Review | Open Access

Energy Materials

Kwon *et al. Energy Mater.* **2026**, *6*, 600085 **DOI:**10.20517/energymater.2026.42

Spatially resolved modulation of the electrode-electrolyte interface in high Li-stoichiometric battery anodes

Jin Yong Kwon[1,#], Younsang Cho[1,#], Gijung Lee[1,#], Dong-Yeob Han[2,*], Jaegeon Ryu[1,*]

Keywords:
High Li-stoichiometric anodes, electrode-electrolyte interface, spatial architecture, solid electrolyte interphase layer, interfacial strategies

Citation: Kwon, J. Y.; Cho, Y.; Lee, G.; Han, D. Y.; Ryu, J. Spatially resolved modulation of the electrode-electrolyte interface in high Li-stoichiometric battery anodes. *Energy Mater.* **2026**, *6*, 600085. https://dx.doi.org/10.20517/energymater.2026.42

Received: 25 Mar 2026 **First Decision:** 9 May 2026 **Revised:** 30 Jun 2026 **Accepted:** 17 Jul 2026 **Published:** 27 Jul 2026

Academic Editor: Jiaqi Huang
Copy Editor: Fangling Lan
Production Editor: Fangling Lan

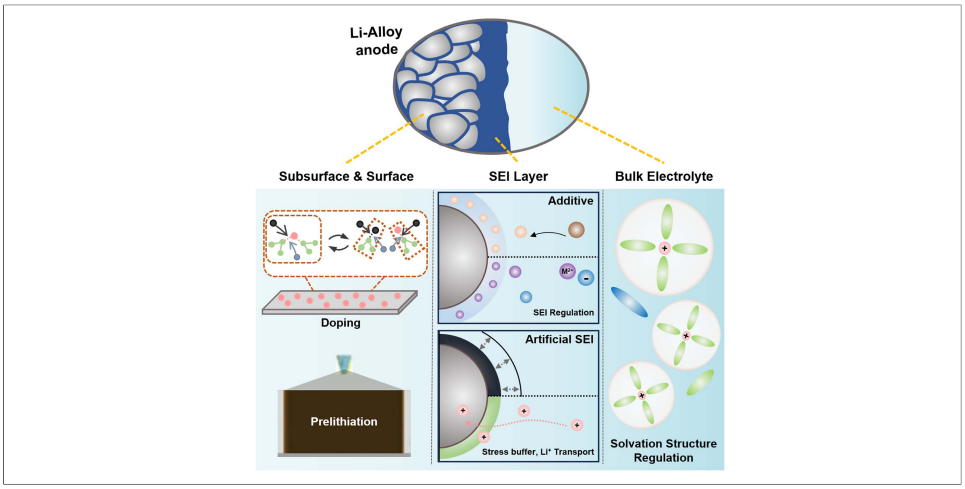

Abstract

High Li-stoichiometric battery anodes (e.g., Si, Ge, Sn, P, Sb, Bi) with exceptional theoretical capacities and favorable lithiation potentials are promising to surpass the energy limitations of existing rechargeable batteries. Yet, these anodes suffer from large volume fluctuations, unstable interfacial reactions, and the difficulty of maintaining an intact solid electrolyte interphase layer, all of which hinder their practical application. Numerous strategies have been developed to stabilize the electrode-electrolyte interface to overcome these challenges. In fact, these approaches can be systematically categorized according to their spatial proximity to the interface, ranging from surface-level modifications to bulk-level structural designs. The continued advancement of such spatially resolved strategies offers an attractive pathway to achieve durable and high-performance electroarchitectures. In this review, we first discuss the fundamental aspects, encompassing the spatial structures and functional roles that emerge at the electrode-electrolyte interface. Thereafter, interfacial strategies are presented in terms of their spatial location, spanning from the electrode subsurface to the bulk, while addressing both liquid electrolyte and solid-state electrolyte systems. By presenting a spatial framework for

Check for updates

[1]Department of Chemical and Biomolecular Engineering, Sogang University, Seoul 04107, Republic of Korea.
[2]Walker Department of Mechanical Engineering, The University of Texas at Austin, Austin, TX 78712, USA.
[#]Authors contributed equally.

[*]**Correspondence to:** Dr. Dong-Yeob Han, Walker Department of Mechanical Engineering, The University of Texas at Austin, Austin, TX 78712, USA. E-mail: dyhan@utexas.edu; Dr. Jaegeon Ryu, Department of Chemical and Biomolecular Engineering, Sogang University, 35 Baekbeom-ro, Mapo-gu, Seoul 04107, Republic of Korea. E-mail: jryu@sogang.ac.kr

interfacial engineering, this review provides new insights and future research directions for constructing more stable interfaces in Li-alloying anodes.

INTRODUCTION

With the rapid advancement of portable electronics, electric vehicles, and smart grid technologies, the pursuit of rechargeable batteries with high energy density and enhanced safety has become increasingly critical. Despite continuous advancements, the energy storage capabilities of conventional lithium-ion batteries (LIBs) with graphite anodes are approaching their energy density limits, prompting the need for alternative anode materials[1,2]. Among various anode candidates, high lithium (Li)-stoichiometric anodes including group IV elements (e.g., Si, Ge, Sn) and group V elements (e.g., P, Sb, Bi) stand out as promising alternatives, offering high theoretical capacities and favorable lithiation potential above the threshold for Li plating[3]. In this review, these materials are referred to as Li-alloying anodes because they store Li through alloying reactions and offer high theoretical capacities with favorable lithiation potentials above the threshold for Li plating. As summarized in Table 1, these high-Li-alloying anodes exhibit diverse electrochemical characteristics that influence their suitability for high-energy applications. Furthermore, high Li-stoichiometric anodes exhibit relatively low chemical reactivity and a reduced tendency toward dendritic growth, thereby improving cycle stability in conventional liquid electrolytes (LEs). These characteristics also render high Li-stoichiometric anodes particularly attractive for application in all-solid-state batteries (ASSBs), where interfacial stability and dendrite suppression are of paramount importance[4,5].

Compared with graphite and Li metal anodes, Li-alloying anodes require a distinct combination of interfacial properties. Graphite primarily depends on a stable solid electrolyte interphase (SEI) formed on an intercalation host with limited volume change, whereas Li metal requires an interface that regulates Li plating and stripping while suppressing dendritic growth[9]. Li-alloying anodes differ from both systems because the Li storage process involves alloying and dealloying reactions accompanied by repeated surface reconstruction[10]. Their interface should therefore combine mechanical adaptability, strong adhesion to the evolving electrode surface, repeated passivation of newly exposed active material, and uniform Li^+ transport across a deforming SEI[11].

These requirements are difficult to satisfy because Li-alloying anodes inevitably undergo severe volume expansion and contraction during cycling, which trigger a cascade of mechanical and interfacial degradation[12]. The repeated volume fluctuations induce internal structural disintegration, leading to fracture of active particles, disruption of percolative conductive networks, and eventual electrical isolation of the fractured domains[13]. Concurrently, the newly exposed particle surfaces readily react with the electrolyte to produce an unstable, thick SEI layer, resulting in excessive Li consumption and elevated interfacial resistance. Even in solid-state electrolytes (SSEs), the mechanically unstable nature of high-Li-stoichiometric anodes poses new interfacial challenges[14]. During repeated dimensional changes, the mechanical mismatch between the expanding anodes and the rigid SSEs leads to delamination, void formation, and contact loss at the interface[15]. This interfacial failure not only disrupts ionic pathways but also induces heterogeneous lithiation kinetics, exacerbating stress localization and accelerating further crack propagation[16,17]. Furthermore, persistent interfacial impedance buildup due to interlayer disruption and interfacial structural fatigue ultimately compromises the long-term stability and coulombic efficiency (CE). These multifaceted challenges underscore the critical need for engineered electrode-electrolyte interfaces that can simultaneously accommodate volume fluctuations and maintain robust ion transport pathways.

The electrode-electrolyte interface serves as a complex but essential regulator of electrochemical behavior, regardless of the type of electrolyte. The SEI, widely recognized as the key interfacial component, is generally

Table 1. Physical and electrochemical properties of various high Li-stoichiometric anodes

	High Li-stoichiometric anode	Density (g cm^{-3})	Lithiated phase	Volume change (%)	Average potential *vs.* Li/Li$^+$ (V)	Theoretical gravimetric capacity (mAh g^{-1})	Theoretical volumetric capacity (mAh cm^{-3})
Group IV elements	Si[6]	2.33	$Li_{4.4}Si$	420	0.4	4,200	9,786
	Ge[6]	5.32	$Li_{4.4}Ge$	370	0.5	1,625	8,645
	Sn[6]	7.26	$Li_{4.4}Sn$	260	0.6	994	7,216
Group V elements	P[7]	2.34	Li_3P	300	0.75	2,596	6,075
	Sb[8]	6.7	Li_3Sb	200	0.9	660	4,422
	Bi[8]	9.78	Li_3Bi	215	0.8	385	3,765

formed spontaneously on the anode surface via electrolyte decomposition and interfacial reactions during the initial charging process, once the anode potential falls below the thermodynamic stability window of the electrolyte[18,19]. An ideal SEI prevents further electrolyte decomposition and enables rapid Li^+ conduction through the layer while inhibiting electron transport. Beyond its ion-selective and passivating functions, the charge transfer dynamics at the electrode-electrolyte interface are strongly influenced by the thickness and composition of the SEI[20]. A thicker SEI imposes additional resistance to charge transfer, thereby limiting reaction rates. Moreover, because Li^+ undergoes desolvation before migrating to the electrode surface, variations in interfacial structure also affect the efficiency of this desolvation step, leading to different charge transfer dynamics compared with those in the bulk electrolyte[21]. Such interfacial characteristics not only determine charge transfer behavior but also influence the spatial distribution of Li within the electrode during cycling, as they govern Li^+ transfer across the interface and subsequent diffusion through the electrode bulk[22]. Therefore, the influence of the interface spans multiple dimensions, with its effects varying according to the spatial position and structural relationship to the interfacial layer.

Significant efforts have been dedicated to tailoring the electrode-electrolyte interface through various strategies (i.e., chemical modification[23], artificial interlayer deposition[24], structural optimization[25], and engineering of electrolyte composition[26]), aiming to improve interfacial stability and charge-transfer kinetics. However, when these studies are organized mainly around individual strategies, such as surface coating, electrolyte additives, artificial interphases, or electrode architectures, it can be difficult to identify where interfacial failure begins and where each strategy primarily acts[27]. Gradient design introduces directional changes within a specific electrode, coating layer, or interphase, whereas spatially resolved modulation in this review uses the spatial location of interfacial phenomena to compare surface/subsurface reactions, SEI evolution, electrolyte-structure effects, ion transport, and solid-state contact failure[28]. Each spatial regime demands distinct chemical and structural approaches to effectively regulate interfacial reactions and ion transport. Moreover, the nature of the interface and its governing mechanisms differ significantly between liquid and solid-state systems. Yet, a comprehensive understanding of these spatial and phase-dependent interfacial phenomena remains limited. Therefore, this review provides a systematic analysis of interfacial engineering strategies from a spatial perspective, highlighting how spatially resolved modulation at the immediate interface and beyond can regulate interfacial dynamics and improve long-term stability in both LEs and SSEs.

To improve readability, the manuscript is organized by the spatial position where each interfacial phenomenon mainly occurs. Section "FUNDAMENTALS OF THE ELECTRODE-ELECTROLYTE INTERFACE" establishes the fundamental structure and role of the electrode-electrolyte interface. The discussion then moves from the electrode side to the electrolyte side: Section "ELECTRODE SURFACE AND SUBSURFACE REGION (~10 Å)" addresses the surface and subsurface regions, Section "SOLID

ELECTROLYTE INTERPHASE LAYER DESIGN IN LIQUID & SOLID ELECTROLYTE SYSTEMS (1~50 nm)" focuses on SEI and interphase design, Section "INTERFACIAL ELECTROLYTE STRUCTURE IN LIQUID ELECTROLYTE SYSTEMS (50~100 nm)" examines the electrolyte environment near the interface in LEs, and Section "INTERFACIAL ION TRANSPORT BARRIERS IN SOLID-STATE ELECTROLYTE SYSTEMS" discusses ion transport barriers and contact failure in SSEs. This organization links surface reactions, SEI evolution, electrolyte structure, and solid interface failure to the spatial domains in which they are most relevant. By uncovering key spatial factors governing interfacial behavior, we aim to guide the design of advanced Li-alloying anodes for high-performance energy storage systems. Although Li-alloying anodes store Li through alloying reactions, their interfacial failure modes are not identical across materials. Phosphorus anodes can involve dissolution and shuttling of lithium polyphosphide species, whereas Sn, Pb, and Bi anodes are strongly affected by phase evolution, stress accumulation, and contact instability during repeated alloying and dealloying. While this review addresses the broad class of Li-alloying anodes, it predominantly employs Si as the primary model system. Since Si possesses the highest theoretical capacity among Li-alloying anodes, it has been the subject of the most extensive research, providing a robust foundation for illustrating interfacial engineering concepts that are highly transferable to other materials.

FUNDAMENTALS OF THE ELECTRODE-ELECTROLYTE INTERFACE

In LIBs, the electrode-electrolyte interface serves as a multifunctional region governing ion transport and redox kinetics. This interface becomes particularly important in systems employing Li-alloying anodes, which exhibit high theoretical capacities but undergo severe volume changes during cycling. Under these highly dynamic conditions, the interface should simultaneously serve as an ionic conductor, an electronic barrier, and a mechanically robust buffer. The contrasting properties of LEs and SSEs further complicate interfacial behavior, reinforcing the need for a more detailed analytical framework[29]. A spatially resolved approach provides a clearer understanding of how localized chemo-structural evolution governs interfacial function. Repeated expansion and contraction of high-capacity anodes generate region-specific degradation such as SEI fracture, particle disintegration, and ion flux, directly impairing ionic accessibility, reaction uniformity, and long-term stability. Since conventional uniform models cannot adequately capture these localized dynamics, a spatial framework is essential. By relating electrolyte phase to site-specific interfacial evolution and identifying spatial criteria that govern stability, this approach provides practical guidance for the design of robust interphases in next-generation LIBs.

Figure 1 outlines the electrode-electrolyte interfaces, spanning from the electrode bulk and surface to the bulk electrolyte. Rather than conveying mechanistic details, this figure introduces the spatial scope for discussing interfacial phenomena in Li-alloying anodes throughout this review. Clearly delineating the electrode subsurface, the SEI layer, and the bulk electrolyte as separate regions, it establishes the structural basis for the subsequent analysis. Each domain will be examined individually regarding its specific impact on interfacial stability and electrochemical performance.

Spatial architecture of the electrode-electrolyte interface

Li^+ transport across the electrode-electrolyte interface arises from both migration and diffusion, with their relative contributions varying with electrolyte type [Figure 2A][30]. The predominance of either mechanism is intrinsically linked to the physical phase and structural characteristics of the electrolyte, with LEs and SSEs exhibiting fundamentally divergent interfacial dynamics and transport behaviors.

In LEs, ionic transport is primarily governed by migration, as solvated species readily respond to applied electric fields[31,32]. As illustrated in Figure 2B, the LE interface consists of an electric double layer (EDL) and an adjacent diffusion layer[33,34]. Within this region, solvated Li^+ accumulates near the negatively polarized electrode, forming layered architectures that gradually transition into the bulk electrolyte. This interfacial

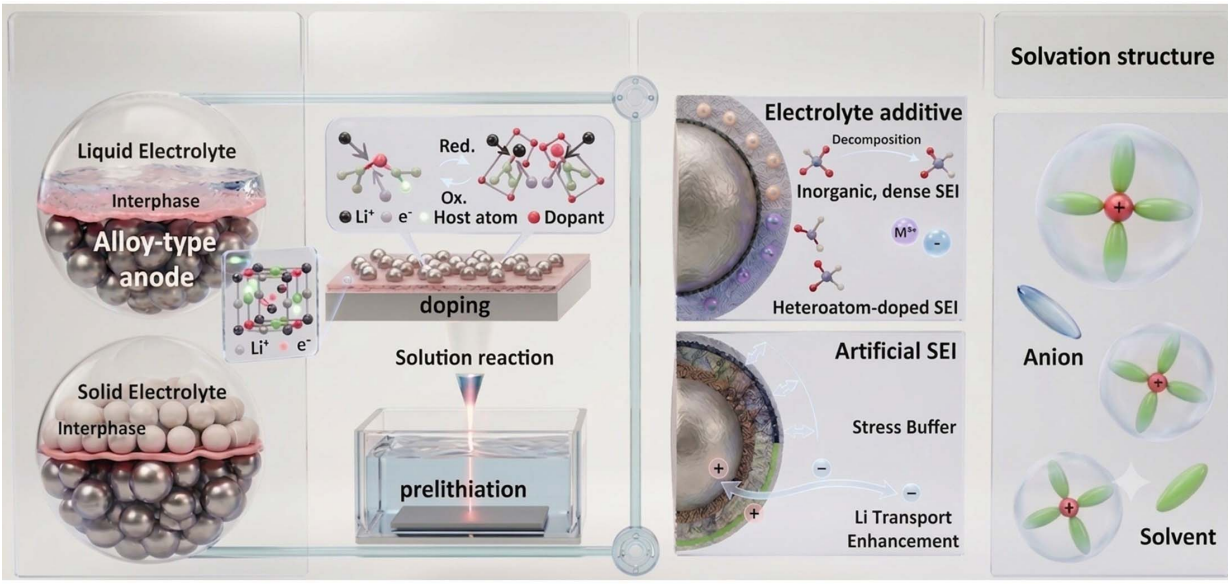

Figure 1. Schematic of spatial architecture from electrode to bulk electrolyte.

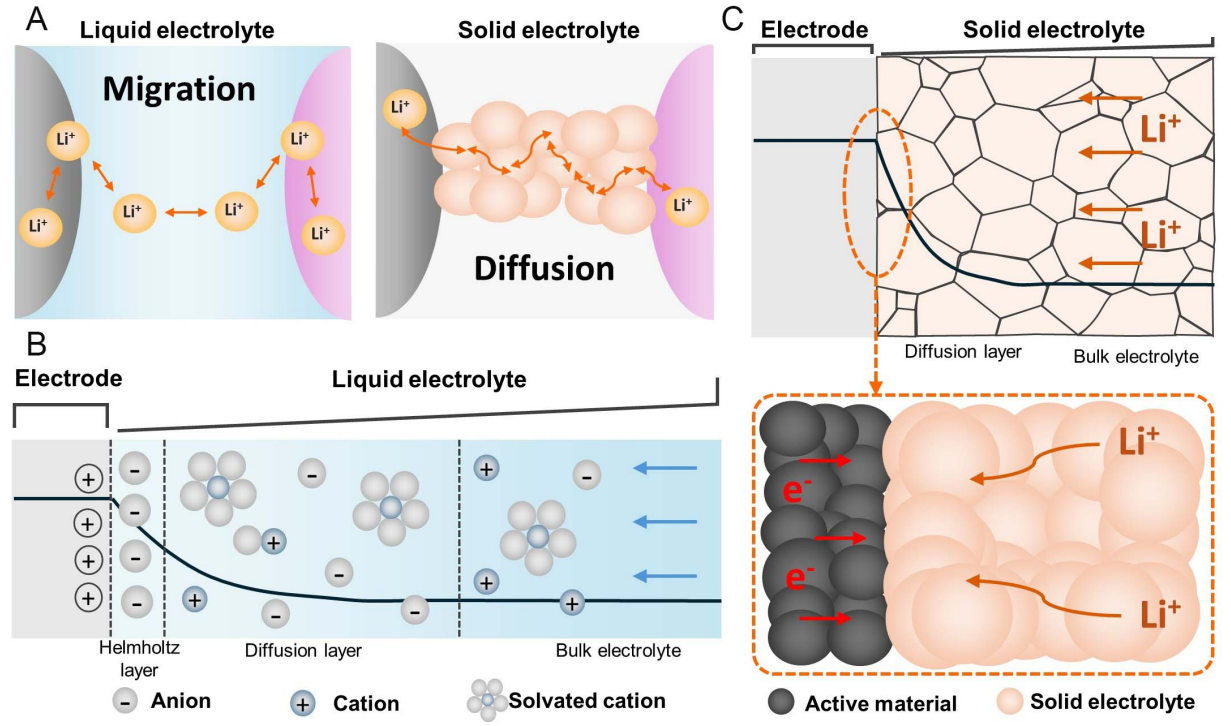

Figure 2. Schematic of (A) Li^+ transport mechanisms in liquid and solid electrolytes, (B) a typical electrode-liquid electrolyte interface with electrochemical components, and (C) electrode-solid electrolyte interfaces in the ASSBs.

organization not only reflects electrostatic structuring but also modulates the spatial availability of mobile Li^+ for electrochemical reactions. Under the influence of potential gradients, Li^+ moves rapidly across this region, ensuring efficient access to active sites and alleviating local depletion through field-driven redistribution[35]. Such transport responsiveness is particularly important in high-capacity anodes, where current density and ion flux often fluctuate sharply. However, under high-rate operation, limited salt concentrations, or poor electrode-electrolyte contact, even migration-dominated systems may experience transient Li^+ depletion, leading to increased overpotentials and heterogeneous interfacial reactivity[36].

The electrode-electrolyte interface in SSEs exhibits distinct structural and chemical constraints that critically influence Li^+ transport[4]. Solid-solid contact often creates physical gaps, mechanical stress, or unstable interphases due to chemical interactions between the electrode and electrolyte[37]. These interfacial features increase resistance and hinder ion transfer, a problem further compounded by space-charge layers that alter the local Li^+ chemical potential. In contrast to LEs, where solvated ions migrate through a flexible fluid layer, ion transport in SSEs entirely depends on solid-state diffusion. As shown in Figure 2C, Li^+ moves through lattice vacancies or interstitial pathways, making mobility highly dependent on lattice geometry, grain boundaries, and interfacial integrity[38]. The intrinsic abruptness in both structural and compositional aspects of these interfaces significantly exacerbates their susceptibility to interfacial defects, positioning such defects as pivotal determinants in constraining the electrochemical performance of ASSB systems[39].

Intrinsic chemo-mechanical deviations in Li-alloying anodes, especially volume changes during cycling, can further degrade interfacial integrity by introducing external stress and compromising contact, which increases resistance[40]. In LE-based systems, the electrolyte's fluidity helps maintain contact with the active material during such changes, whereas the rigidity of SSEs limits their ability to maintain interfacial continuity[41]. Thus, Li^+ transport in solids is inherently constrained by the mechanical and structural stability of solid-solid interfaces. This contrast, highlighted in Figure 2B and C, defines two distinct paradigms of interfacial ion transport: migration-driven conduction across diffuse, solvent-mediated interfaces in liquid systems *vs*. diffusion-limited conduction across rigid, lattice-bound interfaces in SSEs. Although the transport pathways differ, LE and SSE interfaces share a common requirement: stable Li^+ delivery must be maintained while parasitic reactions at the electrode surface are suppressed[42]. In LEs, this requirement is mainly addressed at the liquid-electrolyte interface, where solvation, desolvation, and electrolyte decomposition govern SEI formation[43]. In SSEs, it is addressed at the solid-solid interface, where lattice diffusion, chemical compatibility, and contact retention determine whether Li^+ pathways remain continuous during electrode volume changes[40]. These shared requirements and phase-dependent differences provide the basis for comparing interphase formation in liquid and solid-state systems in the following section.

Importantly, these interfacial processes should not be considered independently, as electrochemical performance ultimately emerges from the coupled interplay between ion solvation, interphase formation, Li^+ transport, and interfacial chemical evolution. In LE systems, the solvation structure of Li^+ determines desolvation behavior at the electrode surface, which subsequently influences electrolyte decomposition pathways and SEI composition. The resulting SEI then governs Li^+ transport kinetics and interfacial resistance, thereby affecting reaction uniformity, rate capability, and cycling stability. Similarly, in SSE systems, Li^+ diffusivity, interfacial chemical compatibility, and contact retention collectively regulate the formation and evolution of solid-state interphases, which in turn determine the continuity of Li^+ transport pathways and electrochemical accessibility. As these processes evolve during cycling, localized changes in surface chemistry can induce spatial heterogeneity in ion transport and reaction kinetics, ultimately manifesting as performance decay. Therefore, a comprehensive understanding of Li-alloying anode interfaces requires an integrated framework that links interfacial chemistry, transport behavior, and electrochemical outcomes across multiple spatial domains.

Comparative interfacial formation: liquid *vs.* solid electrolyte

The formation of the SEI at the interface between electrode and electrolyte constitutes a highly dynamic and multifaceted process, governed by a complex interplay of electrochemical, chemical, and mechanical phenomena[44,45]. This complexity is particularly pronounced in high-capacity anode systems, where repeated lithiation and delithiation cycles induce significant structural transformations and continuous interfacial evolution[46-48].

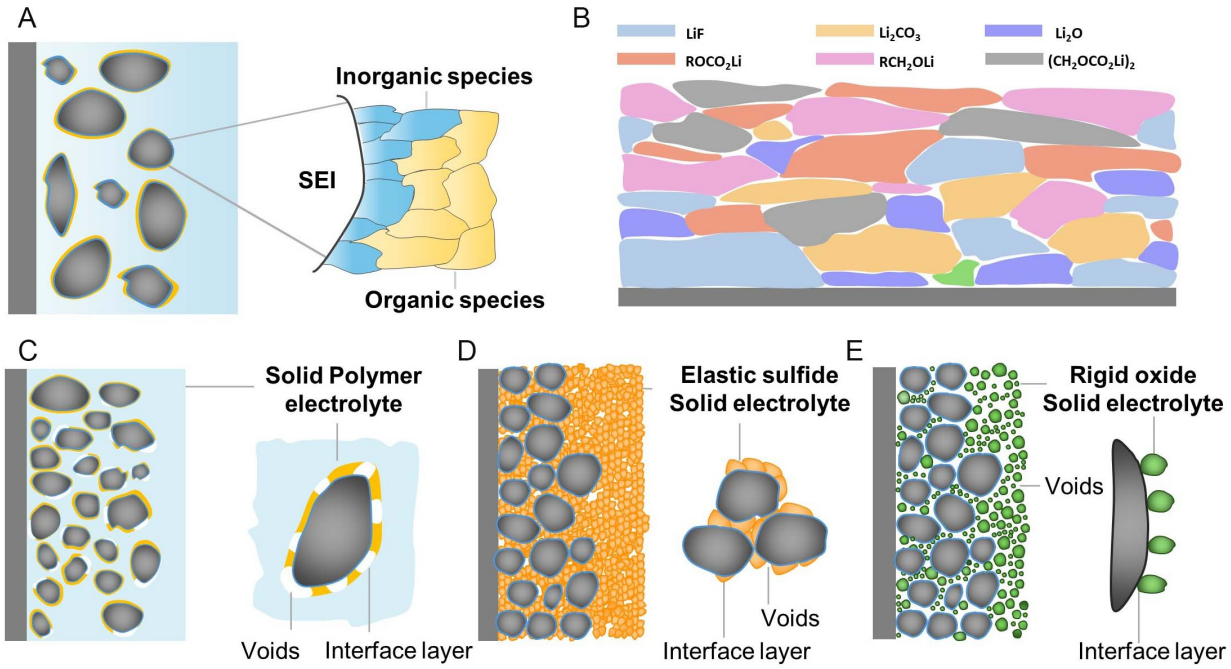

Figure 3. Schematic of (A) interfacial formation in LE systems, (B) mosaic SEI structure, (C) interfacial formation of solid polymer electrolytes, (D) elastic sulfide-based solid electrolytes, and (E) rigid oxide-based solid electrolytes. (A, C-E) Reproduced with permission from ref.[55], under CC BY 4.0 license.

Various conceptual models have been proposed to describe the SEI, reflecting its structural complexity and dynamic formation[49-51]. Among these, one of the earliest and most widely accepted is the bilayer model, which has served as a foundational framework for understanding SEIs formed in LE systems[52]. As illustrated in Figure 3A, this model depicts the SEI as a layered structure composed of an inorganic-rich inner region and an organic-rich outer region[53-55]. This stratification arises from the sequential reduction of electrolyte components, governed by their Lowest Unoccupied Molecular Orbital (LUMO) energy levels and constrained by the system's electrochemical stability window (ESW)[56-58].

However, the bilayer model provides an oversimplified view that fails to capture the spatial and chemical heterogeneity observed under realistic cycling conditions. As shown in Figure 3B, the SEI more accurately adopts a mosaic-like morphology, consisting of irregularly distributed inorganic and organic domains[27,54,59,60]. The inorganic constituents, such as lithium fluoride (LiF), lithium oxide (Li_2O), and lithium carbonate (Li_2CO_3), are typically crystalline and result from the reduction of anions and electrolyte impurities, predominantly localizing near the electrode surface[61]. In contrast, the organic components, including lithium alkyl carbonates ($ROCO_2Li$), lithium alkoxides (ROLi), and polymerized solvent fragments, are amorphous and mechanically softer, arising from solvent decomposition. This heterogeneous architecture is further modulated by local variations in current density, electrode topography, and the solvation environment. In Li-alloying anodes, which undergo pronounced volumetric expansion, such spatial non-uniformity can precipitate mechanical degradation, interfacial rupture, and chemically heterogeneous SEI growth during prolonged cycling[62,63].

In ASSBs, interfacial dynamics differ fundamentally due to the absence of a liquid phase and the imposition of direct solid-solid contact[64]. As shown in Figure 3C, solid polymer electrolytes (SPEs), exemplified by polyethylene oxide (PEO) doped with Li salts such as lithium bis(trifluoromethanesulfonyl)imide (LiTFSI), initially form conformal contacts with the anode owing to their viscoelastic properties[65]. However, during electrochemical cycling, mechanical incompatibilities arising from the substantial volume changes of

Li-alloying anodes lead to interfacial deterioration, including crack initiation and void formation. Concurrently, electrochemical decomposition of both the polymer matrix and the salt yields unstable SEI constituents, including polyether segments, ROLi species, and sulfonyl-derived fragments, which are structurally disordered and chemically labile[66-68].

Figure 3D highlights the behavior of sulfide-based SSEs (e.g., lithium argyrodite (Li_6PS_5Cl) and lithium germanium phosphorus sulfide ($Li_{10}GeP_2S_{12}$)), which exhibit chemical reactivity with low potential anodes[69,70]. Even in the absence of an applied bias, these materials undergo decomposition at the interface, yielding inorganic SEI species such as lithium sulfide (Li_2S), lithium phosphide (Li_3P), and Li_xPS_y. These decomposition products can form compact interphases with moderate Li^+ conductivity. However, their low electronic conductivity, coupled with mechanical stress accumulation, frequently leads to interfacial instability characterized by fracture and delamination over extended cycling periods[71,72].

As illustrated in Figure 3E, oxide-based SSEs, including garnet-type $Li_7La_3Zr_2O_{12}$ (LLZO) and Na super ionic conductor (NASICON)-type $Li_{1+x}Al_xTi_{2-x}(PO_4)_3$ (LATP), exhibit notable electrochemical stability but are thermodynamically incompatible with Li-alloying anodes[73-75]. Interfacial reactions typically result in the formation of insulating and mechanically rigid products such as Li_2O, lithium hydroxide (LiOH), and Li_2CO_3. These products form non-conformal, brittle interphases that impede ion transport and give rise to localized contact loss, microcracking, and the eventual development of electronically and ionically inactive "dead zones"[76]. The inability of ceramic electrolytes to accommodate anode volume changes further exacerbates these degradation pathways.

Collectively, these interfacial formation mechanisms modulated by electrolyte chemistry, anode surface reactivity, and mechanical dynamics give rise to pronounced spatial heterogeneity in SEI composition and morphology across different electrochemical systems. Instead of a uniform passivation layer, the SEI develops as a structurally and chemically complex interface, exhibiting localized variations that evolve over time. This non-uniformity intensifies during battery cycling, as repeated mechanical, chemical, and electrochemical stresses gradually change the structure of the interphase. Understanding the spatial distribution and temporal evolution of these heterogeneous interphases is therefore essential for elucidating their role in long-term interfacial stability and guiding the rational design of durable battery interfaces. These aspects are explored in greater detail in the subsequent section.

Key interfacial roles in high-capacity anodes

The SEI formed on Li-alloying anodes needs to fulfill a diverse set of interfacial roles to ensure stable battery operation under dynamic electrochemical conditions[77,78]. Most critically, it acts as an electrical insulator, preventing further electrolyte reduction by blocking electron transfer from the anode surface[79]. Simultaneously, it should allow selective and efficient Li^+ transport across the interface to sustain ionic conductivity[80]. These requirements are further compounded by the need for the SEI to behave as a buffer layer that accommodates the considerable volume fluctuations inherent to alloy systems. Li-alloying anode materials exhibit substantial volumetric changes during lithiation and delithiation, ranging from moderate (~50%) in Sn-based systems to extreme expansions exceeding 300% in Si and other capacity anodes. The SEI should maintain physical integrity and interfacial adhesion throughout these transformations, without cracking or delaminating. In addition, it is required to prevent chemical degradation and thermal decomposition over extended cycling, particularly under elevated temperatures or high current densities[81,82]. These overlapping demands, including electrochemical selectivity, mechanical adaptability, and environmental stability, render the SEI a uniquely multifunctional interphase, as schematically illustrated in Figure 4A.

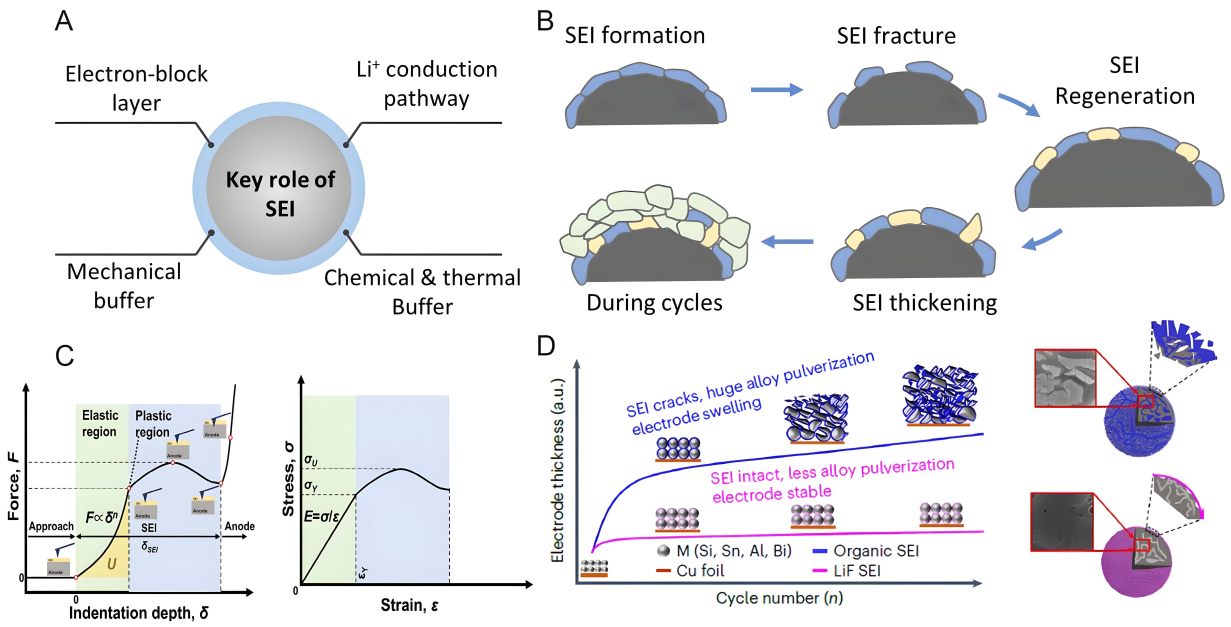

Figure 4. Schematic of (A) the key role of SEI, (B) SEI fracture and regeneration during cycling. (C) Force-displacement curve and stress-strain curves of SEI. (B and C) Reproduced with permission from ref.[84]. Copyright 2024, Wiley-VCH GmbH. (D) Comparison between thick-fragile SEI and thin-tough SEI. (Reproduced with permission from ref.[92]. Copyright 2022, Wiley-VCH GmbH).

However, in Li-alloying anodes, these multifunctional properties of SEI are rarely realized under practical cycling conditions due to their inherently large volume fluctuations. As shown in Figure 4B, the SEI is highly susceptible to mechanical failure when the anode undergoes repeated expansion and contraction. During lithiation, the active material swells, stretching the SEI; during delithiation, shrinkage can result in tensile stress, leading to cracks and partial detachment[83]. Once fractured, the exposed anode surface reacts with the electrolyte, initiating new reduction reactions that form additional SEI[84]. This repetitive rupture-regeneration cycle gradually thickens the interphase and disrupts its compositional and structural uniformity. The newly formed SEI often differs in chemical makeup and mechanical properties from the original layer, leading to spatial inhomogeneity in Li^+ transport pathways. Over time, the accumulation of decomposition products increases interfacial resistance, consumes electrolyte and active Li, and degrades overall cell performance. Insufficient mechanical compliance of the SEI can also destabilize the electrode structure itself or even promote dendritic growth under localized current concentrations[84]. These degradation pathways indicate that cycling stability strongly depends on the mechanical ability of the SEI to preserve interfacial continuity on a volume-changing electrode surface. Insufficient toughness, deformability, or interfacial cohesion causes repeated alloy expansion and contraction to generate cracks, partial delamination, and continuous SEI regeneration[85]. These processes accelerate active Li consumption, electrolyte depletion, and interfacial resistance growth. Stable cycling therefore requires SEI architectures that can mechanically accommodate volume fluctuations during cycling while maintaining electronic passivation and Li^+ transport[86].

The mechanical behavior of the SEI under localized stress determines structural integrity and functional longevity, particularly in alloying anodes with large volume fluctuations during cycling[87]. As illustrated in Figure 4C, indentation experiments offer a quantitative framework for probing the deformation and failure mechanisms of the SEI under compressive loading[84]. The force-displacement curve reveals the progressive mechanical response of the SEI through distinct regimes. At low loads, the SEI exhibits elastic deformation, characterized by a linear relationship between force and displacement and complete recovery upon unloading[88]. With increasing load, the curve deviates from linearity, signaling the transition into a plastic

regime wherein the SEI undergoes irreversible structural reconfiguration. Further displacement may result in mechanical rupture or full penetration of the SEI layer. The terminal indentation depth serves as a proxy for estimating SEI thickness, governing both mechanical resilience and ionic conductivity. Complementarily, the stress-strain curve encapsulates the same deformation process from a different perspective. The initial slope corresponds to the elastic modulus, reflecting the SEI's intrinsic stiffness. Beyond the yield point, the material enters a strain-tolerant regime culminating in fracture, which denotes the material's limit under tensile or compressive stress. Brittle SEI layers tend to fracture prematurely, undermining interfacial cohesion and exposing the reactive anode surface to continuous electrolyte attack[89]. Conversely, a more compliant SEI can accommodate mechanical strain without delamination, thereby maintaining interfacial contact and prolonging electrochemical stability.

These experimental insights highlight the importance of understanding not only the average mechanical properties of the SEI, but also their spatial variation across the interface. As discussed in Section "Comparative interfacial formation: liquid *vs.* solid electrolyte", the SEI often exhibits a bilayered architecture comprising a mechanically robust, inorganic-rich inner layer and a more ductile, organic-rich outer layer[90]. This stratified configuration provides both chemical and mechanical gradation, effectively mitigating stress localization[91]. The inner layer, intimately bonded to the anode, ensures interfacial passivation and electronic insulation. Simultaneously, the outer layer functions as a mechanical buffer, absorbing deformation and arresting crack propagation. Such synergistic mechanical coupling is crucial for preserving the integrity of the SEI against the backdrop of pronounced anode expansion and contraction. Designing an optimal SEI, therefore, requires more than the maximization of either stiffness or compliance. Instead, a mechanically balanced SEI, capable of elastoplastic accommodation in harmony with the dynamic anode morphology, is essential for sustaining interfacial cohesion and electrochemical performance over extended cycling. Ultimately, the SEI's ability to accommodate localized mechanical stress dictates whether it functions as a protective barrier or deteriorates into a locus of failure.

The critical influence of SEI quality on interfacial performance is exemplified in Figure 4D, which compares two structurally distinct interphases representative of thick and fragile *vs.* thin and tough SEI formation in Li-alloying anodes[92]. In the mechanically fragile case, the SEI is excessively thick, mechanically unstable, and poorly integrated with the active material surface. This fragile interphase fails to accommodate volumetric changes during cycling, leading to interfacial detachment, internal fragmentation of the electrode, and spatially heterogeneous Li^+ flux. Such non-uniform ion distribution accelerates local stress buildup, uneven lithiation, and ultimately interfacial degradation. By contrast, the thin and tough SEI is conformal, mechanically robust, and maintains intimate contact with the electrode[93]. It maintains intimate contact with the electrode surface while supporting uniform Li^+ transport across the interface, even under repeated deformation. Recent studies demonstrated that through targeted interfacial design, such compliant and stable SEI structures could effectively suppress structural failure and enhance long-term electrochemical performance[47,61]. While their findings were specific to Si, the underlying design principles such as stress accommodation, interfacial adhesion, and transport uniformity are broadly applicable to other Li-alloying systems. This comparison underscores that SEI effectiveness is governed not simply by its composition or morphology, but by its ability to maintain structural and functional integrity in response to the dynamic behavior of Li-alloying anodes. For reliable, high-performance energy storage, the SEI must be mechanically integrated with the anode to preserve strong interfacial adhesion and structural continuity, allowing it to deform in concert with the host material during volume changes without losing its protective or ionic transport functions. Because these mechanical and electrochemical requirements can vary across different regions of the electrode, achieving durable performance ultimately requires a spatially resolved understanding of the interface, beginning with the surface and subsurface domains that will be discussed in the following section. To facilitate this discussion, Table 2 summarizes the key characterization techniques

commonly used to probe the spatial heterogeneity of battery interphases across different length scales[94-96].

ELECTRODE SURFACE AND SUBSURFACE REGION (~10 Å)

Among the spatial domains for addressing interfacial challenges, the surface and near-surface regions of the electrode, being closest to the electrode-electrolyte boundary, play a crucial role in determining interfacial stability, charge-transfer kinetics, and the formation of the SEI. Representatively, these specific domains encompass the electrode bulk, subsurface, and surface. Unlike bulk properties, surface electronic structures, termination states, and subsurface defects strongly influence how the electrode interacts with the electrolyte, especially during the initial cycles when electrolyte decomposition and interfacial reactions are most pronounced. These surface-related features not only govern the thermodynamic driving force for electrolyte reduction but also significantly affect the binding energies of Li^+ and decomposition species on the electrode surface. Particularly for high-capacity Li-alloying anodes, intrinsic limitations such as low surface electronic conductivity or an unfavorable Fermi level (E_F) frequently trigger uncontrolled electrolyte decomposition, resulting in the formation of a fragile and resistive organic-dominated SEI layer. To mitigate these issues, strategic interventions including artificial surface modification and prelithiation have been actively developed to reconfigure the surface electronic states and promote a chemically and mechanically stable interphase. In this section, we explore the role of surface electronic structures in electrode-electrolyte interactions and discuss how surface and subsurface modifications can be employed to enhance electrochemical performance.

Surface electronic structure and its role in electrolyte decomposition

The surface electronic structures of electrode materials serve as a key factor in electrochemical reactions occurring at the electrode-electrolyte interface. Unlike the bulk, which exhibits well-defined electronic bands, the surface presents localized states, reconstruction, or termination-dependent variations that significantly affect the Fermi level (E_F) position, surface dipoles, and charge distribution. These features of the surface determine how electrons are transferred across the interface and directly govern the energy level alignment between the E_F of the electrode and the frontier orbitals (HOMO and LUMO) of the electrolyte[77]. Among the key properties of surface electronic structure, the E_F represents the electrochemical potential of electrons in the electrode under equilibrium[97]. In particular, the extent of overlap or separation between the E_F of the electrode and the ESW dictates whether parasitic reactions such as electrolyte oxidation or reduction occur.

To better understand this interaction, a simplified energy diagram is presented in Figure 5, highlighting how the electrode's surface electronic structure and work function dictate the open circuit voltage (OCV) and electrochemical stability, which in turn control interfacial phenomena such as electrolyte decomposition and SEI formation during initial cycling. The work function refers to the minimum energy required to remove an electron from the electrode surface and reflects the material's tendency to donate electrons[98]. Under equilibrium conditions, the OCV is determined by the difference between the anode (Φ_A) and cathode (Φ_B) work functions, while the alignment of the E_F of the electrode with the electrolyte's HOMO-LUMO gap dictates the thermodynamic stability of the interface[99]. During charging, the E_F of the anode rises and surpasses the LUMO of the electrolyte, triggering reductive decomposition and SEI formation. Once the SEI layer is established, it effectively shifts the LUMO upward and blocks further electron transfer, thus stabilizing the interface against continued electrolyte reduction[100]. Meanwhile, on the cathode side, the E_F drops below the HOMO of the electrolyte, initiating oxidative decomposition[101]. This leads to the formation of a cathode-electrolyte interphase (CEI), which passivates the surface and prevents further oxidative reactions, thereby maintaining interfacial stability.

With this understanding of interfacial electronic alignment, tuning the surface electronic structure can directly influence interfacial reactions. Enhancing the work function of the electrode surface in contact with the electrolyte can effectively suppress ongoing electrolyte decomposition during repeated cycling. For

instance, Lee *et al.* demonstrated that the silicon dioxide (SiO_2)-rich surface of the Si-based negative electrode initially exhibits a high work function, which effectively suppresses the reduction of electrolyte components during SEI formation[102]. Therefore, tuning the work function of the electrode surface provides a viable approach to control the interfacial electron transfer kinetics and mitigate undesirable side reactions. In addition, modulating the E_F of the electrode offers a route to control interfacial reactivity and suppress undesirable side reactions with the electrolyte. To this end, a wide range of strategies has been developed to modify the surface electronic structure of electrode materials, thereby enhancing interfacial stability and overall electrochemical performance. In the following sections, we will explore these surface engineering techniques in detail, highlighting how specific modifications such as surface termination, doping, and pre-lithiation can be employed to strategically tailor the surface and subsurface chemistry of electrode materials.

Surface termination strategies

Systematic modulation of surface termination has emerged as a powerful strategy for tailoring electronic boundary conditions in high Li-stoichiometric anodes. Termination species, such as fluorine and nitrogen, alter the local bonding environment as well as the E_F and electrode work function. Moreover, certain surface terminations directly contribute to the formation of chemically and mechanically robust SEI components. Notably, the elemental nature of the termination affects both the chemical composition and electrochemical functionality of the resulting SEI, such as ionic conductivity and electron-blocking ability[27]. For instance, Huang *et al.* synthesized a surface fluorinated vertical graphene carbon layer on SiO_x (SiO_x@vG-F) via the pyrolysis of the polyvinylidene fluoride (PVDF)[103]. The density functional theory (DFT) calculations revealed that fluorine termination on the SiO_x@vG-F electrode significantly enhances binding energy with Li^+ by 12.1 kcal mol^{-1} compared to the unmodified surface, attributed to the strong affinity between fluorine atoms and Li^+ [Figure 6A]. This surface fluorination also drives the preferential formation of LiF-rich SEI. Among various SEI components, LiF is well known for its wide band gap (~13.6 eV) and intrinsically low electronic conductivity, which effectively suppresses electron tunneling across the electrode-electrolyte interface[103]. Consequently, the formation of an inorganic-based SEI layer contributes to improved interfacial stability and enhanced long-term cycling performance of the Si-based electrode[104]. Also, Fang *et al.* modified the surface of Si via coating of fluorinated alucone (AIFHQ)[105]. The electrode with the AIFHQ reveals fast interfacial kinetics via the galvanostatic intermittent titration technique (GITT) and diffusion simulation results. The introduction of AIFHQ facilitates the formation of a LiF-enriched SEI that enables a robust interface and enhances Li^+ diffusion kinetics[105]. The calculated Li^+ diffusion coefficient reaches 2.10×10^{-10} cm^2 S^{-1}, which is nearly two times higher than that of the unmodified Si electrode (1.13×10^{-10} cm^2 S^{-1}), ultimately contributing to improved electrochemical performance in the Si anode. In summary, the introduction of fluorine functionalities modulated the surface chemistry and electronic properties of the electrode, thereby facilitating the controlled formation of a LiF-predominant SEI and establishing a stable electrode-electrolyte interface essential for high-performance LIBs.

In addition to fluorination, nitrogenation is a promising surface termination approach that can modulate the chemical properties of the electrode. In general, the incorporation of nitrogen atoms into the graphene lattice introduces an electronic donor state close to the E_F, which enhances electronic conductivity and modulates interfacial reactivity by altering the local electronic environment[106]. From this perspective, nitrogenation of the surface is expected to enhance interfacial kinetics and facilitate charge transfer across the interface. Tan *et al.* incorporated nitrogen atoms into the surface of the Si anodes through nitrogen gas plasma treatment[85]. In the case of nitrogen-treated electrodes, the substitutional incorporation of nitrogen leads to an elongation of Si-Si bond lengths, thereby resulting in a reduction in the binding energy of elemental Si. Such structural modification allows efficient charge transfer by lowering the activation energy required for

Table 2. Comparison of representative characterization techniques for probing the spatial features of interphase

Technique	Impedance analysis (EIS/DRT)	Neutron-based methods	Raman mapping	X-ray tomography (CT)	AFM & nanoindentation	XPS depth profiling	TOF-SIMS	Cryo-TEM
Spatial resolution	Macroscopic scale	10~100 nm	0.5~1 μm	0.05~10 μm	1~10 nm	1~10 nm	1~5 nm	0.1~1 nm
Chemical & structural sensitivity	Differentiates interphase, grain boundary, and charge-transfer phenomena based on distinct relaxation times	Uniquely sensitive to light isotopes, precisely maps Li concentration gradients and bulk structural evolution	Maps molecular vibrations, functional groups, and phase transitions (e.g., crystalline-to-amorphous transformation)	Low chemical contrast for light elements, but excellent density contrast for tracking volume expansion and crack propagation	Low chemical sensitivity, but exceptional sensitivity to localized mechanical properties (modulus, adhesion, stress)	Quantitative elemental composition and accurate mapping of chemical oxidation states along the depth profile	Unsurpassed isotopic and molecular fragment sensitivity; ideal for differentiating organic/inorganic SEI constituents	Highly sensitive to atomic lattice, SEI morphology, and spatially resolved chemical oxidation states
Operando/*in situ* compatibility	High: Non-destructive technique for continuous cell monitoring	High: Neutrons highly penetrate heavy cells and dense electrode materials	High: Routinely utilized with optical window cells for *in-situ* tracking	High: Non-destructive 3D morphological tracking inside electrochemical cells	High: Electrochemical AFM allows direct observation in liquid electrolytes	Moderate: Ambient-pressure XPS exists, but standard profiling is *ex-situ*	Low: Strictly requires an ultra-high vacuum environment	Low: Requires cryogenic freezing to preserve transient/reactive states
Limitations & challenges	Lacks direct spatial imaging Highly convoluted signals require rigorous physical validation via equivalent circuit modeling	Requires large-scale reactor facilities Relatively poor spatial resolution compared to electron microscopy	Weak signals for thin inorganic SEI components Significant interference from background fluorescence	Poor contrast for inorganic/organic SEI layers Susceptible to beam-induced heating and radiation damage during extended scans	Limited to surface topography	Ar-ion sputtering can alter the intrinsic chemical states Poor lateral resolution	Destructive technique (sputtering) Matrix effects heavily complicate quantitative analysis	Extremely localized sampling Complex sample preparation High cost

Li^+ diffusion from the surface into the bulk of the electrode Figure 6B[107]. Also, Song *et al*. demonstrated that surface modification with nitride compounds yields much higher electronic conductivity, thereby improving charge-transfer kinetics[108]. Beyond the improved charge transport, the increased mechanical robustness facilitated more reversible electrochemical behavior by preserving structural integrity over prolonged cycling. In light of these benefits, surface modulation of electrode materials promotes beneficial interfacial chemistry and accelerates charge transfer processes, contributing to enhanced cycling reversibility and interfacial robustness in high-Li-stoichiometric anodes. Ultimately, the rational design of surface terminations should focus on a synergistic approach: manipulating the local electronic environment to accelerate interfacial charge transfer, while simultaneously directing the formation of a chemically and mechanically robust SEI layer for long-term cycling stability.

Prelithiation and doping to modify interfacial potential and reactivity

Li-alloying anodes exhibit exceptionally high theoretical capacities but suffer from significant initial consumption due to the formation of a SEI and irreversible lithiation of the host material[109]. This results in a low initial coulombic efficiency (ICE), which poses a critical challenge for practical full-cell integration, especially

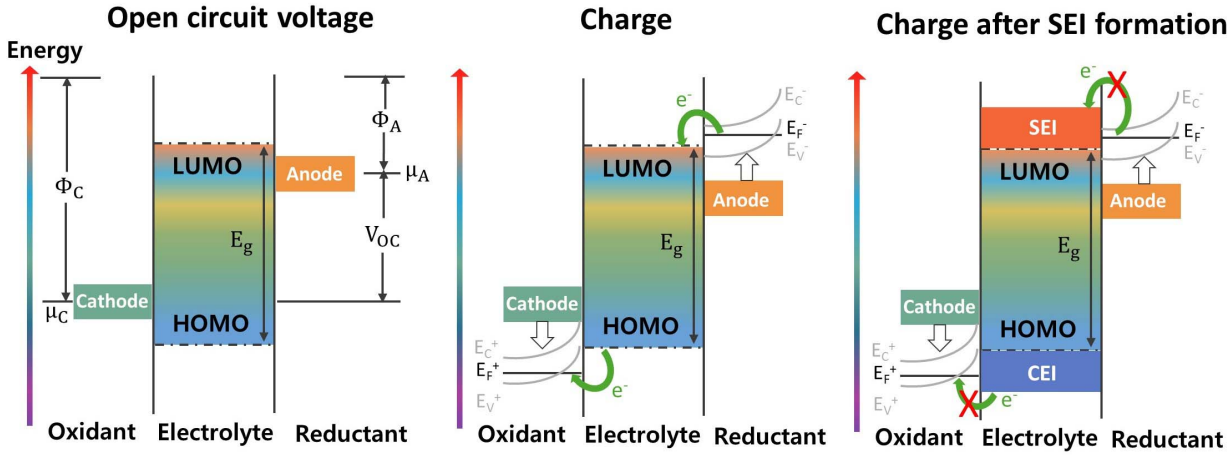

Figure 5. Energy diagram of a rechargeable battery with anode and cathode.

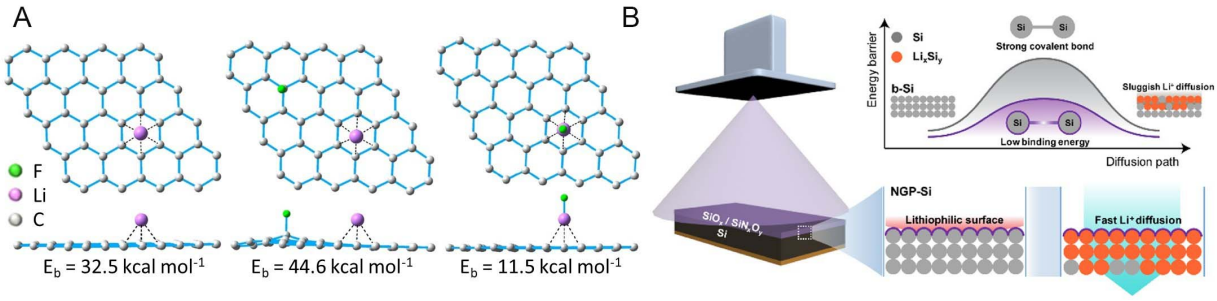

Figure 6. (A) The binding energy of SiO_x/vG and SiO_x/vG-F electrodes with Li^+. Reproduced with permission from ref.[103]. Copyright 2024, Wiley. (B) Nitrogen plasma-induced Lithiophility and Si-Si weakening for fast Li^+ diffusion. Reproduced with permission from ref.[107]. Copyright 2022, American Chemical Society.

when paired with conventional cathodes. To mitigate this issue, prelithiation strategies have been widely explored across various electrolyte systems to compensate for the irreversible capacity loss and stabilize the interfacial potential during early cycling. For example, Wang *et al.* employed lithium-biphenyl (Li-Bp)/Tetrahydrofuran (THF) to achieve chemical prelithiation at the P/C anodes, which increased Li compensation and consequently improved the ICE to 93% under full prelithiation[110]. During chemical prelithiation, an artificial SEI layer was generated on the P/C anode surface, which stabilized the interface and prevented further Li consumption; even if the SEI was partially reconstructed, the associated Li loss could still be compensated by the preloaded active Li within the prelithiated P/C composite. Beyond restoration of Li inventory, prelithiation can influence interfacial evolution by moderating initial electrolyte decomposition and promoting the formation of a compact SEI[111]. This controlled interfacial reconstruction helps suppress localized reactions and reduce interfacial resistance, thereby enhancing long-term electrochemical stability. Furthermore, prelithiation can effectively modulate the electrode's E_F, thereby reducing interfacial reactivity[112]. For instance, Kim *et al.* investigated the effect of controlled prelithiation on interfacial potential by varying the external shorting time between c-SiO_x and Li metal in LEs[113]. As the contact time increased, the voltage progressively decreased along a single plateau, indicating continuous alloying to form Li-Si phases. By monitoring the OCV after each interval, they demonstrated that tuning the interfacial potential through prelithiation could effectively enhance the ICE and modify the interface structure[113]. Specifically, the SEI formed on prelithiated electrodes was observed to be richer in inorganic components such as LiF and Li_2O, which is attributed to the varying lithiation current profiles during prelithiation compared to the constant current applied to conventional electrodes[111]. This tailored interfacial

chemistry contributed to extended cycle life. Also, prelithiation strategies have been conducted in SSEs. Ham *et al*. propose a straightforward pressure-driven prelithiation approach for the Si anode during ASSB fabrication[109]. During the pressure-induced lithiation, the incorporation of Li into Si enhances its electronic conductivity, rising from 10^{-4} to 10 S cm^{-1} as the Li content increases from Li_0Si to Li_2Si Figure 7A. As the Li content in Si increases, the reduced interfacial resistance facilitates more efficient charge transport, leading to lower cell overpotentials and improved ICE. Consequently, the enhanced interfacial kinetics contribute to more stable cycling performance. Beyond simply incorporating Li into the electrode structure, prelithiation can also actively affect interfacial characteristics, particularly by steering the initial formation pathway of the SEI. Jang *et al*. utilized a molecularly engineered Li-arene complex (LAC) with a low potential, enabling simultaneous chemical lithiation of the Si/SiO_x surface and *in situ* formation of a protective interfacial layer Figure 7B[109,114]. The infiltration of the LAC solution into the electrode enables uniform Li distribution across the entire electrode, in contrast to solid Li sources that often lead to localized overlithiation. Notably, the Si particles exhibited spatially uniform expansion after prelithiation, inducing homogeneous lithiation, which in turn alleviates interfacial stress. Additionally, the protective layer formed from the LAC solution evenly covers the surface of the prelithiated anode, providing enhanced stability during exposure to dry air and ultimately leading to longer battery cycle life. Consequently, these findings collectively highlight that prelithiation of the electrode is effective in compensating initial capacity loss, while also playing a pivotal role in regulating interfacial potential and reactivity. Thus, prelithiation provides a route to stabilize early interfacial evolution by coupling Li compensation with controlled interphase formation[111]. Despite these benefits, practical use of prelithiation remains limited by the need to precisely control the lithiation degree across the electrode. Because prelithiation directly changes the Li inventory and initial electrode potential, a slight mismatch in lithiation degree can leave Li-deficient or over-lithiated regions, promoting non-uniform interfacial fractions during early cycling. This challenge becomes more critical in thick or high-loading electrodes, where long transport pathways and contact heterogeneity can lead to depth-dependent lithiation[115]. In addition, chemical prelithiation methods must minimize residual reagents and by-products, whereas mechanical prelithiation requires uniform contact and pressure control between the electrode and Li source. These requirements become particularly important when prelithiation is considered for roll-to-roll electrode processing and large-format cell manufacturing[116]. Therefore, practical prelithiation should be optimized to regulate the Li inventory in a controlled manner, improving ICE while preserving lithiation uniformity, stable interfacial reactivity, and full-cell balance.

Heroatom doping is a widely employed approach in engineering active materials to tailor the local bonding environment and electronic density of states (DOS) of host materials, thereby introducing potentially more active or reactive sites[117]. Therefore, doping of electrode materials can weaken covalent bonds susceptible to Li^+ interaction, leading to controlled bond dissociation within the electrode matrix. As a result, previously inaccessible polarized bonds become exposed to Li^+, generating new active sites that facilitate faster redox kinetics. Zhou *et al*. demonstrated that sulfur doping in black phosphorus (S/bP) beyond a critical concentration of 1 atom% enhances exchange current densities and reduces the activation barriers for lithiation and delithiation[118]. In Figure 7C, S/bP destabilizes bonds during lithiation by promoting the cleavage of staggered P-S and P-P bonds upon electron injection. This leads to the fragmentation of the S/bP lattice into smaller nanoribbons, whereas pristine bP maintains its structure under similar conditions. Ultimately, the bond cleavage induced by sulfur doping exposes new active sites, which not only accelerate the intrinsic redox kinetics of the Li-alloying reaction but also reduce the interfacial energy barrier for charge transfer. This dual effect facilitates rapid ion-electron coupling across the electrode-electrolyte interface and enables high-rate lithiation dynamics conducive to fast charging operation. In addition to sulfur, P doping can effectively alter the electronic structure of Si-based anodes owing to its large atomic radius and strong electron-donating character, thereby promoting Li insertion and extraction[119]. Lv *et al*. synthesized P-doped porous Si nanoparticles (SiNPs) via a combination of ball milling and acid etching[120]. The incorporation of P

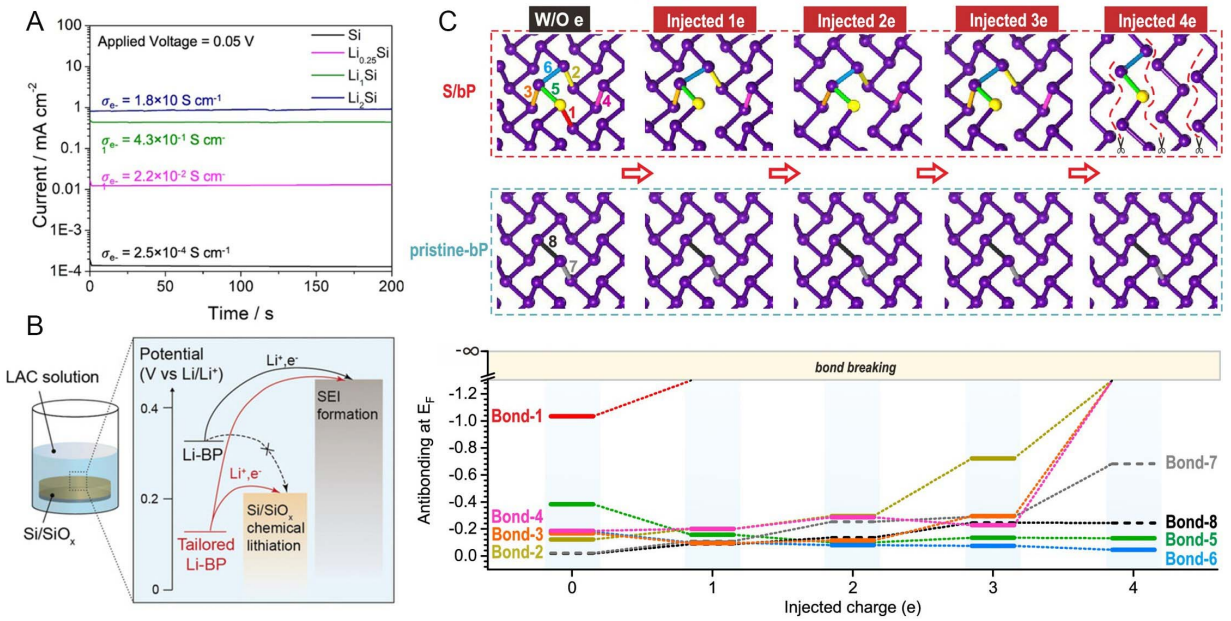

Figure 7. (A) Enhanced electronic conductivity of Si upon lithiation. Reproduced with permission from ref.[109]. Copyright 2024, Author(s), licensed under a Creative Commons CC BY license. (B) Energy level alignment for chemical lithiation and SEI formation governed by Li-BP complex potential. Reproduced with permission from ref.[114]. Copyright 2020, Wiley. (C) Comparison of bond evolution and antibonding states near E_F in S/bP and pristine-bP under initial lithiation. Reproduced with permission from ref.[118]. Copyright 2024, American Chemical Society.

atoms into the Si lattice profoundly alters its electronic structure, increasing the intrinsic conductivity by 8 to 9 orders of magnitude compared to undoped SiNPs. This dramatic enhancement in electrical conductivity potentially reduces interfacial resistance, which leads to excellent rate performance. In addition, the P-doped porous SiNPs mitigate the mechanical stress associated with Si volume expansion and stabilize the interface during cycling, promoting long-term electrochemical stability. Collectively, these results underscore the importance of heteroatom doping as a versatile strategy for engineering the local chemical environment and electronic structures of Li-alloying anodes, offering a promising route to improve redox kinetics.

More broadly, the anode surface modification strategies discussed in this section regulate different spatial domains and therefore mitigate different degradation pathways. Surface termination acts primarily at the outermost electrode surface, where it adjusts Li^+ adsorption, electron transfer, and the chemical route of initial SEI formation[102]. This approach can promote favorable interphase components and suppress excessive electrolyte reduction, although its performance can be limited by incomplete coverage, chemical instability of the modified surface, or increased resistance when the surface layer is overly insulating[121]. Prelithiation mainly regulates the surface and near-surface lithiation state by compensating for initial Li loss and moderating interfacial potential during early cycling. Its benefits depend on spatially uniform Li distribution, because non-uniform or excessive lithiation can generate local stress, heterogeneous potential distributions, and uncontrolled SEI growth. Heteroatom doping extends further into the subsurface or near-bulk region by modifying the local chemical environments, electronic conductivity, and Li-alloying kinetics[122]. This strategy can improve charge transfer and reduce internal kinetic barriers, but its effectiveness depends on dopant homogeneity, phase stability, and retention of the intrinsic capacity of the active material. These comparisons indicate that surface and subsurface modification strategies should be selected according to the dominant failure location and the targeted interfacial function, rather than retreated as equivalent approaches for general interface stabilization.

SOLID ELECTROLYTE INTERPHASE LAYER DESIGN IN LIQUID & SOLID ELECTROLYTE SYSTEMS (1~50 nm)

SEI layer, positioned on top of the electrode subsurface and in direct contact with the electrolyte, significantly affects the interfacial properties over a wider spatial range. Therefore, designing and optimizing the SEI layer is considered a critical factor that governs the electrochemical performance, cycling stability, and safety of high-capacity anode materials. Although the SEI has conventionally been described as a simple electron-blocking barrier that prevents continuous electrolyte decomposition, it also serves essential roles in enabling selective Li^+ conduction and in alleviating the mechanical degradation of Li-alloying anodes. This function is particularly important for high Li-stoichiometric anode materials, which undergo substantial volume fluctuations during cycling. In such anode systems, the SEI layer must demonstrate mechanical robustness, chemical stability, and high ionic conductivity, as its chemical composition and thickness directly influence cycle reversibility and the structural integrity of the electrode. A well-designed SEI can buffer interfacial stress, prevent crack propagation, and maintain uniform charge distribution during operation. Under these demanding operations, the repetitive structural fracture of the interphase and subsequent parasitic electrolyte consumption constitute the dominant degradation phenomena. To mitigate these critical failures, engineering tailored electrolyte additives or designing artificial SEI architectures has emerged as a vital strategy to precisely govern the interfacial chemistry and evolution.

This section explores recent strategies to regulate the formation and properties of SEI layers using electrolyte additives, artificial coatings, and polymeric binders. Moreover, the discussion will extend to the interfacial instability unique to solid-state systems, where both mechanical stress and chemical degradation directly influence the reorganization of the SEI layer.

Solvent and salt decomposition-induced solid electrolyte interphase construction

Carbonate-based electrolyte additive

Unsaturated ester-based electrolyte additives were first reported for stabilizing high-capacity anode materials. Owing to their high reduction potential and reactive functional groups, such as fluoroethylene carbonate (FEC), vinylene carbonate (VC), and dimethylvinylene carbonate (DMVC), undergo preferential electrochemical decomposition at the early stage of cycling. These additives help form an inorganic-based or mechanically stable SEI that can effectively impede the disintegration of the electrode structure. Among these, FEC additives are widely employed due to their ability to generate a LiF-rich interface, which possesses effective electron-insulating properties and SEI breakdown prevention capability due to its mechanical rigidity[90]. At the atomic level, the decomposition of FEC typically proceeds via single-electron reduction to generate fluoride radicals and ethylene-based fragments at around 1.5 V[123].

$$FEC + e^- + Li^+ \rightarrow VC + LiF \quad (1)$$

$$FEC + e^- + Li^+ \rightarrow CH_2{=}CF + Li_2CO_3$$

$$nCH_2{=}CF \rightarrow [\text{-}CH_2\text{-}CF\text{-}]_n \rightarrow [\text{-}CH{=}CH\text{-}]_n + LiF \quad (2)$$

The radicals rapidly react with Li^+ to form LiF and are included in the inner SEI layer in a nanocrystalline shape, which can modulate crystal structure and chemical functions[124]. Following the initial reduction, the unsaturated intermediates undergo radical polymerization and subsequent de-fluorination even below 1.0 V, producing additional LiF. Due to their wide bandgap and electronic insulation properties, they serve as effective barriers that suppress further electrolyte reduction by electronically passivating the Si surface. At the same time, their mechanical rigidity improves the structural resilience against repetitive stress from large

volume fluctuations. Furthermore, although bulk and non-uniform LiF is known to be ionically resistive, nanoscale LiF domains, particularly at SEI grain boundaries or amorphous interphases, may facilitate localized Li^+ migration through space-charge-assisted transport or interfacial hopping mechanisms[125]. These combined effects allow FEC-derived SEIs to act as selective and protective ionic conductors.

Recent studies have elucidated that LiF, generated from FEC decomposition, is not merely confined within the SEI but can also chemically interact with the Si surface, leading to a form of interfacial doping Figure 8A[126]. This interfacial embedding alters the local chemical environment by stabilizing undercoordinated Si atoms and generating a fluorine-rich boundary layer. As a result, LiF doping disrupts long-range ordering in lithiated Si, leading to local lattice disorder at the interface. This structural modulation increases the energy barrier for the nucleation of crystalline $Li_{15}Si_4$, a phase known to accelerate electrode degradation due to its large volume change and high stiffness. The suppression of this crystalline phase fundamentally alters the lithiation behavior of Si. Without FEC, the system tends to form c-$Li_{15}Si_4$ after full lithiation, particularly at low rates or high depths of discharge. However, in FEC-containing systems, the lithiation pathway is redirected toward amorphous Li_xSi phases that are mechanically softer and electrochemically more reversible[126]. Cryo-transmission electron microscope (TEM) and selected area electron diffraction (SAED) studies confirm the absence of diffraction spots associated with c-$Li_{15}Si_4$ under such conditions. This pathway shift is beneficial for both mechanical stability and chemical reversibility. Amorphous Li_xSi reduces irreversible Li trapping and promotes more homogeneous delithiation[127]. Furthermore, the presence of LiF at the interface may regulate local Li^+ diffusivity and prevent over-lithiation at grain boundaries. In summary, FEC enables a coupled mechanism of surface doping and phase control, offering a chemically grounded route to stabilize both interfacial structure and electrochemical performance in Si anodes[128].

On the other hand, a VC-based electrolyte additive has been developed for high-capacity anode materials, where its reduction primarily forms a polycarbonate-based SEI layer. While decomposition of the FEC additive poses a risk of generating HF during radical reaction, which significantly affects the abuse influence on active materials, VC additives have the advantage of producing negligible harmful byproducts from their decomposition. In particular, VC additives decompose via a two-electron reduction mechanism, opening the vinylene ring and subsequent polymerization into polycarbonate-type structures[129]. The initial reduction typically occurs at a relatively high potential (1.2~1.4 V *vs.* Li/Li^+), forming linear or crosslinked poly (VC) chains on the anode surface. These polymeric species integrate into the SEI as electronically insulating yet highly ionically permeable layers[130]. Therefore, VC-derived SEI tends to be thinner and more elastic than FEC-derived SEI, offering improved conformal coverage over expanding Si surfaces. As a result, previous work has shown that only 1% VC addition to the electrolyte can promote the formation of initial VC-derived SEI at higher potentials and inhibit the reduction decomposition of electrolyte solvent[131]. However, due to its compact structure and lack of intrinsic defects, the VC-derived SEI exhibits relatively low Li^+ conductivity, which can limit high-rate performance despite its excellent interfacial stability[103].

Similar additives with VC that contain vinyl groups are reported as vinyl ethylene carbonate (VEC)[132] and methylene ethylene carbonate (MEC)[133]. While VC undergoes rapid electrochemical ring-opening polymerization, additional alkyl substituents in MEC and VEC stabilize the vinyl group and suppress uncontrolled radical polymerization. Therefore, cells employing VEC and MEC as electrolyte additives demonstrated significantly lower concentrations of $ROCO_2Li$ in the SEI, as confirmed by X-ray photoelectron spectroscopy (XPS) and nuclear magnetic resonance (NMR) analysis, compared to those using VC[133]. The reduced presence of these unstable carbonate species correlates with enhanced SEI stability, leading to improvements in cycle retention and rate capability. Further, to overcome the limitations of VC and FEC, DMVC derivatives were rationally designed by introducing functional side groups such as

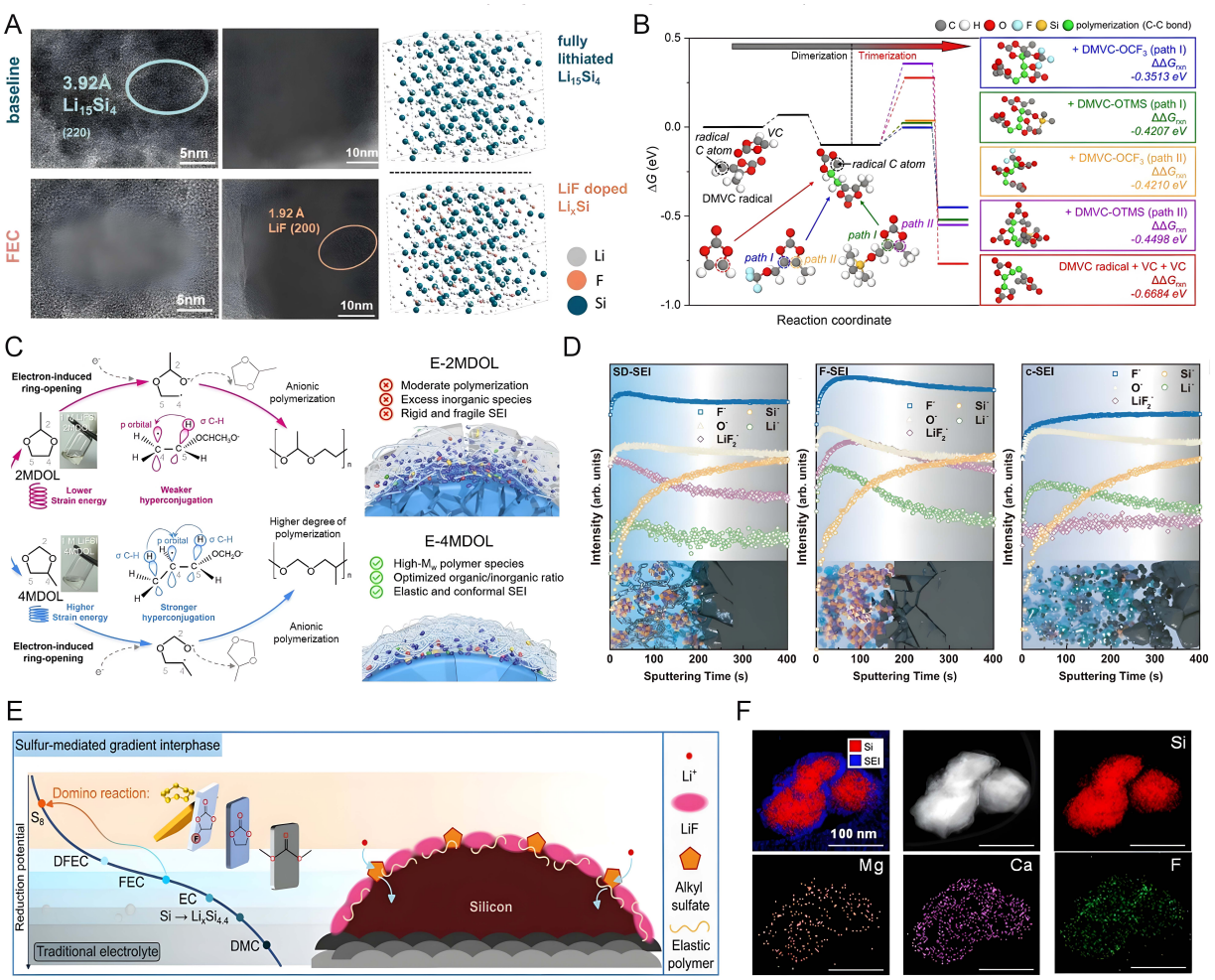

Figure 8. (A) TEM images and schematic images of FEC electrolyte additive forming LiF dopant into Si crystal structure. Reproduced with permission from ref.[126]. Copyright 2023, American Chemical Society. (B) Relative Gibbs free energies of DMVC additive and VC dimer trimerization route reacting with VC, DMVC-OCF_3, or DMVC-OTMS. Reproduced with permission from ref.[134]. Copyright 2021 Author(s), licensed under a Creative Commons CC BY license. (C) Schematic diagram of the selective methylation design of cyclic ether molecules and mechanistic comparison of ring-opening polymerization. Reproduced with permission from ref.[137]. Copyright 2024, Wiley. (D) TOCF-SIMS secondary ion images of the cycled micron-sized Si electrodes showing selectively dissolving SEI component. Reproduced with permission from ref.[43]. Copyright 2023, Author(s), licensed under a Creative Commons CC BY license. (E) Conceptual illustration of domino reactions involving the electrochemical reduction of elemental sulfur. Reproduced with permission from ref.[145]. Copyright 2023, American Chemical Society. (F) TEM-element mapping of Si and mixed cation-based SEI components derived from multivalent ion additive. Reproduced with permission from ref.[152]. Copyright 2024, American Chemical Society.

trimethylsilyloxy (-OTMS) and -OCF_3 to tailor their reduction behavior and interfacial reactivity Figure 8B[134]. Upon one-electron reduction, DMVC undergoes selective ring-opening at the vinylene site, generating carbon-centered radicals that proceed through either homocoupling (path I) or hetero-radical recombination with co-additives (path II). These radical pathways promote thermodynamically favorable C-C bond formation, leading to the growth of cross-linked polycarbonate networks that serve as mechanically adaptive SEI layers. In particular, OTMS-containing species contribute to PF_5 scavenging and effectively suppress the formation of HF and alkyl carbonate byproducts. The resulting SEI exhibits a spatially graded architecture, composed of a soft, polymer-rich outer layer and a rigid, LiF/SiO_x-enriched inner region. This heterogeneous modulus distribution enables anisotropic stress dissipation and prevents interfacial fracture, thereby enhancing the mechanical and electrochemical stability of high-capacity Si anodes under repeated volume changes.

Non-carbonate organic-based electrolyte engineering

Compared to conventional carbonate-based additives, ether-based and other non-carbonate organic electrolyte components offer key advantages for stabilizing Li-alloying anodes, though their low oxidative stability poses a challenge for compatibility with high-voltage cathodes[135]. Such stabilization is closely associated with the ability of these components to modulate the local solvation environment and determine the preferential reduction of electrolyte species at the anode surface. Their lower viscosity and weaker Li^+ coordination promote anion-rich solvation structures, facilitating salt-anion decomposition and the formation of an inorganic-rich SEI[135]. Beyond solvation control, these additives often undergo selective decomposition or generate reduction products that contribute to the formation of desirable SEI components. For example, 1,3-dioxolane (DOL) derivatives can undergo electron-triggered ring-opening polymerization to form conformal, elastic SEI that effectively buffers volume changes in Si anodes[136]. Unlike carbonates, which tend to fragment into gaseous or brittle species, non-carbonate molecules are more chemically tunable and frequently contain polymerizable or surface-reactive groups, enabling *in situ* interfacial network formation. These mechanistic benefits collectively allow for improved interfacial stability, chemical uniformity, and mechanical resilience in high-capacity anode materials. Additionally, selective methylation of DOL at specific ring positions enables precise modulation of its electrochemical decomposition pathways and SEI structure[137]. In particular, 2-methyl-DOL (2MDOL) and 4-methyl-DOL (4MDOL) undergo electron-induced ring-opening reactions, but with markedly different outcomes [Figure 8C][137]. DFT analysis reveals that 4MDOL exhibits greater ring strain and stronger hyperconjugation, which facilitate more efficient anionic polymerization into longer-chain oligomers, resulting in a highly crosslinked and elastic SEI matrix. In contrast, 2MDOL exhibits lower ring strain and weaker hyperconjugation, producing shorter polymer chains and a less cohesive SEI structure[137]. The SEI derived from 4MDOL exhibits superior nanophase separation, comprising flexible ether-rich domains and discrete LiF clusters, which effectively buffer Si volume changes and enhance interfacial stability.

In addition to constructing inorganic-based SEI by decomposition of electrolyte additives, SEI engineering via direct decomposition of electrolyte solvent is also considered an effective strategy[138]. Adopting tetrahydrofuran (THF) and fluorinated co-solvents such as 2-methyltetrahydrofuran (2-MeTHF) or Bis(2,2,2-trifluoroethyl) ether (BTFE) enables selective formation of LiF-based SEI due to their reductive instability at low potentials[139,140]. In particular, fluorinated solvents undergo preferential electron-induced cleavage of C-F or P-F bonds near the anode surface, leading to the localized generation of fluoride species. These species readily react with Li^+ to precipitate LiF at the interface. The solvent decomposition pathway competes with salt-derived SEI formation and can dominate in low dielectric media or localized high-concentration environments, yielding a uniform and robust interphase. Instead of controlling electrolyte decomposition to induce selective interphase formation, selective SEI dissolution was introduced as a new strategy for designing desirable SEI. By incorporating a high donor-number solvent, γ-butyrolactone (GBL), into the electrolyte, soluble organic SEI species such as lithium ethylene dicarbonate (LEDC), lithium ethyl carbonate (LEC), and lithium fluorophosphates undergo gradual dissolution [Figure 8D][43]. This process shifts the dynamic equilibrium at the interface, driving the transformation of the SEI composition toward thermodynamically stable, insoluble inorganic species such as LiF. Additionally, the removal of low-modulus organic phases suppresses interfacial creep and fracture, while exposing reactive sites that promote further inorganic deposition. The dissolution-driven evolution results in a mechanically coherent and ionically conductive SEI tailored by interfacial solubility control rather than direct decomposition pathways.

Across carbonate and non-carbonate electrolyte components, SEI regulation differs in how electrolyte species are delivered to the anode surface, decomposed, and retained within the near-surface interfacial region[141]. Carbonate-based components generally couple electrolyte reduction with SEI construction near the anode surface, as their decomposition products are retained, polymerized, or incorporated into LiF-rich,

polycarbonate-rich, or compositionally graded interphases[134]. Non-carbonate components can redistribute this sequence between the near-surface electrolyte and the growing SEI by regulating Li^+ coordination, anion participation, reductive decomposition, or fluorinated solvents, ring-opening polymerization, or selective dissolution[43,142]. Accordingly, SEI formation is governed by the identity of the initially reduced species, the local availability of reactive electrolyte species, and the retention or removal of decomposition products within the interphase. Such spatially differentiated control is important for Li-alloying anodes, where SEI chemistry must remain coupled with interfacial continuity during repeated volume changes

To mechanically stabilize and achieve rapid Li^+ transportation, introducing heteroatom-based compounds into the SEI layer is considered an effective strategy. For instance, sulfur-containing additives such as 1,3-propane sultone (PS) decompose to generate Li_2SO_3 and Li_2S upon electrochemical reduction, which contribute to a flexible yet robust SEI architecture[143]. These sulfur-rich species provide enhanced mechanical adaptability during Si volume fluctuations and facilitate Li^+ transport through the SEI. In particular, SiO_x-based anodes benefit from early passivation by sulfur-containing additives, which selectively reduce at lower potentials, suppressing further solvent decomposition[144]. However, conventional approaches for designing sulfur-containing additives often relied on multistep or complicated synthesis steps, which were sophisticated and unsuitable for industrial scaling. To address this, recent work suggested a sulfur atom-mediated domino reaction-derived SEI layer. As illustrated in Figure 8E, the introduction of elemental sulfur (S_8) initiates a sequence of reduction-triggered reactions known as a domino process[145]. Upon early-stage reduction, S_8 decomposes to generate reactive sulfur-centered intermediates, which undergo subsequent transformation into alkyl sulfate and sulfonate species. These intermediates readily graft onto the Si surface or pre-existing SEI components. In parallel, conventional solvents such as FEC and EC are reduced at lower potentials, contributing LiF and polycarbonate components, respectively. The resulting gradient interphase exhibits a sulfur-rich outer layer comprising Li-alkyl sulfates and elastic polymeric domains that provide mechanical compliance, while an inner region rich in LiF ensures dense ionic blocking. Such sulfur-mediated layering imparts high interfacial elasticity, as confirmed by a uniform increase in Derjaguin-Muller-Toporov (DMT) modulus measured by atomic force microscopy (AFM). Additionally, the dense inner structure and elastic outer layer mitigate the growing excessive SEI layer; the domino-reaction-induced SEI layer exhibits uniform and thin morphology in the TEM image.

Inorganic-based electrolyte additive

As well as organic compounds used for electrolyte additives, inorganic additives (salt, metal-ligand material, siloxane) were also explored to enhance the mechanical robustness and chemical stability of SEI[146]. In contrast to conventional organic additives, which typically generate polymeric or carbonate-based SEI components through electrochemical decomposition, metal-containing additives offer distinct mechanistic advantages by participating in the formation of inorganic-rich interfacial layers. Specifically, these additives can decompose metal fluorides, oxides, or silicates, which can serve as thermodynamically/mechanically stable and ionically conductive SEI constituents. In certain decomposition routes, metal ions can also be incorporated into the SEI, forming metal-doped or alloy-derived interphases that further suppress interfacial degradation[147]. These inorganic phases act as effective physical barriers against continuous electrolyte decomposition as well as facilitate more uniform Li^+ transport across the electrode-electrolyte interface, thereby improving both the electrochemical stability and the mechanical robustness of the SEI under the large volume fluctuations. Thereby, metal-based additives have emerged as promising candidates for stabilizing high-capacity anode materials.

Salt-based additives were employed to enable facile decomposition and direct integration into the SEI structure and to enhance its stability and chemical functionality. Heteroatom boron-nitrogen-containing salts act as effective precursors for artificial SEI formation, improving interfacial crack prevention and ion

transport. Among boron-containing salts, lithium bis(oxalato)borate (LiBOB) and lithium difluoro(oxalato)borate (LiDFOB) decompose preferentially at higher potentials than conventional electrolyte solvents, yielding borate, oxalate, and fluoroborate fragments. These decomposition products form a crosslinked, inorganic-rich interphase composed of Li-O-B and B-F networks. Such structures provide high chemical stability, mechanical rigidity, and resistance to further electrolyte reduction[148]. For instance, lithium metaborate ($LiBO_2$) and lithium tetraborate (LiB_4O_7) exhibit a Young's modulus 2 times higher than that of LiF and a lower activation energy for Li^+ transportation, favorable for high-capacity anodes[149]. In particular, chemical reduction of LiDFOB promotes the formation of lithium oxalate (Li_2CO_3) and crosslinked oligoborate-based polymers. XPS analysis of SEI formed in LiDFOB-containing electrolytes reveals a higher ratio of B-F to B-O bonding states, consistent with polymeric boron-containing structures and suppressed inorganic LiF content. This composition yields a more elastic and stress-buffering interphase that accommodates large volume changes while limiting electrolyte decomposition[150]. On the other hand, nitrogen-containing salts such as lithium nitrate ($LiNO_3$) decompose to generate nitrogen-rich species, including lithium nitride (Li_3N) and NO_x fragments[151]. Li_3N is an effective electron insulator that suppresses further electrolyte decomposition while enhancing Li^+ transport across the SEI, thus effectively mitigating continuous electrolyte breakdown. Also, the combined use of B- and N-based salts enables the formation of a conformal and ion-conductive SEI that regulates interfacial reactions and improves long-term stability.

Instead of Li-based salts, multivalent metal (K, Ca, Mg)-based salts have also been reported for incorporating metal components into the SEI[152]. Multivalent metal salts such as Magnesium(II) Bis(trifluoromethanesulfonyl)imide ($Mg(TFSI)_2$) and Calcium(II) Bis(trifluoromethanesulfonyl)imide ($Ca(TFSI)_2$) contribute to interfacial and bulk stabilization of Si anodes through distinct mechanisms. Ca^{2+} reacts with fluorinated species in the electrolyte to form Calcium fluoride (CaF_2), which precipitates as a compact and chemically stable surface layer. This CaF_2-based SEI acts as a physical barrier that suppresses further electrolyte decomposition and inhibits Li loss during storage. Mg^{2+} shows lower surface reactivity but participates in structural stabilization by partially incorporating into the Si during lithiation. This incorporation promotes the formation of Li-Mg-Si ternary phases, which reduce local lattice distortion and enhance the mechanical stability of lithiated Si. Collectively, these processes result in a thinner and more uniform SEI layer that contains Ca and Mg metal, both enhancing cycle life and reducing undesirable side reactions Figure 8F. Additionally, the combination of surface passivation by Ca-containing SEI and bulk phase stabilization by Mg incorporation leads to improved long-term calendaring aging stability even at the elevated temperatures, particularly under extended voltage hold conditions[152,153]. Beyond compositional SEI control via salt additives, modifying the surface work function of Si electrodes has been reported as an effective strategy to regulate SEI. The native SiO_2 surface of Si-based anodes exhibits a high work function (~6.24 eV), limiting initial electrolyte reduction and SEI formation. The addition of indium acetate (InAc) additives lowers the local work function through surface adsorption and partial In deposition, thereby promoting faster and more uniform EC reduction. Partial lithiation of In to Li-In phases also serves as an electron sink, enhancing reduction kinetics. Time-of-Flight Secondary Ion Mass Spectrometry (TOF-SIMS) and XPS confirm that InAc enables compact SEI formation, suppressing uncontrolled electrolyte decomposition during cycling and storage.

Since the exhibition of high compatibility with Si due to its repeated Si-O-Si structure, siloxane-based compounds demonstrate particularly notable effects on high-capacity anodes, especially in Si anodes. Fluorinated cyclic siloxanes have been reported as effective interfacial modifiers for Si/C electrodes[154]. Upon electrochemical reduction, they can undergo ring-opening reactions and subsequently condense with surface hydroxyl groups or native silicon oxide (SiO_x). This process leads to the formation of a siloxane-oxide hybrid network that becomes integrated into the SEI. During this transformation, fluorine atoms are released and can form LiF. Rather than creating a continuous LiF film, these reactions tend to yield LiF domains that are

locally distributed. The resulting SEI consists of both organic siloxane-derived components and inorganic species such as Si-O-Si and LiF, leading to a heterogeneous and multiphase interfacial structure. This SEI has been described as exhibiting gradients in composition and mechanical properties, with softer organic regions near the electrolyte and stiffer, inorganic-rich regions closer to the electrode surface[155]. These gradients may contribute to stress redistribution and suppression of mechanical degradation during volume changes of the Si electrode. Such interfacial engineering strategies demonstrate the tunability of silane-derived SEI architectures in both chemical composition and mechanical performance. Notably, (3-Aminopropyl)triethoxysilane (APTES) forms a surface-bound layer via hydrolysis and condensation, introducing C-N bonding and thermally stable SiO_2 domains, which suppress lithium hexafluorophosphate ($LiPF_6$) hydrolysis and minimize carbonate solvent decomposition at elevated temperatures[85]. On the other hand, trialkoxyvinylsilane undergoes reductive decomposition prior to bulk solvent breakdown, forming robust Si-O and Si-F-bonded interphases that suppress solvent consumption and reinforce the SEI against volume fluctuations of Si. TOF-SIMS analysis revealed that silane-derived fragments and localized inorganic species such as LiF and Li_xSiO_y exist within the SEI, suggesting a composite and interpenetrating network. Overall, while these diverse inorganic-based electrolyte additive strategies present challenges regarding non-uniform dispersibility or the potential for excessive decomposition, they offer the advantage of enabling precise control over SEI composition and structure, which can be fundamentally modulated through chemical decomposition reactions. Such mechanistically tailored interphases offer a versatile framework to improve the interfacial structure durability and electrochemical stability of high-capacity anodes under extreme cycling conditions. To achieve ultimate interfacial durability in high-capacity Si anodes, the design of electrolyte additives must evolve toward constructing a spatially graded, organic-inorganic hybrid SEI. This multidimensional approach leverages inorganic species to form a rigid, ion-conductive inner barrier, while utilizing organic/polymeric networks as an elastic outer layer to dynamically dissipate stress during severe volume fluctuations.

Artificial solid electrolyte interphase design by functional material coating

Carbon coating strategies

Carbon coating is a simple but effective method for stabilizing the interface of a high-capacity anode by enhancing both mechanical strength and electron-transport properties[156]. Various carbon materials are employed as coating materials, while the degree of carbonization and thickness of the carbon coating critically affect interfacial properties and electrochemical performance of the anode. For instance, heat treatment temperature directly influences carbon ordering, as low-temperature carbonization results in an amorphous carbon structure, while high-temperature treatment induces the formation of more graphitized, ordered carbon layers. Consequently, as shown in Figure 9A, amorphous carbon significantly reduces the internal resistance of the electrode both in the SEI layer and the charge transfer region during cycling. These results indicate that the elasticity and lower Young's modulus of amorphous carbon effectively release inner stress and stabilize SEI[157]. Additionally, while excessive carbon coating impedes electron conductivity due to a disordered isotropic structure, a proper carbon coating layer exhibits increased conductivity and effectively inhibits excessive SEI layer generation and assists in the formation of an inorganic-based SEI layer[158,159].

Unlike conventional carbon coating, graphene coating on the high-Li stoichiometric anode has been researched due to the high electronic conductivity and mechanical properties of graphitic carbon[160]. Coated graphene supports the intrinsic low conductivity of the Li-alloying anode, which leads to stable SEI generation at the initial cycle, and its high mechanical modulus prevents the SEI layer from cracking[161]. When graphene nanosheets are applied to tin, graphene additionally buffers the large inner stress and maintains continuous electron pathways, thereby mitigating pulverization and preserving interfacial integrity, while their high surface area and lithiophilic defect sites promote uniform Li nucleation and deposition[162]. However, due to defect sites in graphene, the layered structure easily collapsed, and fractures

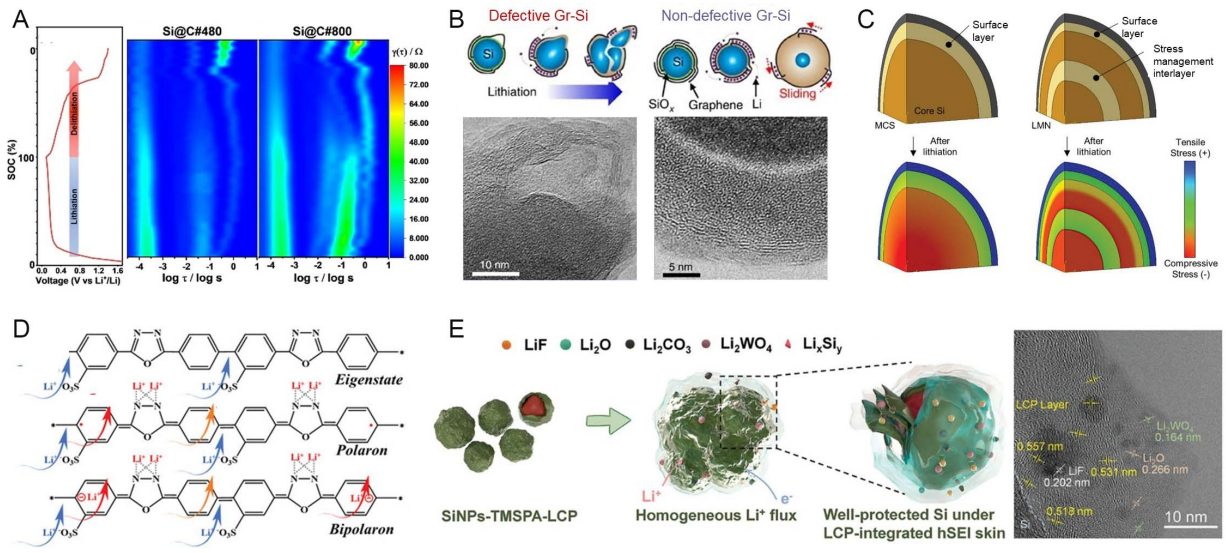

Figure 9. (A) DRT function for the Si@C electrode, which was carbonized at different temperatures. Reproduced with permission from ref.[157]. Copyright 2022, American Chemical Society. (B) Schematic images and TEM images of lithiated Gr-Si NPs for both non-defective and defective graphene encapsulation. Reproduced with permission from ref.[163]. Copyright 2015, Author(s), licensed under a Creative Commons CC BY license. (C) Schematic cross-sectional view showing hoop stress before cycling and after lithiation by finite element modeling (FEM) calculation during lithiation. Reproduced with permission from ref.[178]. Copyright 2019, Wiley. (D) Structural change of Li doping into conductive polymer coating layer. Reproduced with permission from ref.[188]. Copyright 2023 Wiley. (E) Integrating SEI into the conductive coating layer enhanced structural stability. Reproduced with permission from ref.[187]. Copyright 2022, Wiley.

of the coating layer occurred due to dramatic volume expansion. To address this limitation, a direct chemical vapor deposition approach was developed to grow defect-free and SiC-free graphene layers on the Si surface Figure 9B. By introducing carbon dioxide (CO_2) as a mild oxidant, interfacial reactions between Si and carbon precursors were suppressed, forming uniform graphene layers parallel to the Si substrate[163]. These defect-free layers accommodate the ~300% volumetric expansion of Si through a sliding mechanism between adjacent layers that consequently leads to non-defective Gr-Si exhibiting stable layering morphology. Further research was achieved by introducing covalent bonding between graphene and Si[164]. This approach strengthens interfacial adhesion while maintaining dynamic interlayer mobility. The result is a mechanically robust yet adaptive shell that effectively disperses internal stress and mitigates SEI cracking. Collectively, these strategies demonstrate that controlling the structural integrity of graphene and its interaction with Li-alloying anodes are crucial to stabilizing the electrode-electrolyte interface under repeated cycling conditions.

Additionally, carbon coating effectively suppresses the unstable side reaction of the Si anode during calendar aging[165]. This protective layer minimizes direct contact between the lithiated Si and the electrolyte, thereby hindering undesired interfacial reactions such as $LiPF_6$ decomposition and subsequent formation of LiF, $Li_xPO_yF_z$, or Li_2CO_3[166]. Moreover, the carbon layer interrupts the internal electron-conduction pathway from Li_xSi to nearby graphite or electrolyte components, blocking local electron transfer that otherwise triggers thermodynamically favorable electrolyte reduction. This suppression delays the onset of side reactions that are activated by increased storage temperature and reduced energy barriers in unprotected Si[167]. Mechanistically, the carbon coating increases the effective energy barrier (ΔE_a) for electron tunneling and solvent decomposition, thus reducing the likelihood of SEI thickening and continuous electrolyte consumption. By stabilizing interfacial energetics and limiting charge carrier leakage, the carbon layer passivates the surface of Li_xSi and mitigates the spatially inhomogeneous interphase growth that typically accelerates during prolonged rest.

Inorganic coating strategies

Inorganic coatings have emerged as one of the most effective strategies to stabilize Si anodes. These coatings act as mechanical buffers, chemical barriers, and ion-conductive layers, thereby preserving electrode integrity and extending cycle life. The mechanisms of their function depend on the coating material's chemical composition, structural properties, and interaction with Li and electrolyte components. Metallic coatings such as Ni, Cu, Fe, and Ag form conductive shells around Si particles, promoting electron transport and mechanical confinement[168]. For instance, Ni coatings undergo interfacial alloying to form NiSi phases via thermal diffusion, which not only serve as conductive anchors but also generate chemically bonded interfaces that resist delamination[169]. Cu, while electrochemically inert, offers ductility and forms conductive networks that facilitate Li^+ flux and buffer internal stress[168]. Ag coatings also significantly improve conductivity and reduce SEI reformation[170].

In contrast, metal oxides such as Al_2O_3, TiO_2, and SiO_2 form passivation layers with high mechanical strength and chemical stability of the Li-alloying anode interface[171]. Al_2O_3 and ZnO, with their Lewis acid-base characteristics, can scavenge HF and block electron tunneling, thereby preventing electrolyte decomposition while maintaining Li^+ permeability through nanochannels[172]. Moreover, their high Young's modulus allows them to confine Si expansion, while their porous morphology enables Li diffusion. TiO_2-based coatings demonstrate dual advantages of being highly mechanically robust and chemically stable in Li environments[173]. In core-shell Si@TiO_2 composites, the hollow void between the Si core and TiO_2 shell accommodates volume change, while the outer TiO_2 shell suppresses electrolyte intrusion and SEI instability[174]. Moreover, TiO_2 can suppress oxygen evolution from the Si-based anode during overcharging and enhance interfacial stability. These coatings also regulate interfacial Li transport and stress buffering, thereby mitigating fracture-driven delamination and preserving both structural and electrochemical coupling across the interface. Further, composite designs incorporating Si embedded in SiO_x matrices offer synergistic benefits by combining high electrochemical activity with structural integrity by absorbing internal stress and preserving structural cohesion. The oxide matrix serves as a robust scaffold that preserves electrical connectivity and mitigates mechanical stress during volume fluctuations[175]. A particularly promising direction involves forming artificial SEI layers using SiO_x coating. For instance, engineered Si@SiO_x structures incorporate a sacrificial SiO_x shell that reacts with Li to form a stable interphase composed of Li_2O and lithium silicates (Li_4SiO_4, Li_2SiO_3)[176]. These compounds form a mixed ionic-electronic conductive network that buffers stress and reduces interfacial impedance. Studies have shown that the optimal thickness of the SiO_2 layer provides a good balance between mechanical strength and Li^+ permeability[177], while excessively thick layers hinder Li^+ diffusion, and too thin layers fail to suppress undesirable SEI formation. Furthermore, the multi-layer lamellar structure of the SiO_2 layer effectively acts as a stress-dissipating layer that relieves the inner stress of the active material Figure 9C[178]. Another critical inorganic coating is silicon oxycarbide (SiOC), which is typically formed through the pyrolysis of siloxane-based precursors. SiOC consists of an amorphous Si-O-C glassy matrix embedded with free carbon, enabling it to participate in Li storage while simultaneously functioning as a mechanically resilient binder[179]. By bridging adjacent SiNPs and accommodating their volume fluctuations during cycling, SiOC enhances structural integrity. Furthermore, its dense and chemically inert nature suppresses electrolyte penetration and facilitates the formation of a partially self-healing SEI, contributing to long-term interfacial stability.

Functional organic material coating strategies

In recent work, functional polymer coatings have been widely introduced to modify the interface of high-capacity anodes. Non-conductive polymers such as poly(methyl methacrylate) (PMMA) serve as artificial SEI by physically isolating the highly reactive Si surface from LEs. These coatings suppress continuous electrolyte decomposition and inhibit the formation of thick, resistive interphases. PMMA provides a thin, elastic film capable of coordinating solvated Li^+ through ester groups, promoting ionic conductivity while

accommodating the large volume changes of Si[180]. In parallel, Li-conducting covalent organic frameworks (COF) have demonstrated promise as pre-defined artificial interphases[181]. These COF coatings possess highly ordered channels that facilitate directional Li^+ conduction while simultaneously excluding solvent molecules. By regulating Li^+ flux and shielding the Si surface from direct exposure to the electrolyte, the COF layer promotes the formation of stable SEI components such as LiF and Li_xSiO_y and suppresses excessive decomposition of carbonate and phosphate solvents. Electrochemical measurements have confirmed the absence of initial cathodic decomposition peaks and improved impedance profiles, indicating effective interfacial passivation and controlled SEI evolution[182]. These ionically selective and mechanically robust interphases significantly improve the stability of the electrolyte interface and minimize the dynamic instability commonly observed in conventional SEI layers.

Functional polymer coatings offer additional advantages by integrating mechanical compliance with simultaneous ion and electron transport[183,184]. Such materials utilize conjugated backbones and polar side groups to provide Li coordination, redox activity, and charge delocalization. For instance, *in situ*-polymerized conducting hydrogels have also demonstrated conformal coating of SiNPs, where the hydrophilic polymer matrix swells in the presence of electrolyte to promote Li^+ conduction while buffering mechanical stress. The polymeric network functions as a dual ion-conductive and protective barrier that regulates interfacial reactions and delays SEI growth. Additionally, π-conjugated polymers such as poly(thiophene) or poly(3,4-ethylenedioxythiophene) can form polaron or bipolaron states, which can coordinate with Li^+ during cycling, enhancing Li^+ transport while maintaining electronic connectivity across the interphase Figure 9D[185,186]. These features allow the conductive coating to act not only as a protective layer but also as a dynamic ion-conductive matrix. Also, self-layered conductive polymer coating strategies by introducing tungstic acid can integrate SEI components such as LiF and Li_2WO_4. Further, incorporating SEI into the conductive layer leads to homogeneous Li^+ flux and contributes to the formation of uniform, chemically stable hybrid interphases Figure 9E[187]. These layers mitigate local overpotentials and block direct electrolyte contact, resulting in well-protected Si surfaces with minimized interfacial degradation. Similarly, sponge-like porous conductive polymer coatings leverage their interconnected pore structure to enhance ion diffusion, while the elastic, conductive layer accommodates Si expansion and maintains electrochemical integrity. These coatings enable spatially uniform SEI formation and reduce impedance buildup during long-term cycling[188]. Collectively, conductive polymer coatings represent a promising strategy for realizing stable and efficient Si anodes by unifying structural adaptability, ionic selectivity, and electrochemical activity within a single interfacial layer.

Conductive polymer binders such as polyfluorene-based copolymers and their thermally hierarchical ordered structure (HOS) actively regulate the SEI formation process by modulating both interfacial chemistry and Li^+ transport. The polar side chains and conjugated backbone of conductive polymer binder facilitate strong adhesion to native SiO_x and allow for efficient ionic conduction across the interface[189]. Upon thermal annealing, the binder undergoes a hierarchical π-π stacking transition into an ordered structure, which reinforces interfacial mechanical stability and promotes selective ion and solvent transport[190]. This ordered arrangement suppresses uncontrolled decomposition of carbonate solvents and directs SEI evolution toward more stable, inorganic-rich compositions. Specifically, HOS inhibits the excessive generation of Li_2CO_3 and $ROCO_2Li$ while enriching the SEI with LiF and Li_xSiO_y components, as confirmed by XPS. This results in a thinner, denser, and more ionically conductive SEI that effectively suppresses parasitic reactions and enhances long-term cycling. Additionally, modulating the chemical structure of the binder can directly influence SEI chemistry by the spontaneous decomposition of the binder itself[191]. DFT calculations reveal that the LUMO energy level of the fluorinated binder lies below that of ethylene carbonate (EC), diethyl carbonate (DEC), and even their complexes with $LiPF_6$, inducing preferential reduction at the binder site during initial lithiation. In particular, sulfonyl fluoride ($-SO_2F$) groups in the fluorinated binder act as

electron-accepting moieties that undergo reductive cleavage at low potentials, releasing F^-, which subsequently reacts with Li^+ to form LiF. This preferential reduction of the binder occurs before electrolyte solvent decomposition, enabling direct LiF formation through the targeted cleavage of F-containing bonds within the binder structure. Molecular dynamics simulations confirm that the binder-integrated SEI exhibits localized LiF clusters with minimal organic content. Unlike traditional SEI derived from random solvent decomposition, this binder-directed mechanism yields chemically homogeneous and mechanically robust interphases with enhanced ionic conductivity, even under lean-electrolyte additive conditions. In conclusion, the rational design of functional coating materials must converge toward a dual-adaptive interfacial strategy: ensuring structural resilience to withstand severe volume fluctuations, while simultaneously governing SEI evolution through intentional electronic passivation and preferential sacrificial reduction [Table 3].

Solid-state electrolytes: reaction-induced interphases

Interfacial instability of high-capacity anode in the solid-state electrolyte system

Despite the promising gravimetric and volumetric capacities of Li-alloying anodes, their application in ASSBs remains hindered by severe interfacial instability, while SSEs offer several intrinsic advantages. Their solid nature enables physical confinement of active materials, which can assist in suppressing the extreme (~300%) volume expansion during operation and mitigating mechanical pulverization/delamination. In addition, the absence of volatile organic solvents enhances thermal stability and safety. While the ionic conductivity of many SSEs tends to be lower than that of conventional LEs, sulfide-based SSEs exhibit room-temperature Li^+ conductivities on the order of 10^{-3} to 10^{-2} S cm^{-1}, approaching that of LEs[70]. These attributes make SSEs especially promising for high-capacity Li-alloying anodes in next-generation ASSBs. Nevertheless, despite these advantages, Li-alloying anodes suffer from problems, such as the formation of a space-charge layer due to differences in chemical potential and carrier density between the contacting phases. This electrostatically driven region redistributes mobile ions, creating local deviations in stoichiometry and shifting the onset potentials for interfacial redox reactions. Over repeated cycling, such a non-uniform ion distribution can intensify interfacial impedance growth, promote uneven lithiation, and interact synergistically with the mechanical stress field generated by large volume changes[40]. Moreover, Si and Sb anodes, for example, the alloying/dealloying process often leaves the particles in an unrecovered morphology after delithiation, forming void-shell structures that elevate the charge transfer resistance[192]. The repeated contraction not only generates mechanical stress but also accelerates interfacial chemical degradation, as the evolving fracture network exposes fresh reactive surfaces to the SSE, promoting continuous interphase growth and altering its composition over cycling[193]. As illustrated in Figure 10A, XPS analysis of Si anodes cycled in sulfide-based SSEs reveals dynamic changes in chemical states upon operation[194]. During the first lithiation, the Si 2p spectra indicate a progressive conversion from native SiO_2, Li_4SiO_4-like silicates, and Li_xSi alloys. Simultaneously, the Li 1s and O 1s spectra reflect the accumulation of Li_2CO_3 and Li-silicate species, suggesting ongoing interfacial reactions between SSEs and the reduced Si surface. Upon delithiation, only partial reversibility is observed, with residual Li-silicate phases persisting at the interface, thus contributing to interfacial irreversibility and impedance growth.

Figure 10B further delineates how these reactions translate into structural degradation over repeated cycling[192]. In the pristine Si/SSEs interface, lithiation-induced expansion of Si particles (~300%) exerts mechanical stress on the rigid SSEs matrix, leading to crack formation and loss of interfacial contact. This mechanical detachment impedes both electronic and ionic percolation paths, causing non-uniform lithiation and eventual cell failure. The use of Si-SE-C composites has emerged as a strategy to mitigate this issue by incorporating electronically conductive carbon and elastically compliant binders. These composite frameworks buffer volume change and preserve the electrode-electrolyte interface. During lithiation, such architectures exhibit stable Li^+ conduction channels and enable more homogeneous Li-Si alloying[192]. Upon delithiation, the structural integrity of the interface is better maintained, suppressing void formation and

Table 3. Electrochemical performance comparison of interfacial engineering strategies across different spatial domains of alloying-type anode

SEI formation layer													Electrode subsurface & surface									Spatial range
Binder modification	**Surface modification (metal)**	**Surface modification (organic)**	**Nanostructuring**	**Surface modification (organic)**	**Surface modification (organic)**	**Surface modification (ceramic)**	**Surface modification (carbon)**	**Electrolyte solvent**	**Electrolyte additive**	**Electrolyte additive**	**Electrolyte solvent**	**Electrolyte solvent**	**Electrolyte additive**	**Electrolyte additive**	**Prelithiation**	**Prelithiation**	**Prelithiation**	**Prelithiation**	**Surface nitridation**	**Surface fluorination**	**Surface nitridation**	**Surface fluorination**	**Engineering method**
Si/Gr@G-C	HT-Si@Cu	Si@COF	N-PSi@C	SiNPs-TMSPA-LCP	Si-bPOD	LMN(Si/SiO_x/Si/SiO_x/C)	Gr-Si	μSi	Si	Si@C	SiMP	Si/Gr	Si-C	SiNP	c-SiO_x	μSi	P/C composite	L1Si	SCN1	Si@AlFHQ-20	NGP-Si	SiO_x/vG-F	Active material
1.0 M $LiPF_6$ in EC:DMC:EMC (1:1:1) + 5% FEC	1.0 M $LiPF_6$ in EC/DMC (1:1) + 10% FEC	1.3 M $LiPF_2$ in EC/DEC (1:1) + 10% FEC	1.3 M $LiPF_6$ in EC/DEC (3:7) + 10% FEC	1.0 M $LiPF_6$ in EC/DEC (1:1) + 10% FEC + 1% VC	1.0 M $LiPF_6$ in EC/DMC (1:1) + 5% FEC	1 M $LiPF_6$ in EC/EMC/DEC (3:5:2) + 10% FEC + 0.2% $LiBF_4$ + 0.5% VC + 3% SN + 1% PS	1.0 M $LiPF_6$ in EC/DEC/FEC (2:6:2)	1.0 M $LiPF_6$ in FEC/SL/TTE (2:6:2)	1.2 M $LiPF_6$ in EC/EMC (3:7) + 3% FEC + 0.03M $Mg(TFSI)_2$ + 0.07M $Ca(TFSI)_2$	1.0 M $LiPF_6$ in EC/DEC/EMC (1:1:1) + 10% FEC + 0.2 mg mL^{-1} elemental sulfur	1.0 M $LiPF_6$ in GBL/DEC/FEC (45:45:10)	LiFSI/4MDOL/TTE(1:2.6:3)	1.15 M $LiPF_6$ in EC/EMC (3:7) + 5% FEC + 0.5% VC + 0.5% DMVC-OCF_3 + 0.5% DMVC-OTMS	1.0 M $LiPF_6$ in EC:DEC:EMC (1:1:1) + 10% FEC	1.0 M $LiPF_6$ in EC/DEC (1:1) + 5% FEC	1.0 M $LiPF_6$ in EC/DEC (1:1) + 10% FEC	1.3 M $LiPF_6$ in EC/DEC (1:1) + 10% FEC + 2% VC	Li_6PS_5Cl	1.3 M $LiPF_2$ in EC/DMC (1:1)	1.0 M $LiPF_6$ in EC:DEC:DMC (1:1:1) + 10% FEC	1.3 M $LiPF_6$ in EC/DEC (3:7) + 10% FEC	1.0 M $LiPF_6$ in EC:DEC:DMC (1:1:1) + 5% FEC	Electrolyte
60:20:20	60:20:20	80:10:10	-	80:10:10	80:10:10	80:10:10	80:20:0	60:20:20	80:10:10	96:3:1	80:10:10	85:13:2	96:3:1	70:20:10	80:10:10	70:10:20	70:15:15	-	80:10:10	70:10:20	60:20:20	80:10:10	Electrode composition
5	2	3	2.7	3	3	2	3	4.3	3.5	3	4	1.5	3.2	3	2.36	2.4	0.7	10	2.5	3.84	2.3	-	Areal capacity (mAh cm^{-2})
SiO_x/Gr@G-C||NCM811	Half-cell	Half-cell	N-PS@C||LFP	SiNPs-TMSPA-LCP||NCM811	Si-bPOD||NCM811	Half-cell	Half-cell	μSi||NCA	Half-cell	Si||LFP	Si||NCM811	Si/Gr||NMC622	Si-C||NCM811	Half-cell	Prelithiated-c-SiO_x||NCA	Prelithiated-μSi||LFP	Prelithiated-P/C||$LiCoO_2$	L1Si||$LiCoO_2$	Half-cell	Si@AlFHQ-20||$LiCoO_2$	Half-cell	SiO_x/vG-F||NMC811	Cell configuration
77.8%@200th	85.7%@200th	84%@100th	88%@150th	66%@45th	83.3%@50th	90%@100th	91%@100th	81%@200th	50%@100th	94.4%@100th	83.7%@150th	78.4%@250th	81.5%@400th	73.4%@100th	61.6%@100th	77%@200th	90.9%@2,000th	73.8%@1,000th	59%@50th	70.1%@100th	78.6%@200th	86.4%@200th	Capacity retention
0.2 C	1,000 mA g^{-1}	1,000 mA g^{-1}	5C	0.2 C	0.2 C	0.5 C	0.5 C	0.2 C	0.5 C	0.5 C	0.2 C	0.5 C	1 C	0.5 C	1 C	0.33 C	1 C	5 mA cm^{-2}	600 mA g^{-1}	0.2 C	3,000 mA g^{-1}	200 mA g^{-1}	Currerent density
[183]	[168]	[181]	[156]	[187]	[188]	[178]	[160]	[135]	[152]	[145]	[43]	[137]	[134]	[123]	[113]	[114]	[110]	[109]	[108]	[105]	[107]	[103]	Ref.

delamination. This behavior highlights the chemo-mechanical mismatch between expanding Si and rigid SSEs as a primary cause of capacity fading in ASSBs. The formation of interphases such as Li_4SiO_4 and Li_xSi-S compounds can passivate the interface, but often at the cost of increasing interfacial resistance. Moreover, the low fracture toughness of many sulfide-based SSEs like Li_6PS_5Cl exacerbates mechanical failure, where localized interfacial pressure during cycling exceeds the yield strength of SSEs, leading to irreversible morphological degradation.

Influence of chemical degradation in the solid-state electrolyte system

Chemical degradation at the alloy anode/SSE interface heavily depends on the specific chemistry of the solid electrolyte[40]. In polymer electrolytes, the highly reducing anodes decompose both the polymer matrix and the lithium salt, generating polyether fragments, RoLi species, and sulfonyl derivatives[195]. Although the compliant nature of the polymer phase can partially accommodate volume changes to maintain interfacial contact, these labile products form a disordered interphase that continuously increases impedance during cycling. Sulfide electrolytes are particularly susceptible to reduction by Li-rich alloy phases, yielding products such as Li_2S, Li_3P, and Li_xPS_y[196]. While these species can initially passivate the interface, their progressive accumulation severely impedes Li^+ transport. In contrast, oxide electrolytes exhibit higher intrinsic electrochemical stability; however, their rigid ceramic nature and thermodynamic mismatch with Li-rich alloy surfaces promote the formation of poorly conformal, insulating products like Li_2O, LiOH, Li_2CO_3, and lithium silicates[73]. Therefore, polymer, sulfide, and oxide SSEs must be differentiated not only by their bulk ionic conductivity but also by the chemical composition, mechanical traits, and transport resistance of their respective interfacial products.

Among these systems, sulfide electrolyte represents a key case where chemical degradation and mechanical instability are strongly coupled. Notably, recent studies have demonstrated that, contrary to earlier expectations, incorporating SSEs and conductive carbon directly into Si anodes can trigger interfacial instability. During lithiation, the Si undergoes alloying to form Li_xSi, which exhibits strong reducing characteristics. This highly reactive alloy phase initiates the electrochemical

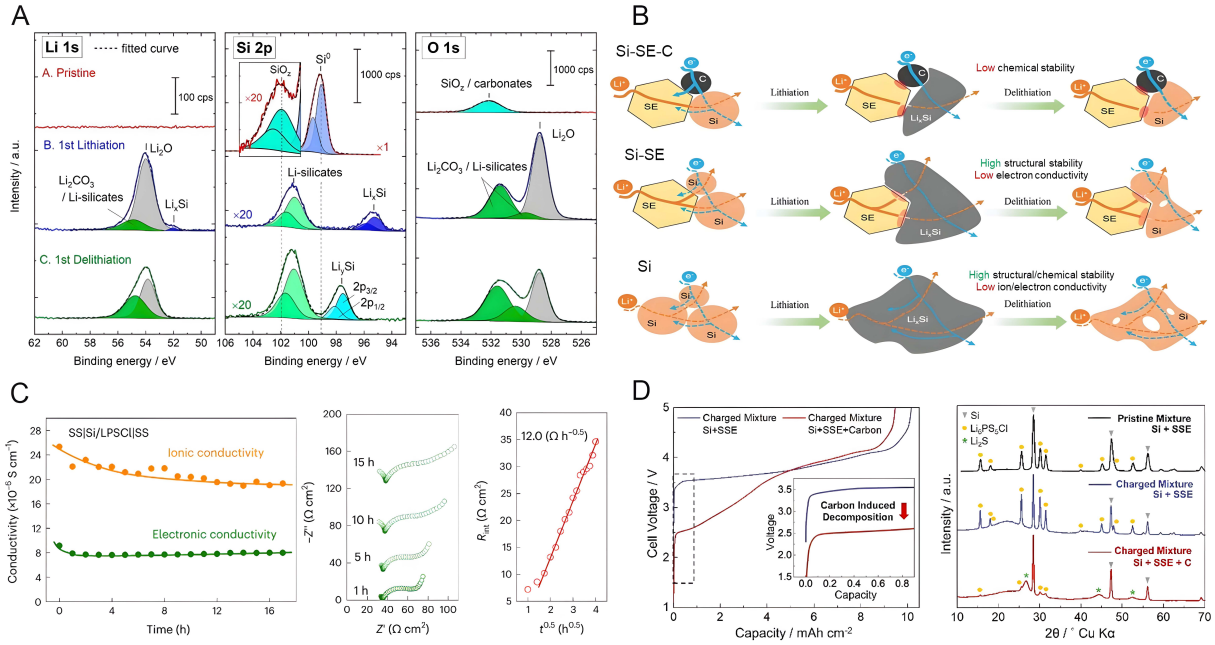

Figure 10. (A) XPS spectra of ASSB Si electrode at the pristine electrode, after first lithiation, and after first delithiation. Reproduced with permission from ref.[194]. Copyright 2020, American Chemical Society. (B) Pros and Cons of the combination of active material/carbon/electrolyte in ASSB. Reproduced with permission from ref.[192]. Copyright 2023, Wiley. (C) Side reaction between carbon additive and solid electrolyte. Reproduced with permission from ref.[40]. Copyright 2024, Author(s), licensed under a Creative Commons CC BY license. (D) Side reaction between Si active material and solid electrolyte. Reproduced with permission from ref.[4]. Copyright 2021, The American Association for the Advancement of Science.

decomposition of sulfide-based SSEs, particularly LPSCl[40]. The reduction is driven by Li atoms migrating from the Li_xSi to the electrolyte interface, where they break the P-S and S-S bonds in the PS_4^{3-} and S^{2-} units Figure 10C. As a result, decomposition products such as Li_2S and Li_3P are formed at the interface[197]. Simultaneously, residual SiO_x on the Si surface reacts with Li to yield Li_xSiO_y and SiO_2. These reactions produce a chemically heterogeneous and electronically insulating interphase that impedes Li^+ transport. This interfacial layer grows progressively with cycling, following a diffusion-limited process. Electrochemical impedance spectroscopy reveals that the interfacial resistance increases proportionally with the square root of time, consistent with Wagner-type diffusion kinetics. Furthermore, this degradation is more severe under high pressure and prolonged resting at low potentials, where the chemical potential of Li is high. Even though no obvious crystalline products are observed at the Si|LPSCl interface in the initial state, high-resolution TEM and XPS analyses after electrochemical cycling confirm the growth of insulating phases. The sulfur 2p spectrum shows an increasing Li_2S signal with each cycle, and the Si 2p spectrum reveals formation of SiO_2 and Li_xSiO_y through side reactions involving SiO_x. The continuous expansion of this interphase not only blocks ion transport but also induces mechanical delamination by weakening interfacial cohesion, particularly under repeated stress induced by Si volume changes.

In parallel, conductive carbon, which is typically added to enhance electrode electronic conductivity, also contributes to electrolyte decomposition in the ASSB system[4]. Carbon surfaces with high electronic conductivity and surface area facilitate electron transfer to the sulfide electrolyte. Even at moderate voltages, this promotes the reductive decomposition of LPSCl at the carbon-electrolyte interface Figure 10D. However, unlike active materials, carbon does not undergo alloying or interfacial passivation. Instead, it continuously donates electrons to the adjacent SSEs, maintaining the reduction pathway throughout cycling. This persistent degradation leads to a growing accumulation of resistive species, which infiltrate the percolating network of the composite electrode. The resultant effect is the disruption of continuous Li^+

conduction pathways and increased ionic and electronic resistance throughout the electrode. Moreover, these side reactions not only degrade the electrochemical performance but also weaken the structural integrity of the composite electrode. Additionally, interfacial degradation originating from both Si and carbon leads to progressive mechanical damage such as particle fracture and delamination within the electrode matrix[198]. The accumulation of interfacial byproducts and localized stress disrupts the continuous network required for efficient ion and electron transport. To address this issue, applying a conformal sulfide electrolyte coating on the conductive carbon has been shown to effectively suppress direct contact between reactive components. This coating limits electron leakage from carbon and buffers mechanical mismatch at the interface, thereby improving both chemical stability and mechanical cohesion in Si-based composite anodes for sulfide-based ASSBs.

INTERFACIAL ELECTROLYTE STRUCTURE IN LIQUID ELECTROLYTE SYSTEMS (50~100 nm)

The spatially heterogeneous nature of the electrode-electrolyte interface in LEs profoundly influences the long-term stability of Li-alloying anodes, particularly through its role in initiating electrolyte decomposition and governing the nucleation of the SEI. Unlike conventional graphite electrodes, which exhibit relatively stable morphologies during cycling, Li-alloying anodes experience dramatic structural and volumetric transformations. These changes impose severe constraints on interfacial coherence and reactivity. Under such dynamic conditions, the electrolyte's capacity to organize solvated ions near the highly reactive anode surface becomes a key determinant of interfacial outcomes. This spatial organization, governed by the structure and evolution of the EDL, extends beyond facilitating ionic conductivity. It plays a pivotal role in defining the initial interfacial chemistry and, consequently, the compositional and morphological features of the nascent SEI. In high-capacity Li-alloying anodes, severe concentration polarization and localized Li^+ depletion within the EDL constitute a dominant degradation phenomenon that accelerates non-uniform SEI growth. To address these critical challenges, strategically tailoring the local electrolyte solvation structure within the EDL has emerged as a primary strategy to ensure homogeneous ion flux and suppress parasitic reactions. Rather than reiterating the well-established functional requirements of the SEI, this section elucidates how the physicochemical properties of the local electrolyte environment, particularly within the EDL, modulate the kinetics and selectivity of interfacial reactions. These interfacial dynamics directly influence SEI growth mechanisms, spatial uniformity, and long-term performance. Understanding and controlling these early-stage processes are critical for engineering robust interphases capable of accommodating the morphological evolution inherent to Li-alloying anodes.

Electric double layer structure

As illustrated in Figure 11A, the EDL near a negatively polarized alloy surface comprises two interfacial zones: the inner Helmholtz plane (IHP), where specifically adsorbed Li^+ and solvent molecules may directly interact with the electrode surface, and the outer Helmholtz plane (OHP), where less tightly bound ionic species reside under the influence of the interfacial electric field[33,199]. Within these regions, the local coordination environment of Li^+ plays a pivotal role in shaping interfacial chemistry. In particular, contact ion pairs (CIPs), resulting from direct Li^+-anion interactions, and aggregates (AGGs), multi-ion complexes involving shared solvent molecules, are prevalent in concentrated electrolytes. These structures not only influence the reduction potential of coordinated species but also act as chemical precursors to SEI components[200]. Their formation is strongly dependent on the electrolyte's salt concentration and the solvation strength between ions and solvents.

This structural differentiation is particularly consequential for Li-alloying anodes, where unstable or inhomogeneous SEI formation can lead to continuous electrolyte decomposition, Li consumption, and mechanical failure of the electrode. The composition and spatial distribution of CIPs and AGGs within the EDL dictate which molecular species are preferentially reduced and, consequently, which fragments become

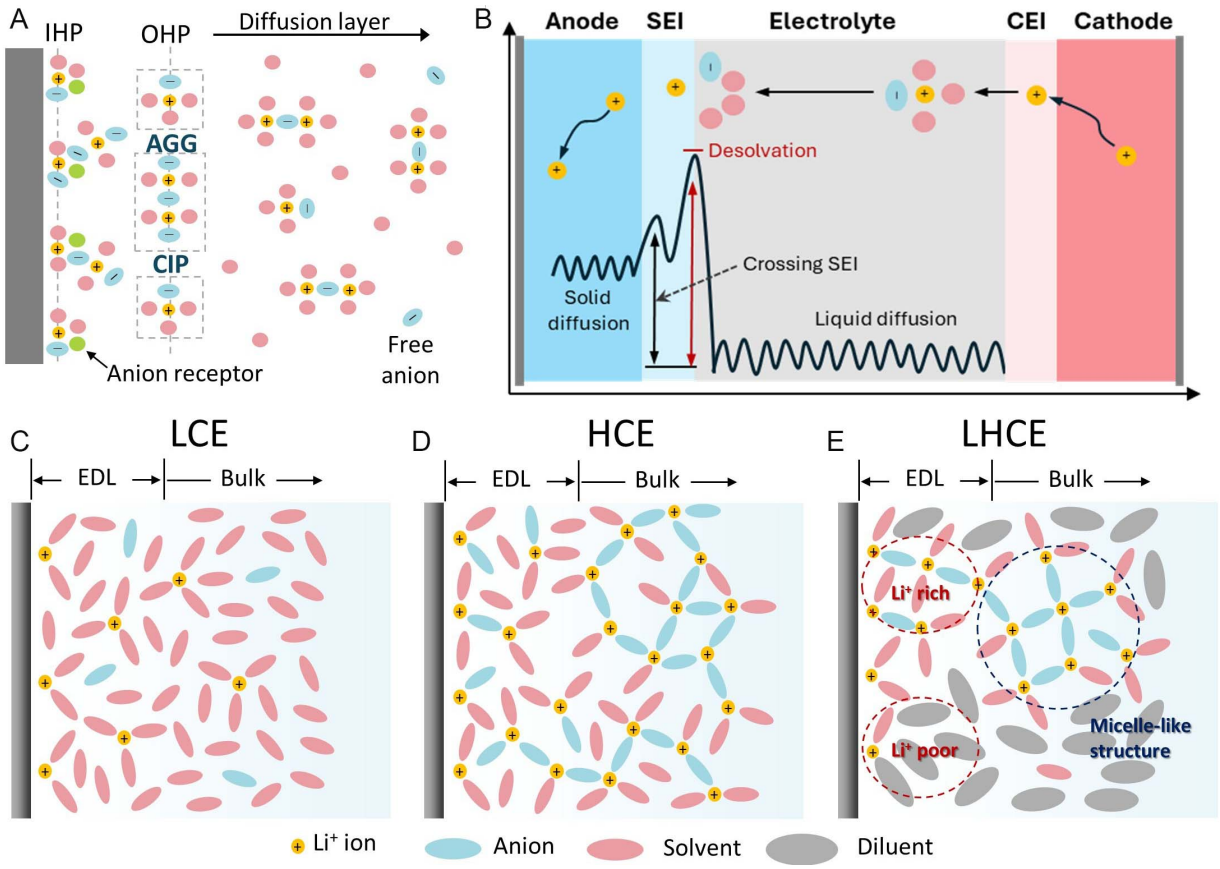

Figure 11. Schematic illustrations of (A) the electrode interface including the IHP, OHP, and diffusion layer, (B) Li^+ transport pathways across the SEI and electrolyte, and (C-E) local electrolyte environments: LCE, HCE, and LHCE near the negatively charged electrode.

incorporated into the SEI[201]. For instance, the reduction of AGG-type clusters that include both solvents and anions can lead to a composite SEI composed of inorganic (e.g., LiF, Li_2O) and organic phases, potentially improving both passivation and mechanical flexibility. Conversely, poorly coordinated solvent molecules or uneven ionic distributions at the interface may promote uncontrolled reduction pathways, producing porous, resistive, or unstable SEI layers.

As shown in Figure 11B, the structural features present at the electrolyte-electrode interface must be understood within the context of dynamic ion transport processes[80,202]. For Li^+ to intercalate into an Li-alloying anode, it should first shed its solvation shell in a desolvation step. This process becomes increasingly energy-intensive when the ion is embedded in strongly coordinated or aggregated solvation environments, such as AGG-like configurations stabilized by robust ion-solvent and ion-anion interactions. Following desolvation, the ion must traverse the SEI, whose transport properties are determined by its chemical composition and morphological characteristics. Formed through initial electrolyte decomposition within the local interfacial environment, the SEI plays a central role in regulating both the kinetics and spatial uniformity of Li^+ flux across the interface[203]. After crossing the SEI, the ion enters the bulk of the active material, where it diffuses through a structurally dynamic lattice. In alloy systems, this phase is shaped by ongoing amorphization, atomic rearrangement, and phase transitions, all of which can significantly influence ion transport pathways and energy barriers. The efficiency and continuity of this multi-step transport process, which comprises desolvation, SEI passage, and solid-state diffusion, are fundamentally influenced by the structure of the EDL that precedes interphase formation. The EDL not only governs the spatial organization of ionic species near the electrode surface but also defines the chemical environment in which

initial interfacial reactions occur[204]. While classical EDL models offer a useful starting point for describing ion distributions near charged interfaces, their assumptions often fail to reflect the complexity of modern battery electrolytes. A deeper understanding of how electrolyte composition shapes EDL architecture and, in turn, modulates downstream interfacial behavior, is therefore essential for the rational design of electrolytes and interphases in alloy-based battery systems[205].

Classical theories of the electric double layer, developed primarily for dilute aqueous electrolytes, provide a conceptual basis for understanding interfacial ion distributions[34]. Early models such as the Helmholtz and Gouy-Chapman frameworks introduced the notion of compact and diffuse ionic layers[206], while the Gouy-Chapman-Stern model added a two-region structure composed of an inner layer of specifically adsorbed ions (the Stern layer) and an outer diffuse layer governed by electrostatics[207]. However, these models rest on oversimplified assumptions such as point-like ions, uniform dielectric media, and continuous solvent behavior, all of which are inadequate for describing concentrated, multicomponent electrolytes[208]. They largely neglect steric effects, discrete solvation motifs, and mesoscale structural heterogeneity, all of which are increasingly important in battery systems employing high salt concentrations or complex solvent architectures. These limitations first become apparent in low-concentration electrolytes (LCEs), where the EDL still adheres relatively well to classical behavior[209]. As shown in Figure 11C, Li^+ is solvated primarily by polar solvents and accumulates near the negatively charged electrode, while anions are repelled from the interface[31]. The resulting EDL is narrow and compositionally simple, with limited ion-ion interactions and minimal structural complexity. In high-concentration electrolytes (HCEs), the elevated salt content promotes extensive ion pairing and aggregation, giving rise to dense EDL regions rich in both Li^+ and coordinating anions. As depicted in Figure 11D, CIPs and AGGs form readily, even within the interfacial zone[210]. While the EDL remains spatially continuous, its local coordination chemistry becomes significantly more complex, with altered reduction dynamics and SEI precursor distributions. The interfacial architecture becomes even more distinct in localized high-concentration electrolytes (LHCEs), where high salt concentrations are combined with inert diluents[211]. These systems exhibit microphase segregation, forming nanodomains in which coordinating components cluster and diluents are excluded from Li^+ solvation shells. As shown in Figure 11E, the EDL splits into a Li^+-rich micelle-like zone adjacent to the electrode and a Li^+-poor, diluent-rich outer region. Despite their low coordinating ability in bulk, diluent molecules, such as fluorinated ethers, can partially solvate interfacial Li^+, shifting their reduction potential and actively participating in SEI formation. Advanced LHCE strategies strategically exploit this microphase segregation to exclude volatile, highly reactive solvents from the immediate electrode surface. By forcing a high local concentration of salt complexes into the inner EDL while maintaining low bulk viscosity, LHCEs effectively suppress solvent co-intercalation and continuous fluid decomposition. Beyond LHCE architectures, weakly solvating electrolytes (WSEs) have emerged as a powerful alternative paradigm for manipulating the EDL without relying on excessive salt quantities or dense diluent networks. By employing solvents characterized by low donor numbers or sterically hindered chelating sites, WSEs intrinsically weaken the competitive Li^+-solvent affinity. This weak solvation energetics naturally drives the system to form extensive CIP and AGG networks at significantly lower, safer salt concentrations than traditional HCEs. Consequently, the EDL in a WSE regime becomes densely populated by anions, which drastically reduces the desolvation energy barrier for Li^+ ions attempting to cross the interface and establishes a highly uniform interfacial ionic flux.

This deliberate enrichment of the EDL with aggregated ionic clusters across modern HCE, LHCE, and WSE designs directly enables the targeted engineering of anion-derived interphases. In an anion-dominated EDL, the preferential electrochemical reduction of heavily paired anions occurs at higher potentials than that of free solvent molecules. This decomposition pathway yields an inorganic-rich SEI layer that provides exceptional mechanical rigidity and high fracture toughness capable of withstanding the intense compressive and tensile stresses generated during alloy lithiation and delithiation. Furthermore, these inorganic phases

offer lower grain-boundary resistance, accelerating solid-state Li^+ diffusion and effectively preventing localized lithium dendrite growth. These observations point to a broader principle: the structure and reactivity of the EDL are not dictated solely by bulk electrolyte properties, but are instead defined by the local coordination environment at the interface. Across electrolyte types, including LCEs, HCEs, LHCEs, and WSEs, the Li^+ coordination environment at the electrode surface governs which species are reduced and how the SEI initiates and evolves.

Therefore, rational electrolyte design for high-performance batteries must go beyond optimizing bulk conductivity or stability. It requires engineering the nanoscale interfacial environment by carefully controlling solvent, salt, and diluent interactions within the EDL to mediate targeted interfacial reactions. By tailoring the structural and energetic availability at the interface, it is possible to construct SEI layers that are chemically selective, mechanically resilient, and ionically conductive, thereby enabling robust cycling in next-generation Li-alloying anode systems.

Li^+ solvation shell chemistry and desolvation kinetics

While the electric double layer dictates the immediate chemical environment experienced by solvated ions near the electrode surface, the mesoscale electrolyte environment, extending tens of nanometers from the interface, plays a similarly pivotal role in shaping interfacial reaction kinetics and spatial uniformity[212,213]. In Li-alloying anodes, particularly under high current densities or with large surface area architectures, the rapid consumption of Li^+ at the electrode surface gives rise to steep concentration gradients perpendicular to the interface. These gradients can emerge even within the initial seconds of operation and are further exacerbated by limited ionic diffusivity in viscous or highly coordinated electrolyte systems.

As illustrated in Figure 12A, the mass transport of Li^+ toward the electrode involves a sequence of interfacial and bulk processes[214]. Initially, solvated Li^+ must undergo desolvation to shed their coordinating solvent molecules before being adsorbed onto the electrode surface, where they participate in charge-transfer reactions. These steps occur primarily within the electric double layer, a nanoscopic region adjacent to the electrode surface. Outside this region, Li^+ must diffuse through the near-surface electrolyte, then convect in the bulk electrolyte, where the ion concentration (C) remains at its initial bulk value (C^0). However, in practical systems, the rate of Li^+ reduction at the interface often surpasses the rate at which Li^+ is replenished from the bulk. This results in a depletion of local Li^+ concentration (C^{Li+}), as reflected in the reduced surface concentration (C^s) relative to C^0. The resulting concentration gradient (as depicted by the red C^{Li+} leads to polarization of the interfacial electrochemical potential, which in turn modifies the reduction environment across the electrode surface[215]. This spatial variation can significantly impact SEI formation[216]. Near regions with sufficient Li^+ supply, desolvated ion clusters, such as CIPs or AGGs, are more likely to be reduced, producing dense and inorganic-rich SEI components[217]. In contrast, Li^+-deficient areas promote the reduction of free solvent molecules, yielding porous, organic-rich SEI. Such heterogeneity in SEI composition and morphology undermines its passivation function and mechanical robustness. In Li-alloying anodes, where volume change is substantial, this non-uniform coverage may exacerbate localized over-lithiation, mechanical stress, and continuous electrolyte decomposition, accelerating performance degradation.

To mitigate such gradient-driven interfacial inhomogeneities, electrolyte systems can be engineered to regulate not only solvation structure but also the spatial profile of reactive species[218-221]. One representative approach, shown in Figure 12B, involves the use of dual salt electrolytes containing anions with differing reduction tendencies and affinities for electrode surfaces[222]. By pairing a conventional anion, such as PF_6^-, with a more surface-reactive species, such as FSI^-, it becomes possible to tailor the interfacial chemistry at each electrode independently. This enables preferential SEI formation at the anode via FSI^- decomposition,

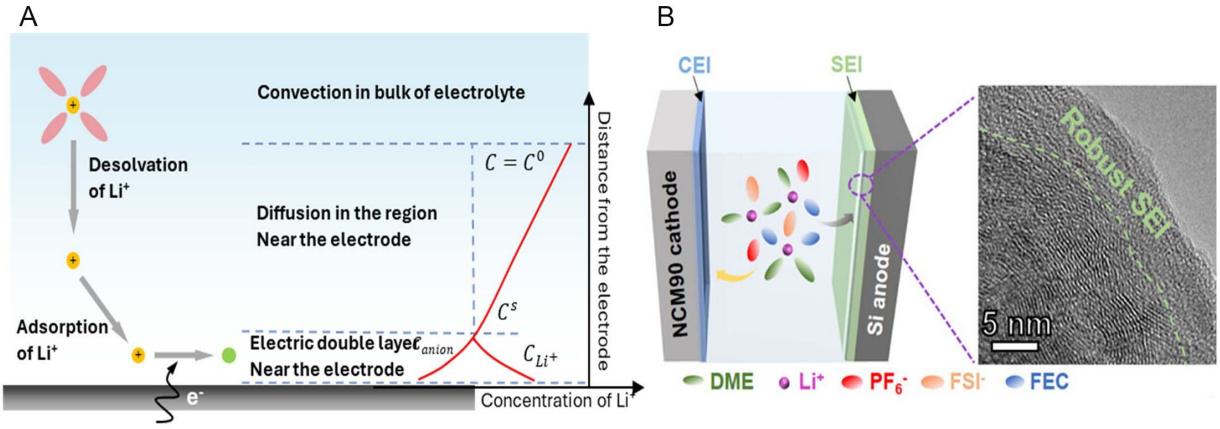

Figure 12. (A) Schematic of mass transfer of Li^+ and corresponding concentration gradient on the electrode surface. (B) Dual salt strategy for robust SEI. Reproduced with permission from ref.[222]. Copyright 2023, American Chemical Society.

while concurrently promoting stable and robust SEI through PF_6^--derived products. Although this strategy does not directly eliminate Li^+ depletion near the interface, it helps compensate for transport limitations by ensuring that interfacial reactions proceed through favorable, selectively reduced species even under steep concentration gradients. As such, dual salt electrolytes represent a broader class of design strategies aimed at decoupling bulk ion transport from interfacial reaction uniformity. By leveraging compositional asymmetry within the electrolyte itself, these approaches contribute to the formation of more coherent and resilient interphases, which are critical attributes for enabling stable cycling of Li-alloying anodes under demanding operating conditions.

Near- interface electrolyte environment

While electrolyte composition plays a critical role in directing interfacial reaction pathways and mitigating gradient-induced instabilities, addressing the structural and mechanical aspects of the near-interface environment is equally essential[223]. Recent efforts have thus expanded beyond chemical optimization to include physical modulation of the mesoscale electrolyte domain and electrode architecture, aiming to achieve spatially uniform ion transport and interfacial robustness under dynamic cycling conditions[224-226]. Chemical strategies alone, however, are often insufficient to accommodate the complex spatial and mechanical demands encountered during battery operation. Ion transport at the interface is governed not only by molecular-scale coordination chemistry but also by the geometry, porosity, and connectivity of the surrounding electrode structure. Structurally engineered electrodes offer complementary avenues to control local ionic flux, mitigate transport bottlenecks, and maintain interfacial stability across diverse operating regimes. Accordingly, various architectural design strategies have been developed to optimize the mesoscale transport environment and enhance the mechanical adaptability of the electrode-electrolyte system.

One effective structural approach involves using porous electrodes with carefully tailored tortuosity and pore-size distributions to promote spatially uniform Li^+ transport and suppress local concentration gradients[227]. As schematically illustrated in Figure 13A, a low-tortuosity, well-connected pore network can reduce concentration polarization near the electrode-electrolyte interface. Although conceptual, this model highlights the fundamental design principle that geometric tuning of porous structures facilitates homogeneous ionic accessibility. Building on this concept, Yang *et al.* developed a Ge/carbon atomic-scale hybrid anode with a micro-nano-gradient porous framework [Figure 13B][228]. This hierarchical structure not only buffered volumetric strain during lithiation/delithiation but also preserved continuous ionic and electronic pathways. Electrochemical measurements confirmed stable SEI formation and improved cycle retention, underscoring the benefits of mesoscale structural integration. Structural modulation has also been

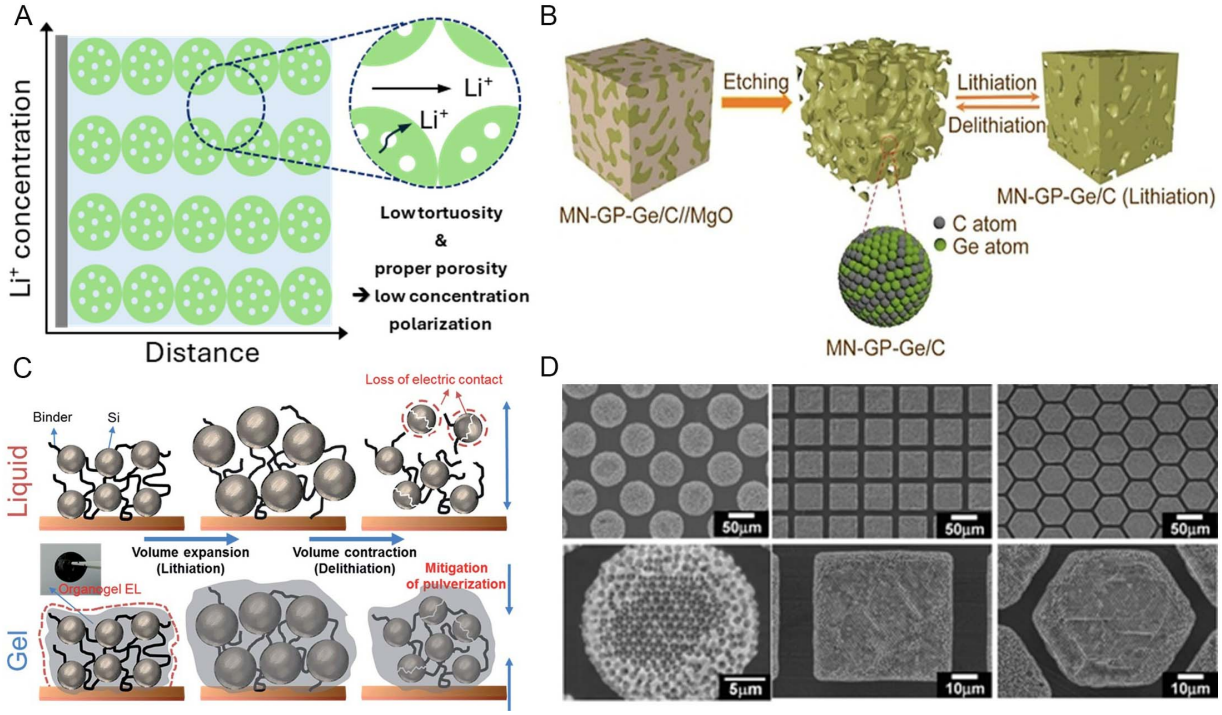

Figure 13. (A) Schematic of the Li^+ mass transport in a well-designed porous anode**.** (B) Schematic of the fabrication process of MN-GP-Ge/C. Reproduced with permission from ref.[228]. Copyright 2021, Wiley. (C) Comparison of Si anode behavior: contact retention and volume buffering in liquid and gel electrolytes. Reproduced with permission from ref.[229]. Copyright 2016, The Royal Society of Chemistry. (D) SEM images of a highly patterned 3-dimensionally ordered macroporous (3DOM) Sn-Ni alloy with various patterns. Reproduced with permission from ref.[230]. Copyright 2011, The Royal Society of Chemistry.

extended to the electrolyte phase. In high-loading Si anodes, Cho *et al.* demonstrated that organogel-based polymer electrolytes can serve as mechanically adaptive media Figure 13C[229]. Unlike conventional LEs, which often fail to maintain interfacial contact under repeated expansion and contraction, the gel system accommodated volume fluctuations while preserving ion transport continuity, thereby mitigating interfacial disintegration. At the surface level, Kotobuki *et al.* introduced a 3D macroporous Sn-Ni alloy anode with integrated micro-patterns designed to redistribute local ionic flux and mechanical stress Figure 13D[230]. This patterned architecture enhanced areal capacity and delayed structural failure during cycling by facilitating spatially uniform interfacial evolution, as validated through post-mortem scanning electron microscope (SEM) analysis.

Structural engineering, encompassing the modulation of bulk porosity, compositional heterogeneity, and interfacial morphology, offers a multifaceted strategy to address the intrinsic challenges associated with Li-alloying anodes. These architectural refinements mitigate mechanical degradation, facilitate spatially homogeneous ion transport, and contribute to the chemical stabilization of the electrode-electrolyte interface. When synergistically integrated with electrolyte formulations tailored for interfacial compatibility and dynamic mechanical compliance, such structural interventions foster the formation of mechanically robust and electrochemically stable SEI architectures. Collectively, these advances delineate a comprehensive design paradigm that unites mesoscale material architecture with electrolyte chemistry to realize durable and high-performance alloy-based energy storage systems.

INTERFACIAL ION TRANSPORT BARRIERS IN SOLID-STATE ELECTROLYTE SYSTEMS

In the ASSB system, where SSEs replace conventional LEs, the electrode-electrolyte interface becomes a dominant factor in determining the overall electrochemical performance. Unlike the LE system, where interfacial contact can be maintained via wetting and fluidic adaptability, solid-state interfaces are prone to

Table 4. Comparison of SEI formation mechanisms between liquid-electrolyte and solid electrolyte systems

Characterization challenges	Mechanical failure modes	Dominant degradation products	Transport limitation	SEI generation driving force	
Nanoscale thickness, compositional heterogeneity, and air sensitivity of SEI species	SEI cracking, rupture, and repeated SEI reformation induced by electrode volume changes	Li_2O, Li_2CO_3, $ROCO_2Li$, ROLi, polymerized fragments	Li^+ diffusion through thickening SEI and concentration polarization	Electrochemical reduction of electrolyte below the ESW	Liquid electrolytes (LEs)
Highly air- and beam-sensitive buried interfaces requiring inert characterization conditions Buried solid-solid interfaces with limited spatial accessibility and low interfacial contrast	Microcracking, localized contact loss, and the generation of electrochemically inactive regions	Polymer-derived decomposition product, polyether, and ROLi	Low ionic conductivity and resistance from decomposition-derived interphase	Electrochemical decomposition of polymer and Li salts under reductive conditions	Solid polymer electrolytes
		Li_2S, Li_3P, and Li_xPS_y	Resistive decomposition products and interfacial contact degradation	Thermodynamic instability and electrochemical reduction at the electrode/electrolyte interface	Sulfide-based SSEs
		Li_2O, LiOH, and Li_2CO_3	Insulating reaction products, grain-boundary resistance, and interfacial contact degradation		Oxide-based SSEs

mechanical mismatch, loss of contact, and the formation of ionically resistive interphases. These challenges are particularly severe in high-capacity Li-alloying anodes, which undergo drastic volume changes during cycling. In such rigid solid-solid configurations, the failure to preserve interfacial integrity leads to localized ion transport bottlenecks, mechanical fracture, and rapid capacity fading. Failure modes at the solid electrolyte interface are highly dependent on the SEEs classification[231]. Polymer-based electrolytes can better accommodate the dimensional variations of Li-alloying anodes through their deformable interfaces, but insufficient mechanical reinforcement can still lead to unstable contact and impedance growth under repeated volume changes[232]. Sulfide electrolytes deliver excellent Li^+ conductivity and interfacial contact, but their stability is compromised by the highly reducing Li-rich alloy surfaces and electronic leakage through conductive networks[4]. Oxide electrolytes offer high chemical stability, yet their extreme rigidity leads to contact loss, brittle fracture, and localized Li^+ transport bottlenecks[233]. These distinct behaviors demonstrate that evaluating interface failure in polymer, sulfide, and oxide systems requires comprehensive criteria encompassing contact retention, mechanical confinement, and Li^+ transport continuity alongside conventional chemical compatibility [Table 4][232].

Fundamentally, this interfacial degradation of Li-alloying anodes in ASSBs originates from a tightly coupled chemo-mechanical loop. As the active particles undergo massive volume expansion during lithiation, intense mechanical stress is generated at the solid-solid boundary. The severity of this stress is inherently governed by the particle size and the mechanical modulus of both the active material and the surrounding SSE. While larger particles are highly susceptible to intra-particle fracture due to accumulated stress, smaller nanoparticles better disperse strain but exponentially increase the interfacial area prone to chemical degradation. Although high external stack pressure is often applied to counteract the resulting contact loss, localized stress exceeding the materials' yield strength accelerates crack propagation rather than mitigating structural damage. Crucially, these mechanical fractures disrupt continuous ionic pathways, severely deteriorating localized Li diffusivity. This sluggish and heterogeneous Li transport induces asynchronous lithiation, generating further localized stress gradients. Ultimately, the reciprocal degradation driven by mechanical failure restricting ion transport and heterogeneous ion flux exacerbating mechanical stress manifests macroscopically as rapid interfacial resistance growth and severe capacity decay.

This section explores recent strategies to address interfacial ion-transport barriers in SSE systems, including crack formation and diffusion-limiting interfacial layers arising from poor contact. Through these discussions, we aim to clarify how mechanical and chemical interfacial mismatches affect ion transport and provide insight into design principles for stable and conductive solid-state interfaces.

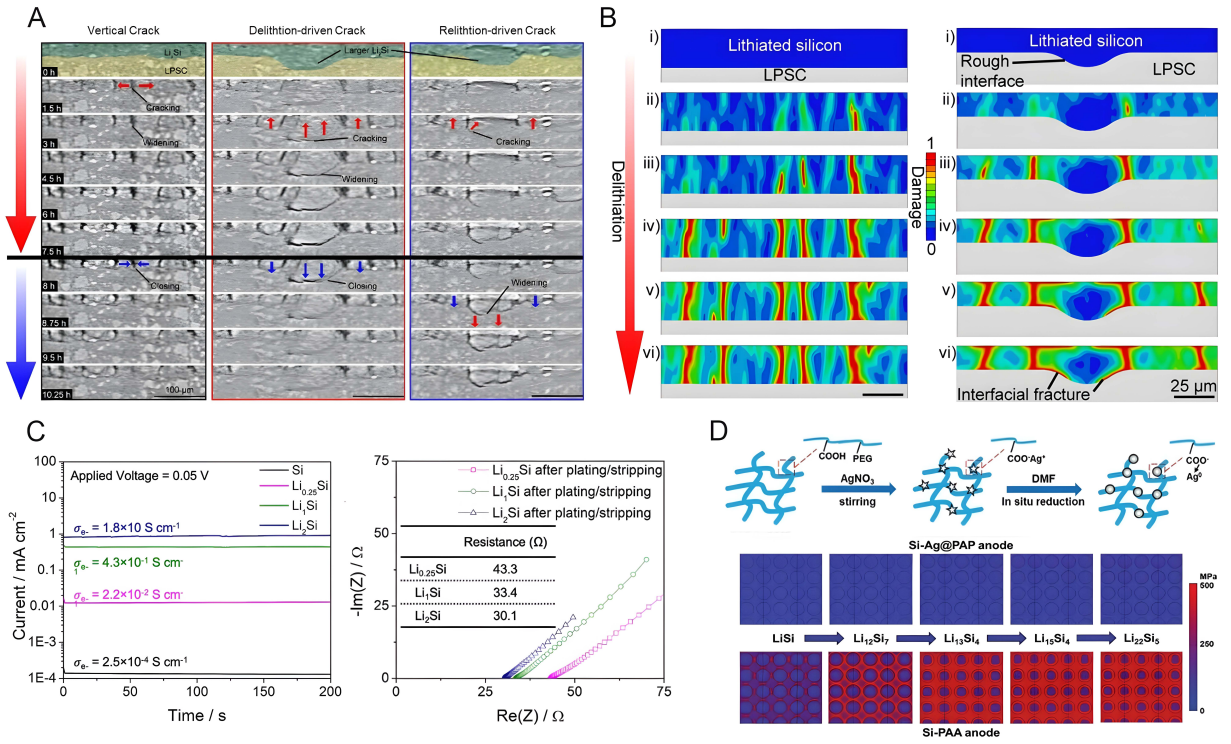

Figure 14. (A) Mechanical fracture mechanisms of the high-capacity anode material electrode in ASSB. (B) Contours of damage evolution in a Li_xSi/LPSC simulation domain with a uniform-thickness electrode and a nonuniform-thickness electrode. (A and B) Reproduced with permission from ref.[231]. Copyright 2024, Author(s), licensed under CC-BY 4.0 license. (C) Ionic conductivity and electrochemical impedance spectroscopy results of prelithiation, modifying surface properties. Reproduced with permission from ref.[109]. Copyright 2024, Author(s), licensed under a Creative Commons CC BY license. (D) Binder engineering strategies for stabilizing the Si anode in ASSB and its stress distribution modeling. Reproduced with permission from ref.[239]. Copyright 2024, Wiley.

Interfacial instability between electrolyte and electrode

Surface crack propagation

In ASSB systems that employ high Li-stoichiometry anodes, interfacial mechanical instability is a critical degradation pathway due to the combined brittleness of active material and sulfide-based SSEs. Cross-sectional observations reveal distinct crack morphologies associated with different stages of electrochemical cycling Figure 14A and B[231]. During the initial lithiation stage, volumetric expansion of Si generates compressive stress, leading to the formation of vertical cracks oriented perpendicular to the electrode plane. These cracks are typically confined and do not propagate extensively over subsequent cycles. In contrast, delithiation results in heterogeneous contraction within the lithiated Si matrix along interparticle boundaries, inducing lateral cracks that propagate parallel to the interface[231]. Upon relithiation, these pre-existing cracks are reactivated and widened due to renewed internal strain, leading to irreversible fracture accumulation. This cyclic process progressively fragments the Si structure, weakens interfacial contact with the electrolyte, and increases cell resistance.

The electrochemical degradation of micro-sized Li-alloying anodes in ASSBs arises from a complex interplay among Li^+ diffusion limitations, internal stress accumulation, and mechanically induced fracture. Tao *et al.* combine experimental observations with finite element modeling to demonstrate that extended Li^+ diffusion pathways in Si particles generate pronounced concentration gradients[234]. These gradients lead to spatially heterogeneous chemical potentials and volumetric expansion, which in turn induce the development of both

hydrostatic and Von Mises stress distributions. Hydrostatic stress, which represents the isotropic component associated with volumetric deformation, appears as compressive near the particle surface and becomes tensile toward the interior. On the other hand, Von Mises stress, a scalar measure that reflects the material's tendency to yield under deviatoric stress, is concentrated in regions where the mismatch in lithiation-induced expansion is most significant. When the magnitude of localized Von Mises stress exceeds the mechanical fracture threshold of active material, cracks are energetically driven to form and propagate through the particle thickness and gradually lead to structural disintegration. The experimentally observed spatial distribution of fractures shows a strong correlation with the high-stress regions and confirms a direct correlation between internal stress fields and mechanical failure. As cycling progresses, the crack network expands and disrupts ionic and electronic conduction pathways, which electrically isolate portions of the active material from the electrochemical process. This degradation is further aggravated by the rigid nature of SSEs, which restrict volumetric accommodation and inhibit stress relaxation, thereby accelerating crack formation and growth. Although the application of external pressure is effective at suppressing interfacial delamination, it does not address underlying causes, such as Li diffusion limitations and internal stress development[39]. Therefore, these results highlight the structural and electrochemical limitations of micro-sized Si in ASSB systems and emphasize the need for nanoscale structural tuning and mechanically adaptive electrode designs to achieve long-term durability.

Interfacial stabilization strategies in the solid-state electrolyte system

To mitigate the severe interfacial issues observed in high-capacity anodes interfaced with SSEs, conformal interfacial engineering has been extensively explored. For instance, the direct contact between highly reactive and volumetrically fluctuating Li-alloying surfaces and sulfide electrolytes often leads to undesirable redox side reactions and interfacial phase reconstruction. One effective interfacial stabilization strategy is designing a thin film-type anode. In particular, atomic layer deposition of tin oxynitride (SnN_y) enables the formation of an amorphous, nanostructured matrix in which Li-Sn alloying occurs within a mechanically compliant Li_3N framework[235]. This conformal coating uniformly covers complex geometries, eliminating local thickness variations that can serve as crack initiation points. The Li_3N matrix exhibits high Li^+ diffusivity, which not only maintains homogeneous lithiation but also buffers the volume changes of Sn nanoparticles through its comparatively elastic nature. By preventing particle aggregation and constraining anisotropic expansion, the nitride layer suppresses stress concentration at the SSE interface, thereby mitigating crack propagation and preserving electrode-electrolyte contact over extended cycling. Another strategy involves the deposition of a thin ceramic interlayer between the Si anode and the sulfide electrolyte, such as Li_6PS_5Cl[236]. This electronically insulating oxide suppresses electronic coupling across the interface, as confirmed by DOS calculations, which show a marked reduction in states near the E_F upon SiO_2 insertion[194]. The suppression of interfacial electronic conduction reduces the driving force for reductive decomposition of the SSEs, thereby stabilizing the chemical environment at the interface. Additionally, the insulating nature of SiO_2 serves as a physical barrier that prevents interdiffusion while still allowing for sufficient Li^+ transport. As a result, ceramic-coated Si-based full-cell pairing with an LFP cathode enables stable operation. In addition to interfacial passivation, prelithiation of Si has emerged as a complementary strategy to improve electrochemical compatibility with sulfide SSEs[109]. Electrochemical impedance spectra indicate that higher degrees of lithiation significantly reduce the interfacial resistance Figure 14C. This reduction is attributed to both enhanced ionic and electronic transport properties of Li-rich silicide phases and their abilities to passivate SEI. Moreover, such prelithiated phases promote more uniform lithiation kinetics and suppress the formation of electrochemically isolated domains, which are prevalent in pristine Si anodes. These effects collectively contribute to improved interfacial charge transfer and mechanical coherence, thereby preventing particle pulverization during cycling in ASSB systems.

Another effective strategy for interfacial stabilization lies in the rational design of functional polymeric binders that accommodate the large volume changes of Si while maintaining chemical compatibility with SSEs[237]. Similar to LE system binder design strategies, a polymer binder consisting of hard and soft segments can buffer mechanical stress cycling by selectively stretching or contracting its segments[238]. This elastic response reduces particle detachment and interfacial cracking, thereby preserving structural integrity over long-term cycling. In addition to segmental elasticity-based binders, another class of polymer architecture has been developed to simultaneously address mechanical resilience and interfacial conductivity. For instance, dual-chemically functionalized binders incorporating *in situ* reduced silver nanoparticles (AgNPs) offer a compelling solution by integrating electronic conduction pathways directly within the polymer matrix. Upon reduction of Ag^+ precursors dispersed in an ether-rich polymer backbone, a percolated Ag network is formed that bridges adjacent Si particles and conductive additives Figure 14D[239]. This embedded metallic network significantly enhances the overall electronic conductivity of the electrode, ensuring efficient charge transport throughout the cycling process. More importantly, the AgNP-embedded polymer exhibits superior mechanical flexibility, with fracture strains exceeding 750%, allowing it to conformally adapt to morphological changes in the Si electrode while maintaining intimate interfacial contact. The effectiveness of binders is further validated by stress distribution modeling during progressive charging stages. Si-Ag@poly (acrylic-co-poly (ethylene glycol) methyl ether methacrylate) (PAP) anode maintains a uniform and low-stress environment throughout the formation of various Li_xSi phases, indicating efficient stress dispersion. Thereby, the Si-Ag@PAP anode maintains its capacity over 2,000 cycles at an extremely high C-rate at 5C under low-pressure conditions (5 MPa). In contrast, the Si-PAA anode exhibits severe and localized stress accumulation, with stress levels exceeding 500 MPa as lithiation proceeds toward $Li_{22}Si_5$[239]. This high internal stress contributes to mechanical failure, such as crack propagation and particle disconnection. The comparative simulation demonstrates that the functional binder effectively buffers internal stresses and suppresses stress-induced interfacial particle cracks by forming a resilient and conductive polymer matrix.

Interfacial contact-derived diffusion layer in solid-state electrolyte

Interfacial ion transport limitation (contact loss)

Beyond the intrinsic cracking problems of high-Li stoichiometry anode materials, failure to establish and maintain interfacial contact with SSEs during operation is a fundamental limitation in ASSB systems. This contact loss, often initiated by mechanical mismatch during repeated lithiation, results in the formation of electrochemically inactive void regions that disrupt ion and electron transport pathways. As a consequence, lithiation becomes increasingly non-uniform, local overpotentials rise, and Li^+ tends to accumulate in isolated domains. These effects collectively reduce active material utilization and CE while accelerating structural degradation and capacity fading over cycling. In the case of the Si anode, a relatively dense Li_xSi layer forms near the surface of the Si electrode, preserving close contact with the adjacent SSE during the initial lithiation Figure 15A. However, the first delithiation induces structural rearrangement within the Si, accompanied by inhomogeneous contraction[40]. As this strain becomes concentrated at specific regions, approximately 2 μm-wide voids begin to emerge where mechanical mismatch disrupts contact. Cross-sectional analyses reveal that these voids arise not from superficial separation but from internal detachment, driven by the accumulation of mechanical stress. With continued cycling, these voids grow larger, exceeding 10 μm after 100 cycles, eventually leading to irreversible disconnection of the electrode-electrolyte interface. This mechanical decoupling leads to electrochemically inactive regions and uneven lithiation patterns, thereby reducing the electrode's active area and degrading coulombic efficiency and capacity retention.

The disruption of Li^+ conduction pathways across the interface stems from both physical detachment and stress-induced damage[39]. Once interfacial voids form, ion transport becomes spatially heterogeneous, and Li^+ redistributes unevenly, guided by local gradients in chemical potential and mechanical stress. These gradients promote the formation of microcracks within the Si phase, further expanding the mechanically

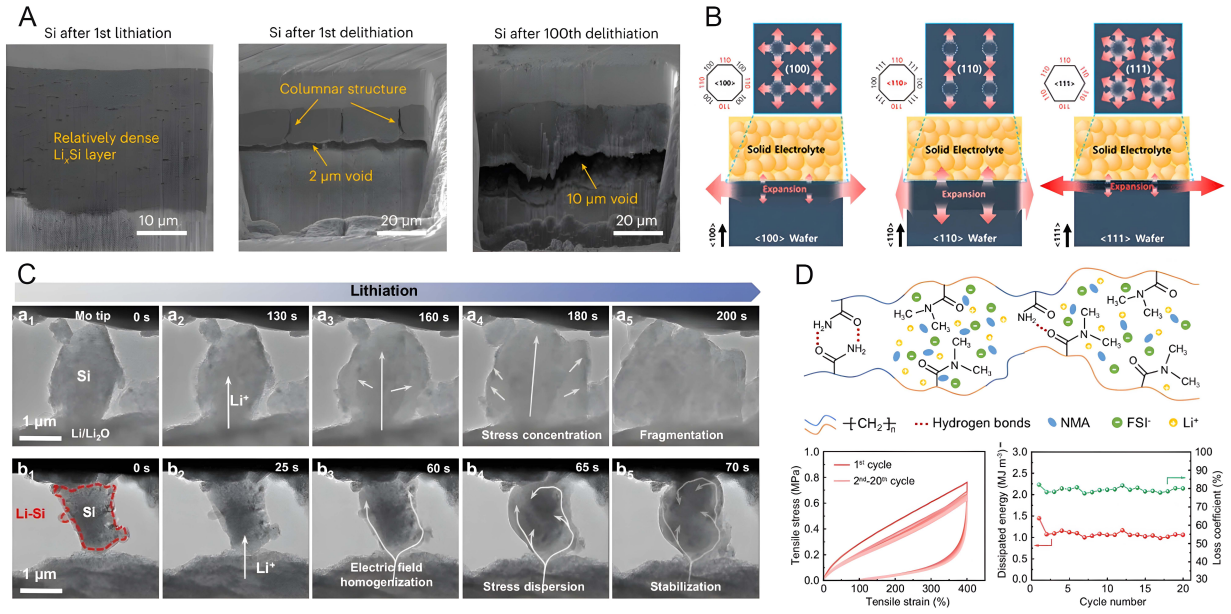

Figure 15. (A) TEM images of contact loss between SSE and electrode during cycling. Reproduced with permission from ref.[40]. Copyright 2024, Author(s), licensed under a Creative Commons CC BY license. (B) Schematic of plane and side views showing major expansion directions along [110] for <100>, <110>, and <111> wafers. Reproduced with permission from ref.[240]. Copyright 2023, American Chemical Society. (C) TEM images of mixing prelithiated Si enable suppressing electrode contact loss and active material expansion. Reproduced with permission from ref.[241] Copyright 2025 Author(s), licensed under a Creative Commons CC BY license. (D) Employing an elastic polymer electrolyte enables maintaining contact without external pressure. Reproduced with permission from ref.[39]. Copyright 2024, Author(s), licensed under a Creative Commons CC BY license.

compromised zone. The damaged interfacial region develops into a diffusion layer that exhibits poor ionic conductivity and diminished electrochemical activity. As a result, interfacial resistance rises, and overall charge-transfer kinetics are hindered. The extent of degradation is also affected by the mechanical characteristics of the SSEs. Thermally densified electrolytes, while initially stable, possess high stiffness and low strain tolerance, making them prone to cracking when Si expands. In contrast, quasi-solid electrolytes can accommodate strain through framework deformation, but suffer from instability in preserving continuous contact under dynamic cycling. These effects underscore the importance of coordinated mechanical design. Maintaining interfacial stability in the Si-based ASSB system requires careful balancing of material rigidity, deformation ability, and pressure-driven stress evolution across the cell.

Strategies for maintaining interfacial contact

Various strategies are applied to the high-capacity anode to maintain interfacial contact in the ASSB system. For instance, engineering the crystallographic orientation of Si wafers has emerged as an effective approach Figure 15B[240]. Among the available orientations, the <110> direction is particularly advantageous due to its large interstitial spacing, which facilitates rapid Li^+ diffusion along the wafer thickness. This directional Li^+ transport minimizes accumulation at the interface, thereby suppressing interfacial stress and mechanical failure. Additionally, surface microstructuring, such as KOH-induced grooving morphology, enhances the physical conformity between the Si electrode and the SSEs. These grooves allow the ductile sulfide-based electrolyte to penetrate and interlock with the electrode surface during cell fabrication, promoting uniform interfacial contact and homogeneous lithiation. As a result, the combination of crystallographic alignment and surface modification plays a critical role in preserving electrode integrity and interfacial stability of ultrahigh areal capacity electrodes (≈ 10 mAh cm^{-2}) under repeated cycling conditions.

To mitigate interfacial degradation without relying on external pressure, a recent study introduced an engineered interfacial architecture composed of a $Li_{21}Si_5$-rich layer and a carbon-sulfide composite interlayer Figure 15C[241]. The Li-rich overlayer, formed through thermal pre-lithiation, alleviates local stress and suppresses the chemical reactivity of pristine Si. Simultaneously, the conductive composite beneath the Si electrode promotes homogeneous current distribution and buffers volumetric strain by accommodating interfacial mismatch. Together, these layers reduce stress concentration and inhibit crack formation, allowing pressure-free cycling while maintaining high capacity retention over 300 cycles. Ultimately, $Li_{21}Si_5$/Si-$Li_{21}Si_5$ anode-based full-cell paired with LCO cathode enables stable operation over 1,000 cycles. In parallel, a quasi-solid-state electrolyte based on a dual-network polymer infused with a deep eutectic mixture solvent has been proposed as an internal mechanical stabilizer Figure 15D[39]. The elastic properties of the polymeric electrolyte provide deformability to accommodate Si expansion and contraction, while preserving continuous contact with the electrode surface. This design obviates the need for stack pressure by enabling reversible structural accommodation during cycling, as evidenced by interfacial stress relaxation in finite-element simulations. The system exhibits stable electrochemical performance over extended cycling under extremely low external pressure conditions (< 1 MPa), highlighting the potential of electrolyte engineering as a complementary strategy to Si-side interfacial control.

CONCLUSION AND OUTLOOK

High Li-stoichiometric anodes undergo substantial volume changes during lithiation, giving rise to interfacial stress, delamination, and unstable SEI formation. In response, numerous interfacial stabilization strategies have been devised according to their spatial relation to the electrode-electrolyte interface. Nonetheless, a comprehensive understanding of how the spatial distribution of chemical modifications governs interfacial behavior remains limited. To this end, this review highlights the significance of spatially resolved modulation of the electrode-electrolyte interface in the context of high Li-stoichiometric anodes. We describe in detail the spatial characteristics of the interface and delineate the contrasting interfacial behaviors and essential roles of LEs and SSEs, while analyzing a range of interfacial engineering strategies categorized by their spatial proximity to the interface. In the subsurface and surface regions of the electrode, modifications such as surface termination, doping, and prelithiation are employed to modulate the local electronic structure, which leads to enhanced interfacial chemical compatibility and mitigates undesirable reactions. Adjacent to the electrode-electrolyte boundary, the incorporation of electrolyte additives or the deposition of artificial layers has been widely utilized to regulate the composition, morphology, and functionality of the SEI, particularly addressing the heterogeneous decomposition behavior at LE interfaces and the inherent instability at the boundary of SSEs. Furthermore, in high Li-stoichiometric anodes, the interfacial configuration is strongly influenced by the EDL structure, Li^+ desolvation kinetics, and the solvation environment near the interface, which collectively govern SEI evolution and spatial lithiation uniformity. In the case of SSEs, cracking at the particle scale and contact loss at localized regions are recognized as key degradation pathways. To address these challenges, recent studies have concentrated on optimizing the mechanical properties and structural design of electrode systems, aiming to preserve interfacial integrity and prevent separation between particles during repeated volume changes. As a result, a deeper understanding of the electrochemical properties associated with these strategies is critical for practical implementation. However, several key challenges still need to be carefully addressed, particularly the interfacial instability arising from surface reactivity and the substantial volume expansion of high-capacity active materials during cycling, which is further aggravated under high areal loading conditions required for enhanced energy density. Herein, we examine the underlying interfacial issues associated with these challenges and outline some perspectives toward future development for High-Li stoichiometric anodes. As a concluding schematic, Figure 16 integrates the major interfacial degradation pathways of Li-alloying anodes with the spatial design strategies proposed throughout this review.

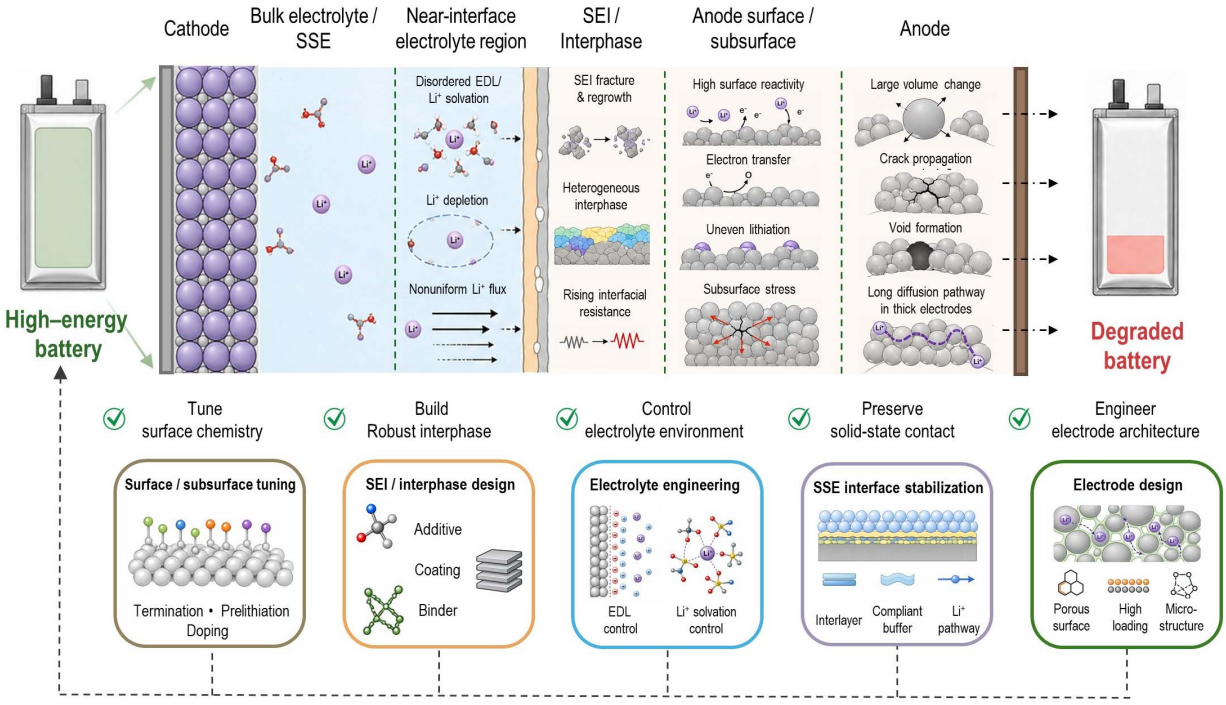

Figure 16. Spatial framework of interfacial degradation pathways and corresponding stabilization strategies for Li-alloying anodes.

(1) Electrolyte-mediated modification of the interface and active material

While surface modification of active materials can mitigate interfacial degradation by tuning surface chemistry or mechanical resilience, such strategies are often constrained by limited tunability and trade-offs with bulk properties. Ultimately, interphases such as SEI are formed through the reductive or oxidative decomposition of electrolyte components, suggesting that the electrolyte governs the composition, structure, and functionality of the interface. Therefore, even well-engineered active material surfaces may be rendered unstable if not matched with a properly formulated electrolyte. In this context, electrolyte design offers a more fundamental and versatile route. The overarching principle must be an electrolyte-centric tailored design that induces the formation of robust interphases while simultaneously mediating surface reactions to chemically modify and stabilize the active material. Such a coupled effect has rarely been explored and must be prioritized through integrated theoretical and experimental approaches in future research to achieve fundamental interfacial stability.

(2) Construction of spatially adaptive interfaces accommodating dynamic volume changes

The large and repeated volume changes of Li-alloying anodes during cycling continuously alter the electrode-electrolyte interface, rendering static interfacial designs insufficient for long-term stability. Future strategies must therefore pivot toward constructing spatially adaptive interfaces that can dynamically respond to the severe mechanical and chemical fluctuations occurring during operation. Promising directions encompass self-healing interphases for crack mitigation, mechanochemically responsive coatings that increase mechanical strength under stress, and stimuli-adaptive materials capable of tuning ionic conductivity to local potential or temperature. By integrating such adaptive functionalities, it becomes possible to maintain interfacial integrity and uniform ion transport even as the electrode undergoes significant morphological evolution.

(3) Advanced characterization and operando spatial mapping-driven digital design of spatially resolved interfaces

A clear understanding of the spatially dependent processes that occur at the electrode-electrolyte interface is critical for advancing alloying-type anodes toward commercial viability. However, experimental insight into these interfacial phenomena is still limited, particularly regarding how compositional and structural gradients evolve under realistic operating conditions. Therefore, to address the current limitation in spatially resolved interfacial analysis, operando characterization tools that can directly visualize interface gradients and spatial distributions are essential. Data obtained from such analyses can form the foundation for data-driven frameworks, including machine learning-guided models, which are capable of predicting and optimizing electrolyte systems concerning spatial distribution and interfacial stability. Collectively, these approaches can accelerate the realization of stable interfaces in high Li-stoichiometric anodes, thus enhancing their practical implementation.

(4) Securing rheological and structural electrode uniformity for high-loading applications

To attain high energy density, it is essential to match the high-loading cathodes with appropriately high-loading anodes. This inevitably leads to increased electrode thickness, which amplifies mechanical stress and poses challenges in maintaining structural integrity during repeated cycling. While strategies such as porous structural design, binder reinforcement, and enhanced interfacial adhesion have been developed to accommodate volume expansion and mitigate degradation, thick electrodes remain inherently prone to cracking. Such mechanical failures compromise the cohesion and continuity of the electrode while simultaneously exposing fresh internal surfaces to sustained contact with the electrolyte. Therefore, beyond conventional structural engineering, the optimal formulation of high-density slurries through advanced rheology modifiers and refined processing techniques is crucial. Preventing crack formation and maintaining continuous electrode uniformity are vital to stabilizing the electrode-electrolyte interface by minimizing spatial disruption under practical, high-loading conditions.

(5) Size-dependent microstructure engineering tailored to electrode architecture

Nanostructured alloying anodes have been widely adopted to alleviate mechanical stress during cycling, enhance Li^+ diffusivity, and maintain morphological preservation by accommodating large volume changes. Despite these advantages, nanostructured materials suffer from side reactions caused by high surface area, unstable SEI formation, and limited tap density, all of which hinder their practical application. From this perspective, microstructured alloying anodes have attracted increasing attention due to their lower surface reactivity, higher volumetric energy density, and improved processability, making them promising candidates for high-loading electrode configurations in next-generation energy storage systems. Given the drastically contrasting interfacial challenges between nano- and microstructured anodes, a strictly size-dependent interfacial design approach is imperative. This tailored strategy must deliberately balance mechanical resilience, reaction kinetics, and long-term interface stability across practical electrode architectures to mitigate particle-scale failure modes effectively.

(6) Utilizing gel polymer electrolytes (GPEs) for interfacial stabilization in Li-alloying anodes

Safety concerns, including the risk of thermal runaway and flammability in LEs, have driven the development of SSEs as safer alternatives. While SSEs offer nonflammability and high thermal stability, their rigid nature exacerbates interfacial contact loss when paired with Li-alloying anodes that undergo large volume changes. This loss of contact increases interfacial resistance, promotes heterogeneous lithiation, and

ultimately accelerates capacity fading. Accordingly, GPEs present a highly promising "phase-hybrid" compromise, uniquely combining the nonflammable and structurally supportive characteristics of SSEs with the highly conformal, space-filling interfacial contact properties of LEs. By integrating GPEs with dynamic Li-alloying anodes, it becomes possible to physically mitigate contact loss and maintain continuous Li-ion pathways, thereby fundamentally suppressing spatially resolved interfacial degradation and vastly improving the practical feasibility of high-capacity Li-alloying anode systems.

DECLARATIONS

Authors' contributions

Data sourcing and collection: Kwon, J. Y.; Cho, Y.; Lee, G.
Editing and supervision: Han, D. Y.; Ryu, J.

Availability of data and materials

Not applicable.

AI and AI-assisted tools statement

During the preparation of this manuscript, ChatGPT (GPT-5.6 Sol, released 2026-07-09) was used solely for language editing. The tool did not influence the study design, data collection, analysis, interpretation, or the scientific content of the work. All authors take full responsibility for the accuracy, integrity, and final content of the manuscript.

Financial support and sponsorship

This work was supported by the National Research Foundation of Korea (NRF) grant funded by the Korean government (MSIT) (RS-2025-16071080) and Korea Toray Science Foundation.

Conflicts of interest

All authors declared that there are no conflicts of interest.

Ethical approval and consent to participate

Not applicable.

Consent for publication

Not applicable.

Copyright

© The Author(s) 2026.

REFERENCES

1. Choi, J. W.; Aurbach, D. Promise and reality of post-lithium-ion batteries with high energy densities. *Nat. Rev. Mater.* **2016**, *1*, 16013. DOI
2. Armand, M.; Tarascon, J. Building better batteries. *Nature* **2008**, *451*, 652-7. DOI PubMed
3. Ko, K.; Sung, K.; Ahn, H. Layer-by-layer-structured silicon-based electrode design for ultrafast lithium-ion batteries. *Korean. J. Chem. Eng.* **2024**, *42*, 1045-53. DOI
4. Tan, D. H. S.; Chen, Y.; Yang, H.; et al. Carbon-free high-loading silicon anodes enabled by sulfide solid electrolytes. *Science* **2021**, *373*, 1494-9. DOI
5. Kim, J.; Choi, J.; Park, J.; Son, H.; Choi, J.; Chae, S. Designing Si anode in sulfide-based all-solid-state batteries: insights from established strategies in lithium-ion batteries. *Korean. J. Chem. Eng.* **2024**, *42*, 1353-64. DOI
6. Li, W.; Sun, X.; Yu, Y. Si-, Ge-, Sn-based anode materials for lithium-ion batteries: from structure design to electrochemical performance. *Small. Methods.* **2017**, *1*, 1600037. DOI
7. Liu, W.; Zhi, H.; Yu, X. Recent progress in phosphorus based anode materials for lithium/sodium ion batteries. *Energy. Storage. Mater.* **2019**, *16*, 290-322. DOI
8. Zhang, W. A review of the electrochemical performance of alloy anodes for lithium-ion batteries. *J. Power. Sources.* **2011**, *196*, 13-24. DOI

9. Sun, Y.; Zhao, C.; Adair, K. R.; et al. Regulated lithium plating and stripping by a nano-scale gradient inorganic-organic coating for stable lithium metal anodes. *Energy. Environ. Sci.* **2021**, *14*, 4085-94. DOI
10. Cao, C.; Abate, I. I.; Sivonxay, E.; et al. Solid electrolyte interphase on native oxide-terminated silicon anodes for Li-ion batteries. *Joule* **2019**, *3*, 762-81. DOI
11. Wu, H.; Chan, G.; Choi, J. W.; et al. Stable cycling of double-walled silicon nanotube battery anodes through solid-electrolyte interphase control. *Nat. Nanotechnol.* **2012**, *7*, 310-5. DOI
12. Chan, C. K.; Peng, H.; Liu, G.; et al. High-performance lithium battery anodes using silicon nanowires. *Nat. Nanotechnol.* **2007**, *3*, 31-5. DOI
13. Ryu, J.; Chen, T.; Bok, T.; et al. Mechanical mismatch-driven rippling in carbon-coated silicon sheets for stress-resilient battery anodes. *Nat. Commun.* **2018**, *9*, 2924. DOI PubMed PMC
14. Lewis, J. A.; Cavallaro, K. A.; Liu, Y.; Mcdowell, M. T. The promise of alloy anodes for solid-state batteries. *Joule* **2022**, *6*, 1418-30. DOI
15. Chen, S.; Cao, Q.; Tang, B.; et al. Chemomechanical pairing of alloy anodes and solid-state electrolytes. *ACS. Energy. Lett.* **2024**, *9*, 5373-82. DOI
16. Cangaz, S.; Hippauf, F.; Reuter, F. S.; et al. Enabling high-energy solid-state batteries with stable anode interphase by the use of columnar silicon anodes. *Adv. Energy. Mater.* **2020**, *10*, 2001320. DOI
17. Cervera, R. B.; Suzuki, N.; Ohnishi, T.; et al. High performance silicon-based anodes in solid-state lithium batteries. *Energy. Environ. Sci.* **2014**, *7*, 662-6. DOI
18. Zhang, Z.; Li, Y.; Xu, R.; et al. Capturing the swelling of solid-electrolyte interphase in lithium metal batteries. *Science* **2022**, *375*, 66-70. DOI
19. Popovic, J. The importance of electrode interfaces and interphases for rechargeable metal batteries. *Nat. Commun.* **2021**, *12*, 6240. DOI PubMed PMC
20. Weng, S.; Zhang, X.; Yang, G.; et al. Temperature-dependent interphase formation and Li^+ transport in lithium metal batteries. *Nat. Commun.* **2023**, *14*, 4474. DOI PubMed PMC
21. Chen, Y.; He, Q.; Zhao, Y.; et al. Breaking solvation dominance of ethylene carbonate via molecular charge engineering enables lower temperature battery. *Nat. Commun.* **2023**, *14*, 8326. DOI PubMed PMC
22. Xu, X.; Martín-Yerga, D.; Grant, N. E.; et al. Interfacial chemistry effects in the electrochemical performance of silicon electrodes under lithium-ion battery conditions. *Small* **2023**, *19*, 2303442. DOI
23. Zhang, X.; Wang, D.; Qiu, X.; et al. Stable high-capacity and high-rate silicon-based lithium battery anodes upon two-dimensional covalent encapsulation. *Nat. Commun.* **2020**, *11*, 3826. DOI PubMed PMC
24. Mu, T.; Sun, Y.; Wang, C.; et al. Long-life silicon anodes by conformal molecular-deposited polyurea interface for lithium ion batteries. *Nano. Energy.* **2022**, *103*, 107829. DOI
25. Park, B.; Lee, S.; Han, D.; et al. Multiscale hierarchical design of bismuth-carbon anodes for ultrafast-charging sodium-ion full battery. *Appl. Surf. Sci.* **2023**, *614*, 156188. DOI
26. Markevich, E.; Salitra, G.; Aurbach, D. Fluoroethylene carbonate as an important component for the formation of an effective solid electrolyte interphase on anodes and cathodes for advanced Li-ion batteries. *ACS. Energy. Lett.* **2017**, *2*, 1337-45. DOI
27. Adenusi, H.; Chass, G. A.; Passerini, S.; Tian, K. V.; Chen, G. Lithium batteries and the solid electrolyte interphase (SEI)—progress and outlook. *Adv. Energy. Mater.* **2023**, *13*, 2203307. DOI
28. Jing, Y.; Wang, Z.; Guo, H.; et al. Functional-oriented design of gradient composite fluoride interphase for enhanced silicon anode performance. *Chem. Sci.* **2026**, *17*, 9971-81. DOI PubMed PMC
29. Yu, X.; Manthiram, A. Electrode-electrolyte interfaces in lithium-based batteries. *Energy. Environ. Sci.* **2018**, *11*, 527-43. DOI
30. Kondo, J.; Iga, Y.; Otani, K.; et al. Enhanced lithium-ion transport at solid-liquid electrolyte interface via inorganic-rich layer for quasi-solid electrolytes. *J. Phys. Chem. C.* **2025**, *129*, 15231-8. DOI
31. Wu, Q.; Qi, Y. Revealing heterogeneous electric double layer (EDL) structures of localized high-concentration electrolytes (LHCEs) and their impact on solid-electrolyte interphase (SEI) formation in lithium batteries. *Energy. Environ. Sci.* **2025**, *18*, 3036-46. DOI
32. Jorn, R.; Kumar, R.; Abraham, D. P.; Voth, G. A. Atomistic modeling of the electrode-electrolyte interface in Li-ion energy storage systems: electrolyte structuring. *J. Phys. Chem. C.* **2013**, *117*, 3747-61. DOI
33. Dunwell, M.; Yan, Y.; Xu, B. Understanding the influence of the electrochemical double-layer on heterogeneous electrochemical reactions. *Curr. Opin. Chem. Eng.* **2018**, *20*, 151-8. DOI
34. Wu, J. Understanding the electric double-layer structure, capacitance, and charging dynamics. *Chem. Rev.* **2022**, *122*, 10821-59. DOI PubMed
35. Lain, M.; Kendrick, E. Understanding the limitations of lithium ion batteries at high rates. *J. Power. Sources.* **2021**, *493*, 229690. DOI

36. Nangir, M.; Massoudi, A.; Tayebifard, S. A. Investigation of the lithium-ion depletion in the silicon-silicon carbide anode/electrolyte interface in lithium-ion battery via electrochemical impedance spectroscopy. *J. Electroanal. Chem.* **2020**, *873*, 114385. DOI
37. Tateyama, Y.; Gao, B.; Jalem, R.; Haruyama, J. Theoretical picture of positive electrode-solid electrolyte interface in all-solid-state battery from electrochemistry and semiconductor physics viewpoints. *Curr. Opin. Electrochem.* **2019**, *17*, 149-57. DOI
38. Yang, H.; Wu, N. Ionic conductivity and ion transport mechanisms of solid-state lithium-ion battery electrolytes: a review. *Energy. Sci. Eng.* **2022**, *10*, 1643-71. DOI
39. Pan, H.; Wang, L.; Shi, Y.; et al. A solid-state lithium-ion battery with micron-sized silicon anode operating free from external pressure. *Nat. Commun.* **2024**, *15*, 2263. DOI PubMed PMC
40. Huo, H.; Jiang, M.; Bai, Y.; et al. Chemo-mechanical failure mechanisms of the silicon anode in solid-state batteries. *Nat. Mater.* **2024**, *23*, 543-51. DOI PubMed PMC
41. Liu, F.; Zeng, Y.; Li, Z.; et al. A gel polymer electrolyte with multiple hydrogen bonding for pressure-free Ah silicon-based pouch cells. *Nat. Commun.* **2025**, *16*, 11708. DOI PubMed PMC
42. Huang, W.; Wang, J.; Braun, M. R.; et al. Dynamic structure and chemistry of the silicon solid-electrolyte interphase visualized by cryogenic electron microscopy. *Matter* **2019**, *1*, 1232-45. DOI
43. Tian, Y.; Tan, S.; Yang, C.; et al. Tailoring chemical composition of solid electrolyte interphase by selective dissolution for long-life micron-sized silicon anode. *Nat. Commun.* **2023**, *14*, 7247. DOI PubMed PMC
44. Han, X.; Lu, L.; Zheng, Y.; et al. A review on the key issues of the lithium ion battery degradation among the whole life cycle. *eTransportation* **2019**, *1*, 100005. DOI
45. Verma, P.; Maire, P.; Novák, P. A review of the features and analyses of the solid electrolyte interphase in Li-ion batteries. *Electrochim. Acta.* **2010**, *55*, 6332-41. DOI
46. Gao, Y.; Yi, R.; Li, Y. C.; et al. General method of manipulating formation, composition, and morphology of solid-electrolyte interphases for stable Li-alloy anodes. *J. Am. Chem. Soc.* **2017**, *139*, 17359-67. DOI
47. Cai, T.; Sun, Q.; Cao, Z.; et al. Electrolyte additive-controlled interfacial models enabling stable antimony anodes for lithium-ion batteries. *J. Phys. Chem. C.* **2022**, *126*, 20302-13. DOI
48. Kolagatla, S.; Collins, G. A.; Kilpatrick, J. I.; Kargin, E.; Ryan, K. M.; Rodriguez, B. J. Cycle-dependent morphology and surface potential of germanium nanowire anode electrodes. *Chem. Commun.* **2023**, *59*, 9203-6. DOI PubMed
49. Song, C.; Han, S. H.; Moon, H.; Choi, N. S. Unlocking fast-charging capabilities of lithium-ion batteries through liquid electrolyte engineering. *EcoMat* **2024**, *6*, e12476. DOI
50. Takenaka, N.; Bouibes, A.; Yamada, Y.; Nagaoka, M.; Yamada, A. Frontiers in theoretical analysis of solid electrolyte interphase formation mechanism. *Adv. Mater.* **2021**, *33*, 2100574. DOI PubMed
51. He, Y.; Wang, J.; Wang, L.; He, X. Thermodynamic understanding of formation and evolution of solid electrolyte interface in Li-ion batteries. *Batteries. Supercaps.* **2024**, *7*, e202400059. DOI
52. Jeong, I.; Kim, S.; Kim, Y.; et al. Toward long-life high-voltage aqueous Li-ion batteries: from solvation chemistry to solid-electrolyte-interphase layer optimization against electron tunneling effect. *Adv. Mater.* **2024**, *37*, 2412652. DOI
53. Heiskanen, S. K.; Kim, J.; Lucht, B. L. Generation and evolution of the solid electrolyte interphase of lithium-ion batteries. *Joule* **2019**, *3*, 2322-33. DOI
54. Krauss, F. T.; Pantenburg, I.; Roling, B. Transport of ions, molecules, and electrons across the solid electrolyte interphase: what is our current level of understanding? *Adv. Mater. Inter.* **2022**, *9*, 2101891. DOI
55. Nie, K.; Hong, Y.; Qiu, J.; et al. Interfaces between cathode and electrolyte in solid state lithium batteries: challenges and perspectives. *Front. Chem.* **2018**, *6*, 616. DOI PubMed PMC
56. Goodenough, J. B.; Kim, Y. Challenges for rechargeable Li batteries. *Chem. Mater.* **2009**, *22*, 587-603. DOI
57. Delp, S. A.; Borodin, O.; Olguin, M.; Eisner, C. G.; Allen, J. L.; Jow, T. R. Importance of reduction and oxidation stability of high voltage electrolytes and additives. *Electrochim. Acta.* **2016**, *209*, 498-510. DOI
58. Peljo, P.; Girault, H. H. Electrochemical potential window of battery electrolytes: the HOMO-LUMO misconception. *Energy. Environ. Sci.* **2018**, *11*, 2306-9. DOI
59. Peled, E.; Golodnitsky, D.; Ardel, G. Advanced model for solid electrolyte interphase electrodes in liquid and polymer electrolytes. *J. Electrochem. Soc.* **1997**, *144*, L208. DOI
60. Mcbrayer, J. D.; Apblett, C. A.; Harrison, K. L.; Fenton, K. R.; Minteer, S. D. Mechanical studies of the solid electrolyte interphase on anodes in lithium and lithium ion batteries. *Nanotechnology* **2021**, *32*, 502005. DOI PubMed
61. Cao, Z.; Meng, H.; Dou, P.; Wang, C.; Zheng, J.; Xu, X. Effects of solid polymer electrolyte coating on the composition and morphology of the solid electrolyte interphase on Sn anodes. *J. Solid. State. Electrochem.* **2016**, *21*, 955-66. DOI
62. Tian, Y.; An, Y.; Zhang, B. Approaching microsized alloy anodes via solid electrolyte interphase design for advanced rechargeable batteries. *Adv. Energy. Mater.* **2023**, *13*, 2302119. DOI

63. Zhu, D.; Zhu, H.; Wu, H.; Yang, C. Bismuth anode engineering for tomorrow's batteries: a review of cutting-edge strategies. *Energy. Storage. Mater.* **2025**, *75*, 103978. DOI
64. Famprikis, T.; Canepa, P.; Dawson, J. A.; Islam, M. S.; Masquelier, C. Fundamentals of inorganic solid-state electrolytes for batteries. *Nat. Mater.* **2019**, *18*, 1278-91. DOI PubMed
65. Nakayama, M.; Wada, S.; Kuroki, S.; Nogami, M. Factors affecting cyclic durability of all-solid-state lithium polymer batteries using poly(ethylene oxide)-based solid polymer electrolytes. *Energy. Environ. Sci.* **2010**, *3*, 1995. DOI
66. Fullerton, W. R.; Li, C. Y. Compliant solid polymer electrolytes (SPEs) for enhanced anode-electrolyte interfacial stability in all-solid-state lithium-metal batteries (LMBs). *ACS. Appl. Polym. Mater.* **2024**, *6*, 7468-77. DOI PubMed PMC
67. Göttlinger, M.; Amrhein, S.; Piesold, C.; Weller, M.; Peters, S.; Giffin, G. A. Development of silicon polymer electrodes with a hybrid polymer electrolyte for all-solid-state lithium-ion batteries. *J. Electrochem. Soc.* **2023**, *170*, 030541. DOI
68. Han, D. Y.; Han, I. K.; Kwon, J. Y.; et al. Covalently interlocked electrode-electrolyte interface for high-energy-density quasi-solid-state lithium-ion batteries. *Adv. Sci.* **2025**, *12*, 2417143. DOI PubMed PMC
69. Seino, Y.; Ota, T.; Takada, K. High rate capabilities of all-solid-state lithium secondary batteries using $Li_4Ti_5O_{12}$-coated $LiNi_{0.8}Co_{0.15}Al_{0.05}O_2$ and a sulfide-based solid electrolyte. *J. Power. Sources.* **2011**, *196*, 6488-92. DOI
70. Grandjean, M.; Pichardo, M.; Biecher, Y.; Haon, C.; Chenevier, P. Matching silicon-based anodes with sulfide-based solid-state electrolytes for Li-ion batteries. *J. Power. Sources.* **2023**, *580*, 233386. DOI
71. Liu, X.; Zhang, N.; Wang, P.; et al. Ionic conductivity regulating strategies of sulfide solid-state electrolytes. *Energy. Storage. Mater.* **2024**, *72*, 103742. DOI
72. Sakuda, A.; Hayashi, A.; Tatsumisago, M. Sulfide solid electrolyte with favorable mechanical property for all-solid-state lithium battery. *Sci. Rep.* **2013**, *3*, 2261. DOI PubMed PMC
73. Ping, W.; Yang, C.; Bao, Y.; et al. A silicon anode for garnet-based all-solid-state batteries: interfaces and nanomechanics. *Energy. Storage. Mater.* **2019**, *21*, 246-52. DOI
74. Ma, X.; Xu, Y.; Zhang, B.; et al. Garnet Si-$Li_7La_3Zr_2O_{12}$ electrolyte with a durable, low resistance interface layer for all-solid-state lithium metal batteries. *J. Power. Sources.* **2020**, *453*, 227881. DOI
75. Zhu, J.; Xiang, Y.; Zhao, J.; et al. Insights into the local structure, microstructure and ionic conductivity of silicon doped NASICON-type solid electrolyte $Li_{1.3}Al_{0.3}Ti_{1.7}P_3O_{12}$. *Energy. Storage. Mater.* **2022**, *44*, 190-6. DOI
76. Zhai, Y.; Kang, W.; Li, Y.; et al. Insights into interfacial issues of layered oxide cathodes and inorganic solid electrolytes. *Energy. Mater. Adv.* **2025**, *6*, 0163. DOI
77. Wang, A.; Kadam, S.; Li, H.; Shi, S.; Qi, Y. Review on modeling of the anode solid electrolyte interphase (SEI) for lithium-ion batteries. *NPJ. Comput. Mater.* **2018**, *4*, 15. DOI
78. Jeong, W. J.; Wang, C.; Yoon, S. G.; Liu, Y.; Chen, T.; Mcdowell, M. T. Electrochemical behavior of elemental alloy anodes in solid-state batteries. *ACS. Energy. Lett.* **2024**, *9*, 2554-63. DOI PubMed PMC
79. Benitez, L.; Cristancho, D.; Seminario, J.; Martinez De La Hoz, J.; Balbuena, P. Electron transfer through solid-electrolyte-interphase layers formed on Si anodes of Li-ion batteries. *Electrochim. Acta.* **2014**, *140*, 250-7. DOI
80. Wang, Q.; Wang, T.; Zhang, P.; et al. Unraveling lithium-ion transport in solid electrolyte interphase: from composition to interface dynamics via molecular dynamics simulations. *Small* **2025**, *21*, 2503340. DOI
81. Parimalam, B. S.; Macintosh, A. D.; Kadam, R.; Lucht, B. L. Decomposition reactions of anode solid electrolyte interphase (SEI) components with $LiPF_6$. *J. Phys. Chem. C.* **2017**, *121*, 22733-8. DOI
82. Yoon, T.; Milien, M. S.; Parimalam, B. S.; Lucht, B. L. Thermal decomposition of the solid electrolyte interphase (SEI) on silicon electrodes for lithium ion batteries. *Chem. Mater.* **2017**, *29*, 3237-45. DOI
83. Liu, Y.; Guo, K.; Wang, C.; Gao, H. Wrinkling and ratcheting of a thin film on cyclically deforming plastic substrate: Mechanical instability of the solid-electrolyte interphase in Li-ion batteries. *J. Mech. Phys. Solids.* **2019**, *123*, 103-18. DOI
84. Li, J. L.; Wang, Y. N.; Sun, S. Y.; et al. Understanding and regulating the mechanical stability of solid electrolyte interphase in batteries. *Adv. Energy. Mater.* **2024**, *15*, 2403845. DOI
85. Tan, T.; Lee, P.; Marium, M.; Zettsu, N.; Yu, D. Y. W. (3-Aminopropyl)triethoxysilane as an electrolyte additive for enhancing the thermal stability of silicon anode in lithium-ion batteries. *ACS. Appl. Energy. Mater.* **2022**, *5*, 11254-62. DOI
86. Shin, H.; Park, J.; Han, S.; Sastry, A. M.; Lu, W. Component-/structure-dependent elasticity of solid electrolyte interphase layer in Li-ion batteries: Experimental and computational studies. *J. Power. Sources.* **2015**, *277*, 169-79. DOI
87. Lee, Y.; Lee, T.; Hong, J.; et al. Stress relief principle of micron-sized anodes with large volume variation for practical high-energy lithium-ion batteries. *Adv. Funct. Mater.* **2020**, *30*, 2004841. DOI
88. Kamikawa, Y.; Amezawa, K.; Terada, K. Elastic-plastic deformation of a solid electrolyte interface formed by reduction of fluoroethylene carbonate: a nanoindentation and finite element analysis study. *J. Phys. Chem. C.* **2020**, *124*, 22488-95. DOI

89. Kumar, R.; Tokranov, A.; Sheldon, B. W.; et al. In situ and operando investigations of failure mechanisms of the solid electrolyte interphase on silicon electrodes. *ACS. Energy. Lett.* **2016**, *1*, 689-97. DOI
90. Chen, J.; Fan, X.; Li, Q.; et al. Electrolyte design for LiF-rich solid-electrolyte interfaces to enable high-performance microsized alloy anodes for batteries. *Nat. Energy.* **2020**, *5*, 386-97. DOI
91. Yi, X.; Qi, G.; Liu, X.; Depcik, C.; Liu, L. Challenges and strategies toward anode materials with different lithium storage mechanisms for rechargeable lithium batteries. *J. Energy. Storage.* **2024**, *95*, 112480. DOI
92. Liu, Q.; Meng, T.; Yu, L.; et al. Interface engineering to boost thermal safety of microsized silicon anodes in lithium-ion batteries. *Small. Methods.* **2022**, *6*, 2200380. DOI
93. Chen, W.; Liao, Y.; Chen, K.; et al. Stable and high-rate silicon anode enabled by artificial poly(acrylonitrile)-sulfur interface engineering for advanced lithium-ion batteries. *J. Electroanal. Chem.* **2023**, *929*, 117093. DOI
94. Zhang, Q.; Xiao, X.; Zhou, W.; Cheng, Y. T.; Verbrugge, M. W. Toward high cycle efficiency of silicon-based negative electrodes by designing the solid electrolyte interphase. *Adv. Energy. Mater.* **2014**, *5*, 1401398. DOI
95. Wang, P.; Yang, H.; Ding, H.; Zhang, N.; Zhao, D.; Li, S. Application of in-situ characterization techniques and artificial intelligence-assisted analysis in studying electrode/electrolyte interface of batteries. *Mater. Scie. Eng. R. Rep.* **2026**, *168*, 101154. DOI
96. Ranque, P.; Gonzalo, E.; Armand, M.; Shanmukaraj, D. Performance-based materials evaluation for Li batteries through impedance spectroscopy: a critical review. *Mater. Today. Energy.* **2023**, *34*, 101283. DOI
97. Minato, T.; Abe, T. Surface and interface sciences of Li-ion batteries. *Prog. Surf. Sci.* **2017**, *92*, 240-80. DOI
98. Hikima, K.; Shimizu, K.; Kiuchi, H.; et al. Operando analysis of electronic band structure in an all-solid-state thin-film battery. *Commun. Chem.* **2022**, *5*, 52. DOI PubMed PMC
99. Schroder, K. W.; Dylla, A. G.; Harris, S. J.; Webb, L. J.; Stevenson, K. J. Role of surface oxides in the formation of solid-electrolyte interphases at silicon electrodes for lithium-ion batteries. *ACS. Appl. Mater. Interfaces.* **2014**, *6*, 21510-24. DOI PubMed
100. Muñoz-MÁrquez, MÁ.; Zarrabeitia, M.; Passerini, S.; Rojo, T. Structure, composition, transport properties, and electrochemical performance of the electrode-electrolyte interphase in non-aqueous Na-ion batteries. *Adv. Mater. Inter.* **2022**, *9*, 2101773. DOI
101. Luo, H.; Zhang, B.; Zhang, H.; et al. Full-dimensional analysis of electrolyte decomposition on cathode-electrolyte interface: establishing characterization paradigm on $LiNi_{0.6}Co_{0.2}Mn_{0.2}O_2$ cathode with potential dependence. *J. Phys. Chem. Lett.* **2023**, *14*, 4565-74. DOI
102. Lee, C. R.; Jang, H. Y.; Leem, H. J.; et al. Surface work function-induced thermally vulnerable solid electrolyte interphase formation on the negative electrode for lithium-ion batteries. *Adv. Energy. Mater.* **2023**, *14*, 2302906. DOI
103. Huang, L. B.; Zhao, L.; Ma, Z. F.; et al. Vertically fluorinated graphene encapsulated SiO_x anode for enhanced Li^+ transport and interfacial stability in high-energy-density lithium batteries. *Angew. Chem. Int. Ed.* **2024**, *63*, e202413600. DOI
104. Cheng, K.; Tu, S.; Zhang, B.; et al. Material–electrolyte interfacial interaction enabling the formation of an inorganic-rich solid electrolyte interphase for fast-charging Si-based lithium-ion batteries. *Energy. Environ. Sci.* **2024**, *17*, 2631-41. DOI
105. Fang, J.; Wu, K.; Qin, L.; Li, J.; Li, A.; Feng, H. Reversible silicon anodes enabled by fluorinated inorganic-organic hybrid coating. *J. Colloid. Interface. Sci.* **2025**, *679*, 819-29. DOI
106. Cho, Y. J.; Kim, H. S.; Im, H.; et al. Nitrogen-doped graphitic layers deposited on silicon nanowires for efficient lithium-ion battery anodes. *J. Phys. Chem. C.* **2011**, *115*, 9451-7. DOI
107. Yeom, S. J.; Wi, T.; Ko, S.; et al. Nitrogen plasma-assisted functionalization of silicon/graphite anodes to enable fast kinetics. *ACS. Appl. Mater. Interfaces.* **2022**, *14*, 5237-46. DOI
108. Song, T.; Kil, K. C.; Jeon, Y.; et al. Nitridated Si-Ti-Ni alloy as an anode for Li rechargeable batteries. *J. Power. Sources.* **2014**, *253*, 282-6. DOI
109. Ham, S.; Sebti, E.; Cronk, A.; et al. Overcoming low initial coulombic efficiencies of Si anodes through prelithiation in all-solid-state batteries. *Nat. Commun.* **2024**, *15*, 2991. DOI PubMed PMC
110. Wang, G.; Li, F.; Liu, D.; et al. High performance lithium-ion and lithium-sulfur batteries using prelithiated phosphorus/carbon composite anode. *Energy. Storage. Mater.* **2020**, *24*, 147-52. DOI
111. Bai, S.; Bao, W.; Qian, K.; et al. Elucidating the role of prelithiation in Si-based anodes for interface stabilization. *Adv. Energy. Mater.* **2023**, *13*, 2301041. DOI
112. Zhang, Q.; Cui, Y.; Wang, E. First-principles approaches to simulate lithiation in silicon electrodes. *Model. Simul. Mater. Sci. Eng.* **2013**, *21*, 074001. DOI
113. Kim, H. J.; Choi, S.; Lee, S. J.; et al. Controlled prelithiation of silicon monoxide for high performance lithium-ion rechargeable full cells. *Nano. Lett.* **2015**, *16*, 282-8. DOI
114. Jang, J.; Kang, I.; Choi, J.; et al. Molecularly tailored lithium-arene complex enables chemical prelithiation of high-capacity lithium-ion battery anodes. *Angew. Chem. Int. Ed.* **2020**, *59*, 14473-80. DOI

115. Lee, J.; Jin, D.; Kim, J. Y.; et al. Dry pre-lithiation for graphite-silicon diffusion-dependent electrode for all-solid-state battery. *Adv. Energy. Mater.* **2023**, *13*, 2300172. DOI
116. Yang, C.; Ma, H.; Yuan, R.; et al. Roll-to-roll prelithiation of lithium-ion battery anodes by transfer printing. *Nat. Energy.* **2023**, *8*, 703-13. DOI
117. Bera, B.; Chakraborty, A.; Kar, T.; Leuaa, P.; Neergat, M. Density of states, carrier concentration, and flat band potential derived from electrochemical impedance measurements of N-doped carbon and their influence on electrocatalysis of oxygen reduction reaction. *J. Phys. Chem. C.* **2017**, *121*, 20850-6. DOI
118. Zhou, E.; Jin, H.; Lv, H.; et al. Solid-state electrocatalysis in heteroatom-doped alloy anode enables ultrafast charge lithium-ion batteries. *J. Am. Chem. Soc.* **2024**, *146*, 20700-8. DOI
119. Zhang, F.; Luo, W.; Yang, J. Interface heteroatom-doping: emerging solutions to silicon-based anodes. *Chem. Asian. J.* **2020**, *15*, 1394-404. DOI PubMed
120. Lv, G.; Zhu, B.; Li, X.; et al. Simultaneous perforation and doping of Si nanoparticles for lithium-ion battery anode. *ACS. Appl. Mater. Interfaces.* **2017**, *9*, 44452-7. DOI
121. Schnabel, M.; Harvey, S. P.; Arca, E.; et al. Surface SiO_2 thickness controls uniform-to-localized transition in lithiation of silicon anodes for lithium-ion batteries. *ACS. Appl. Mater. Interfaces.* **2020**, *12*, 27017-28. DOI
122. Kwon, J. Y.; Cho, Y.; Heo, J. J.; et al. Highly conductive locally graphitized sheath on fibrous micro-Si anode for high-energy Li-ion battery. *J. Power. Sources.* **2025**, *660*, 238530. DOI
123. Schroder, K.; Alvarado, J.; Yersak, T. A.; et al. The effect of fluoroethylene carbonate as an additive on the solid electrolyte interphase on silicon lithium-ion electrodes. *Chem. Mater.* **2015**, *27*, 5531-42. DOI
124. Li, Q.; Liu, X.; Han, X.; et al. Identification of the solid electrolyte interface on the Si/C composite anode with fec as the additive. *ACS. Appl. Mater. Interfaces.* **2019**, *11*, 14066-75. DOI
125. Etacheri, V.; Haik, O.; Goffer, Y.; et al. Effect of fluoroethylene carbonate (FEC) on the performance and surface chemistry of Si-nanowire Li-ion battery anodes. *Langmuir* **2011**, *28*, 965-76. DOI
126. Li, Y.; Cao, Z.; Wang, Y.; et al. New insight into the role of fluoro-ethylene carbonate in suppressing Li-trapping for Si anodes in lithium-ion batteries. *ACS. Energy. Lett.* **2023**, *8*, 4193-203. DOI
127. Gu, M.; Wang, Z.; Connell, J. G.; et al. Electronic origin for the phase transition from amorphous Li_xSi to crystalline $Li_{15}Si_4$. *ACS. Nano.* **2013**, *7*, 6303-9. DOI
128. Xu, Z.; Yang, J.; Qian, J.; et al. Bicomponent electrolyte additive excelling fluoroethylene carbonate for high performance Si-based anodes and lithiated Si-S batteries. *Energy. Storage. Mater.* **2019**, *20*, 388-94. DOI
129. Chen, L.; Wang, K.; Xie, X.; Xie, J. Effect of vinylene carbonate (VC) as electrolyte additive on electrochemical performance of Si film anode for lithium ion batteries. *J. Power. Sources.* **2007**, *174*, 538-43. DOI
130. De La Hoz JM, Balbuena PB. Reduction mechanisms of additives on Si anodes of Li-ion batteries. *Phys. Chem. Chem. Phys.* **2014**, *16*, 17091-8. DOI PubMed
131. Lin, L.; Yang, K.; Chen, H.; Pan, F. *In situ* atomic force microscope observing the effect of vinylene carbonate on the formation of solid-electrolyte interphase layer during the initial cycle. *Funct. Mater. Lett.* **2017**, *10*, 1750052. DOI
132. Yang, Y.; Xiong, J.; Lai, S.; et al. Vinyl ethylene carbonate as an effective SEI-forming additive in carbonate-based electrolyte for lithium-metal anodes. *ACS. Appl. Mater. Interfaces.* **2019**, *11*, 6118-25. DOI
133. Chalasani, D.; Li, J.; Jackson, N. M.; Payne, M.; Lucht, B. L. Methylene ethylene carbonate: novel additive to improve the high temperature performance of lithium ion batteries. *J. Power. Sources.* **2012**, *208*, 67-73. DOI
134. Park, S.; Jeong, S. Y.; Lee, T. K.; et al. Replacing conventional battery electrolyte additives with dioxolone derivatives for high-energy-density lithium-ion batteries. *Nat. Commun.* **2021**, *12*, 838. DOI PubMed PMC
135. Li, A.; Wang, Z.; Pollard, T. P.; et al. High voltage electrolytes for lithium-ion batteries with micro-sized silicon anodes. *Nat. Commun.* **2024**, *15*, 1206. DOI PubMed PMC
136. Yang, W.; Li, S.; Liu, Y.; et al. Selective interfacial polymerization improves reversibility of Si anodes. *Chem. Eng. J.* **2025**, *514*, 163168. DOI
137. Ma, Z.; Ruan, D.; Wang, D.; et al. Selective methylation of cyclic ether towards highly elastic solid electrolyte interphase for silicon-based anodes. *Angew. Chem. Int. Ed.* **2024**, *64*, e202414859. DOI
138. Zeng, G.; An, Y.; Xiong, S.; Feng, J. Nonflammable fluorinated carbonate electrolyte with high salt-to-solvent ratios enables stable silicon-based anode for next-generation lithium-ion batteries. *ACS. Appl. Mater. Interfaces.* **2019**, *11*, 23229-35. DOI
139. Chang, K.; Bui, T. A. N.; Niu, R.; Chen, Y.; Su, Y. Coral-shaped AlSi anode materials for Li-ion batteries enabled by THF-based electrolyte. *J. Energy. Storage.* **2024**, *96*, 112597. DOI
140. Hu, D.; Wu, C.; He, Q.; et al. Novel strategies for constructing highly efficient silicon/carbon anodes: chemical prelithiation and electrolyte post-treatment. *J. Colloid. Interface. Sci.* **2025**, *688*, 215-24. DOI

141. Veith, G. M.; Doucet, M.; Sacci, R. L.; Vacaliuc, B.; Baldwin, J. K.; Browning, J. F. Determination of the solid electrolyte interphase structure grown on a silicon electrode using a fluoroethylene carbonate additive. *Sci. Rep.* **2017**, *7*, 6326. DOI PubMed PMC
142. Yang, G.; Frisco, S.; Tao, R.; et al. Robust solid/electrolyte interphase (SEI) formation on Si anodes using glyme-based electrolytes. *ACS. Energy. Lett.* **2021**, *6*, 1684-93. DOI
143. Lin, F.; Tran, N. T. T.; Hsu, W. Effect of 1,3-propane sultone on the formation of solid electrolyte interphase at Li-ion battery anode surface: a first-principles study. *ACS. Omega.* **2020**, *5*, 13541-7. DOI PubMed PMC
144. Liu, X.; Zhang, T.; Shi, X.; et al. Hierarchical sulfide-rich modification layer on SiO/C anode for low-temperature Li-ion batteries. *Adv. Sci.* **2022**, *9*, 2104531. DOI PubMed PMC
145. Tian, M.; Jin, Z.; Song, Z.; et al. Domino reactions enabling sulfur-mediated gradient interphases for high-energy lithium batteries. *J. Am. Chem. Soc.* **2023**, *145*, 21600-11. DOI
146. Piñuela-noval, J.; Fernández-González, D.; Brutti, S.; et al. Metal carbide additives in graphite-silicon composites for lithium-ion batteries. *ChemElectroChem* **2023**, *10*, e202300339. DOI
147. Uppuluri, R.; Lapidus, S. H.; Zhang, Y.; Vaughey, J. T.; Dogan, F.; Key, B. Electrochemical formation of Li-M-(M′)-Si phases using multivalent electrolyte salt additives. *J. Electrochem. Soc.* **2023**, *170*, 030501. DOI
148. Han, G.; Lee, J.; Choi, J. W.; Park, J. Tris(pentafluorophenyl) borane as an electrolyte additive for high performance silicon thin film electrodes in lithium ion batteries. *Electrochim. Acta.* **2011**, *56*, 8997-9003. DOI
149. Wu, R.; Du, X.; Liu, T.; et al. Robust and fast-ion conducting interphase empowering SiO_x anode toward high energy lithium-ion batteries. *Adv. Energy. Mater.* **2023**, *14*, 2302899. DOI
150. Asheim, K.; Holsen, I. F.; Renmann, V.; et al. Enabling the use of lithium bis(trifluoromethanesulfonyl)imide as electrolyte salt for Li-ion batteries based on silicon anodes and $Li(Ni_{0.4}Co_{0.4}Mn_{0.2})O_2$ cathodes by salt additives. *Batteries. Supercaps.* **2024**, *7*, e202300541. DOI
151. Rynearson, L.; Jayawardana, C.; Yeddala, M.; Lucht, B. L. Improved performance of silicon-containing anodes with organic solvent-solubilized lithium nitrate. *J. Electrochem. Soc.* **2023**, *170*, 060525. DOI
152. Park, S.; Liu, H.; Quinn, J.; et al. Surface and bulk stabilization of silicon anodes with mixed-multivalent additives: $Ca(TFSI)_2$ and $Mg(TFSI)_2$. *ACS. Appl. Mater. Interfaces.* **2024**, *16*, 20341-51. DOI
153. Zhang, Y.; Li, X.; Sivonxay, E.; et al. Silicon anodes with improved calendar life enabled by multivalent additives. *Adv. Energy. Mater.* **2021**, *11*, 2101820. DOI
154. Xu, N.; Sun, Y.; Shi, J.; et al. Fluorinated cyclic siloxane additives for high energy density Li-ion batteries with high nickel cathodes and silicon-carbon anodes. *J. Power. Sources.* **2021**, *511*, 230437. DOI
155. Wei, L.; Jin, Z.; Lu, J.; et al. In-situ construction of hybrid artificial SEI with fluorinated siloxane to enable dendrite-free Li metal anodes. *J. Materiomics.* **2023**, *9*, 318-27. DOI
156. Wang, B.; Ryu, J.; Choi, S.; et al. Ultrafast-charging silicon-based coral-like network anodes for lithium-ion batteries with high energy and power densities. *ACS. Nano.* **2019**, *13*, 2307-15. DOI
157. Tan, W.; Yang, F.; Lu, Z.; Xu, Z. A design strategy of carbon coatings on silicon nanoparticles as anodes of high-performance lithium-ion batteries. *ACS. Appl. Energy. Mater.* **2022**, *5*, 12143-50. DOI
158. Fu, K.; Xue, L.; Yildiz, O.; et al. Effect of CVD carbon coatings on Si@CNF composite as anode for lithium-ion batteries. *Nano. Energy.* **2013**, *2*, 976-86. DOI
159. Qi, C.; Li, S.; Yang, Z.; et al. Suitable thickness of carbon coating layers for silicon anode. *Carbon* **2022**, *186*, 530-8. DOI
160. Wang, B.; Ryu, J.; Choi, S.; et al. Folding graphene film yields high areal energy storage in lithium-ion batteries. *ACS. Nano.* **2018**, *12*, 1739-46. DOI
161. Lu, Y.; Ye, Z.; Zhao, Y.; et al. Graphene supported double-layer carbon encapsulated silicon for high-performance lithium-ion battery anode materials. *Carbon* **2023**, *201*, 962-71. DOI
162. Zhang, C.; Peng, X.; Guo, Z.; et al. Carbon-coated SnO_2/graphene nanosheets as highly reversible anode materials for lithium ion batteries. *Carbon* **2012**, *50*, 1897-903. DOI
163. Son, I. H.; Hwan, Park. J.; Kwon, S.; et al. Silicon carbide-free graphene growth on silicon for lithium-ion battery with high volumetric energy density. *Nat. Commun.* **2015**, *6*, 7393. DOI PubMed PMC
164. Li, Z.; Zhao, Z.; Pan, S.; et al. Covalent coating of micro-sized silicon with dynamically bonded graphene layers toward stably cycled lithium storage. *Adv. Energy. Mater.* **2023**, *13*, 2300874. DOI
165. Bischof, K.; Flügel, M.; Hölzle, M.; Wohlfahrt-Mehrens, M.; Waldmann, T. Aging mechanism for calendar aging of Li-ion cells with Si/graphite anodes. *J. Electrochem. Soc.* **2024**, *171*, 010510. DOI
166. Mcbrayer, J. D.; Rodrigues, M. F.; Schulze, M. C.; et al. Calendar aging of silicon-containing batteries. *Nat. Energy.* **2021**, *6*, 866-72. DOI

167. Sun, K.; Zhang, Z.; Fu, K.; et al. Tracing the origins of calendar aging in Si-containing lithium-ion batteries. *Nano. Lett.* **2025**, *25*, 931-8. DOI
168. Xu, Y.; Zhang, Y.; Hu, Q.; et al. In situ copper coating on silicon particles enables long durable anodes in lithium-ion batteries. *ACS. Appl. Mater. Interfaces.* **2024**, *16*, 5058-66. DOI
169. Wang, F.; Xu, S.; Zhu, S.; et al. Ni-coated Si microchannel plate electrodes in three-dimensional lithium-ion battery anodes. *Electrochim. Acta.* **2013**, *87*, 250-5. DOI
170. Baek, S.; Park, J.; Jeong, Y.; Kim, J. H. Facile synthesis of Ag-coated silicon nanowires as anode materials for high-performance rechargeable lithium battery. *J. Alloys. Compd.* **2016**, *660*, 387-91. DOI
171. Lotfabad, E. M.; Kalisvaart, P.; Kohandehghan, A.; et al. Si nanotubes ALD coated with TiO_2, TiN or Al_2O_3 as high performance lithium ion battery anodes. *J. Mater. Chem. A.* **2014**, *2*, 13746. DOI
172. Zhu, H.; Shiraz, M. H. A.; Liu, L.; Hu, Y.; Liu, J. A facile and low-cost Al_2O_3 coating as an artificial solid electrolyte interphase layer on graphite/silicon composites for lithium-ion batteries. *Nanotechnology* **2021**, *32*, 144001. DOI
173. Jeong, G.; Kim, J.; Kim, Y.; Kim, Y. Multifunctional TiO_2 coating for a SiO anode in Li-ion batteries. *J. Mater. Chem.* **2012**, *22*, 7999. DOI
174. Bai, Y.; Yan, D.; Yu, C.; et al. Core-shell Si@TiO_2 nanosphere anode by atomic layer deposition for Li-ion batteries. *J. Power. Sources.* **2016**, *308*, 75-82. DOI
175. Yang, L. Y.; Li, H. Z.; Liu, J.; Sun, Z. Q.; Tang, S. S.; Lei, M. Dual yolk-shell structure of carbon and silica-coated silicon for high-performance lithium-ion batteries. *Sci. Rep.* **2015**, *5*, 10908. DOI PubMed PMC
176. Chen, T.; Wu, J.; Zhang, Q.; Su, X. Recent advancement of SiO_x based anodes for lithium-ion batteries. *J. Power. Sources.* **2017**, *363*, 126-44. DOI
177. Sim, S.; Oh, P.; Park, S.; Cho, J. Critical thickness of SiO_2 coating layer on core@shell bulk@nanowire Si anode materials for Li-ion batteries. *Adv. Mater.* **2013**, *25*, 4498-503. DOI PubMed
178. Sung, J.; Ma, J.; Choi, S. H.; et al. Fabrication of lamellar nanosphere structure for effective stress-management in large-volume-variation anodes of high-energy lithium-ion batteries. *Adv. Mater.* **2019**, *31*, 1900970. DOI
179. Li, K.; Jiang, Z.; Guo, L.; et al. Polyhedral oligomeric silsesquioxane-based SiOC coating for robust silicon nanoparticle anodes in lithium-ion batteries. *ACS. Appl. Energy. Mater.* **2025**, *8*, 7052-60. DOI
180. Wang, W.; Wang, Y.; Huang, W.; et al. *In situ* developed Si@polymethyl methacrylate capsule as a Li-ion battery anode with high-rate and long cycle-life. *ACS. Appl. Mater. Interfaces.* **2021**, *13*, 6919-29. DOI
181. Ai, Q.; Fang, Q.; Liang, J.; et al. Lithium-conducting covalent-organic-frameworks as artificial solid-electrolyte-interphase on silicon anode for high performance lithium ion batteries. *Nano. Energy.* **2020**, *72*, 104657. DOI
182. Li, X.; Liu, W.; Wang, Y.; et al. Decorating silicon surface by an electroactive covalent organic framework to develop high-performance lithium-ion batteries. *Energy. Storage. Mater.* **2024**, *66*, 103207. DOI
183. Han, D. Y.; Han, I. K.; Son, J.; et al. Molecular engineering of coacervate network binders for stable silicon-based anodes in lithium-ion batteries. *Adv. Funct. Mater.* **2025**, *35*, e09445. DOI
184. Kwon, J. Y.; Lyu, J.; Kim, E.; et al. Assembling a dense grid structure with green polyhydroxyurethane and a high-capacity Si-based anode for lithium ion batteries. *J. Mater. Chem. A.* **2024**, *12*, 15996-6006. DOI
185. Balqis, F.; Eldona, C.; Laksono, B. T.; et al. Conductive polymer frameworks in silicon anodes for advanced lithium-ion batteries. *ACS. Appl. Polym. Mater.* **2023**, *5*, 4933-52. DOI
186. Yu, Y.; Zhu, J.; Zeng, K.; Jiang, M. Mechanically robust and superior conductive n-type polymer binders for high-performance micro-silicon anodes in lithium-ion batteries. *J. Mater. Chem. A.* **2021**, *9*, 3472-81. DOI
187. Pan, S.; Han, J.; Wang, Y.; et al. Integrating SEI into layered conductive polymer coatings for ultrastable silicon anodes. *Adv. Mater.* **2022**, *34*, 2203617. DOI
188. Yu, Y.; Yang, C.; Jiang, Y.; et al. Sponge-like porous-conductive polymer coating for ultrastable silicon anodes in lithium-ion batteries. *Small* **2023**, *19*, 2303779. DOI
189. Wu, M.; Xiao, X.; Vukmirovic, N.; et al. Toward an ideal polymer binder design for high-capacity battery anodes. *J. Am. Chem. Soc.* **2013**, *135*, 12048-56. DOI
190. Zhu, T.; Sternlicht, H.; Ha, Y.; et al. Formation of hierarchically ordered structures in conductive polymers to enhance the performances of lithium-ion batteries. *Nat. Energy.* **2023**, *8*, 129-37. DOI
191. Han, D.; Han, I. K.; Jang, H. Y.; et al. Interface engineering of Si-based anodes with fluorinated binder enabling lean-additive lithium-ion batteries. *Energy. Storage. Mater.* **2024**, *65*, 103176. DOI
192. Cao, D.; Ji, T.; Singh, A.; et al. Unveiling the mechanical and electrochemical evolution of nanosilicon composite anodes in sulfide-based all-solid-state batteries. *Adv. Energy. Mater.* **2023**, *13*, 2203969. DOI

193. Piper, D. M.; Yersak, T. A.; Lee, S. Effect of compressive stress on electrochemical performance of silicon anodes. *J. Electrochem. Soc.* **2012**, *160*, A77-81. DOI
194. Endo, R.; Ohnishi, T.; Takada, K.; Masuda, T. *In situ* observation of lithiation and delithiation reactions of a silicon thin film electrode for all-solid-state lithium-ion batteries by X-ray photoelectron spectroscopy. *J. Phys. Chem. Lett.* **2020**, *11*, 6649-54. DOI PubMed
195. Andersson, E. K. W.; Sångeland, C.; Berggren, E.; et al. Early-stage decomposition of solid polymer electrolytes in Li-metal batteries. *J. Mater. Chem. A.* **2021**, *9*, 22462-71. DOI
196. Narayanan, S.; Ulissi, U.; Gibson, J. S.; Chart, Y. A.; Weatherup, R. S.; Pasta, M. Effect of current density on the solid electrolyte interphase formation at the lithium|Li_6PS_5Cl interface. *Nat. Commun.* **2022**, *13*, 7237. DOI PubMed PMC
197. Tan, D. H. S.; Wu, E. A.; Nguyen, H.; et al. Elucidating reversible electrochemical redox of Li_6PS_5Cl solid electrolyte. *ACS. Energy. Lett.* **2019**, *4*, 2418-27. DOI
198. Kim, J.; Kim, C.; Jang, I.; et al. Si nanoparticles embedded in carbon nanofiber sheathed with Li_6PS_5Cl as an anode material for all-solid-state batteries. *J. Power. Sources.* **2021**, *510*, 230425. DOI
199. Zhang, W.; Lu, Y.; Wan, L.; et al. Engineering a passivating electric double layer for high performance lithium metal batteries. *Nat. Commun.* **2022**, *13*, 2029. DOI PubMed PMC
200. Wu, Q.; Mcdowell, M. T.; Qi, Y. Effect of the electric double layer (EDL) in multicomponent electrolyte reduction and solid electrolyte interphase (SEI) formation in lithium batteries. *J. Am. Chem. Soc.* **2023**, *145*, 2473-84. DOI PubMed PMC
201. Yuan, X.; Cheng, D.; Liu, B.; et al. Engineering battery corrosion films by tuning electrical double layer composition. *Joule* **2024**, *8*, 3038-53. DOI
202. Sun, S.; Zhang, X.; Wang, Y.; Li, J.; Zheng, Z.; Huang, J. Understanding the transport mechanism of lithium ions in solid-electrolyte interphase in lithium metal batteries with liquid electrolytes. *Mater. Today.* **2024**, *77*, 39-65. DOI
203. Kim, J.; Yu, S.; Park, H.; et al. A uniform lithium ion flux and robust interphase enabled by an anion anchoring additive for high energy density Si-based anodes. *J. Mater. Chem. A.* **2026**, *14*, 17831-45. DOI
204. Borodin, O.; Ren, X.; Vatamanu, J.; Von Wald Cresce, A.; Knap, J.; Xu, K. Modeling insight into battery electrolyte electrochemical stability and interfacial structure. *Acc. Chem. Res.* **2017**, *50*, 2886-94. DOI PubMed
205. Li, L.; Fang, C.; Wei, W.; et al. Nano-ordered structure regulation in delithiated Si anode triggered by homogeneous and stable Li-ion diffusion at the interface. *Nano. Energy.* **2020**, *72*, 104651. DOI
206. Tao, H.; Lian, C.; Liu, H. Multiscale modeling of electrolytes in porous electrode: from equilibrium structure to non-equilibrium transport. *Green. Energy. Environ.* **2020**, *5*, 303-21. DOI
207. Burt, R.; Birkett, G.; Zhao, X. S. A review of molecular modelling of electric double layer capacitors. *Phys. Chem. Chem. Phys.* **2014**, *16*, 6519. DOI PubMed
208. Funari, R.; Matsumoto, A.; De Bruyn, J. R.; Shen, A. Q. Rheology of the electric double layer in electrolyte solutions. *Anal. Chem.* **2020**, *92*, 8244-53. DOI PubMed
209. Kang, J.; Lee, I.; Yu, G.; et al. Dual-ionic weakly solvating electrolyte design enables efficient fast-cycling of high-voltage anion shuttle batteries. *Adv. Sci.* **2025**, *12*, e05982. DOI PubMed PMC
210. Chang, C.; Yao, Y.; Li, R.; et al. Stable lithium metal batteries enabled by localized high-concentration electrolytes with sevoflurane as a diluent. *J. Mater. Chem. A.* **2022**, *10*, 9001-9. DOI
211. Efaw, C. M.; Wu, Q.; Gao, N.; et al. Localized high-concentration electrolytes get more localized through micelle-like structures. *Nat. Mater.* **2023**, *22*, 1531-9. DOI
212. Swamy, T.; Chiang, Y. Electrochemical charge transfer reaction kinetics at the silicon-liquid electrolyte interface. *J. Electrochem. Soc.* **2015**, *162*, A7129-34. DOI
213. Chen, X.; Wang, B.; Ye, Y.; Liang, J.; Kong, J. Design of electrodes and electrolytes for silicon-based anode lithium-ion batteries. *Energy. Environ. Mater.* **2024**, *8*, e12838. DOI
214. Xu, X.; Liu, Y.; Hwang, J. Y.; et al. Role of Li-ion depletion on electrode surface: underlying mechanism for electrodeposition behavior of lithium metal anode. *Adv. Energy. Mater.* **2020**, *10*, 2002390. DOI
215. Lee, Y.; Lin, C.; Pai, K.; Chen, C. Control strategy and verification of reducing battery polarization characteristics to improve unmanned aerial vehicles endurance. *J. Power. Sources.* **2024**, *591*, 233787. DOI
216. An, S. J.; Li, J.; Daniel, C.; Mohanty, D.; Nagpure, S.; Wood, D. L. The state of understanding of the lithium-ion-battery graphite solid electrolyte interphase (SEI) and its relationship to formation cycling. *Carbon* **2016**, *105*, 52-76. DOI
217. Yoon, T.; Chapman, N.; Seo, D. M.; Lucht, B. L. Lithium salt effects on silicon electrode performance and solid electrolyte interphase (SEI) structure, role of solution structure on SEI formation. *J. Electrochem. Soc.* **2017**, *164*, A2082-8. DOI
218. Cao, Z.; Zheng, X.; Zhou, M.; et al. Electrolyte solvation engineering toward high-rate and low-temperature silicon-based batteries. *ACS. Energy. Lett.* **2022**, *7*, 3581-92. DOI

219. Dong, S.; Shi, L.; Geng, S.; et al. Breaking solvation dominance effect enabled by ion-dipole interaction toward long-spanlife silicon oxide anodes in lithium-ion batteries. *Nano. Micro. Lett.* **2024**, *17*, 95. DOI PubMed PMC
220. Chen, C.; Zhou, T.; Danilov, D. L.; et al. Impact of dual-layer solid-electrolyte interphase inhomogeneities on early-stage defect formation in Si electrodes. *Nat. Commun.* **2020**, *11*, 3283. DOI PubMed PMC
221. An, J.; Kim, Y.; Woo, H. K.; Choi, Y.; Oh, S. J.; Lee, J. Electrolyte solvents as architects: how solvents guide the spontaneous formation of 3D porous nanostructures in alloy- and conversion-type battery anodes. *Energy. Storage. Mater.* **2024**, *70*, 103478. DOI
222. Liu, G.; Xia, M.; Gao, J.; et al. Dual-salt localized high-concentration electrolyte for long cycle life silicon-based lithium-ion batteries. *ACS. Appl. Mater. Interfaces.* **2023**, *15*, 3586-98. DOI
223. Luo, W.; Chen, X.; Xia, Y.; et al. Surface and interface engineering of silicon-based anode materials for lithium-ion batteries. *Adv. Energy. Mater.* **2017**, *7*, 1701083. DOI
224. Chan, C. K.; Ruffo, R.; Hong, S. S.; Cui, Y. Surface chemistry and morphology of the solid electrolyte interphase on silicon nanowire lithium-ion battery anodes. *J. Power. Sources.* **2009**, *189*, 1132-40. DOI
225. Saverina, E. A.; Sivasankaran, V.; Kapaev, R. R.; et al. An environment-friendly approach to produce nanostructured germanium anodes for lithium-ion batteries. *Green. Chem.* **2020**, *22*, 359-67. DOI
226. Chen, Z.; Cao, Y.; Qian, J.; Ai, X.; Yang, H. Antimony-coated SiC nanoparticles as stable and high-capacity anode materials for Li-ion batteries. *J. Phys. Chem. C.* **2010**, *114*, 15196-201. DOI
227. Zhu, G.; Luo, D.; Chen, X.; Yang, J.; Zhang, H. Emerging multiscale porous anodes toward fast charging lithium-ion batteries. *ACS. Nano.* **2023**, *17*, 20850-74. DOI
228. Yang, Z.; Chen, T.; Chen, D.; et al. A Ge/carbon atomic-scale hybrid anode material: a micro-nano gradient porous structure with high cycling stability. *Angew. Chem. Int. Ed.* **2021**, *60*, 12539-46. DOI
229. Cho, Y.; Park, H.; Lee, J.; et al. Organogel electrolyte for high-loading silicon batteries. *J. Mater. Chem. A.* **2016**, *4*, 8005-9. DOI
230. Kotobuki, M.; Okada, N.; Kanamura, K. Design of a micro-pattern structure for a three dimensionally macroporous Sn-Ni alloy anode with high areal capacity. *Chem. Commun.* **2011**, *47*, 6144. DOI PubMed
231. Nelson, D. L.; Sandoval, S. E.; Pyo, J.; et al. Fracture dynamics in silicon anode solid-state batteries. *ACS. Energy. Lett.* **2024**, *9*, 6085-95. DOI PubMed PMC
232. He, S.; Huang, S.; Liu, X.; et al. Interfacial self-healing polymer electrolytes for long-cycle silicon anodes in high-performance solid-state lithium batteries. *J. Colloid. Interface. Sci.* **2024**, *665*, 299-312. DOI
233. Balaish, M.; Kim, K. J.; Chu, H.; et al. Emerging processing guidelines for solid electrolytes in the era of oxide-based solid-state batteries. *Chem. Soc. Rev.* **2025**, *54*, 8925-9007. DOI
234. Tao, J.; Han, J.; Wu, Y.; et al. Unraveling the performance decay of micro-sized silicon anodes in sulfide-based solid-state batteries. *Energy. Storage. Mater.* **2024**, *64*, 103082. DOI
235. Stewart, D. M.; Pearse, A. J.; Kim, N. S.; et al. Tin oxynitride anodes by atomic layer deposition for solid-state batteries. *Chem. Mater.* **2018**, *30*, 2526-34. DOI
236. Gu, L.; Han, J.; Chen, M.; et al. Enabling robust structural and interfacial stability of micron-Si anode toward high-performance liquid and solid-state lithium-ion batteries. *Energy. Storage. Mater.* **2022**, *52*, 547-61. DOI
237. Hong, S. B.; Jang, Y. R.; Kim, H.; et al. Wet-processable binder in composite cathode for high energy density all-solid-state lithium batteries. *Adv. Energy. Mater.* **2024**, *14*, 2400802. DOI
238. Mao, C.; Dong, J.; Li, J.; et al. Toward practical all-solid-state batteries: current status of functional binders. *Adv. Mater.* **2025**, *37*, 2500079. DOI
239. Wang, Z.; Shen, X.; Chen, S.; et al. Large-scale fabrication of stable silicon anode in air for sulfide solid state batteries via ionic-electronic dual conductive binder. *Adv. Mater.* **2024**, *36*, 2405025. DOI
240. Na, I.; Kim, H.; Kunze, S.; et al. Monolithic 100% silicon wafer anode for all-solid-state batteries achieving high areal capacity at room temperature. *ACS. Energy. Lett.* **2023**, *8*, 1936-43. DOI
241. Zhang, Z.; Zhang, X.; Liu, Y.; et al. Silicon-based all-solid-state batteries operating free from external pressure. *Nat. Commun.* **2025**, *16*, 1013. DOI PubMed PMC

Disclaimer/Publisher's Note: All statements, opinions, and data contained in this publication are solely those of the individual author(s) and contributor(s) and do not necessarily reflect those of OAE and/or the editor(s). OAE and/or the editor(s) disclaim any responsibility for harm to persons or property resulting from the use of any ideas, methods, instructions, or products mentioned in the content.

© The Author(s) 2026. Open Access This article is licensed under a Creative Commons Attribution 4.0 International License (https://creativecommons.org/licenses/by/4.0/), which permits unrestricted use, sharing, adaptation, distribution and reproduction in any medium or format, for any purpose, even commercially, as long as you give appropriate credit to the original author(s) and the source, provide a link to the Creative Commons license, and indicate if changes were made.